UNIVERSITAT DE BARCELONA

Essays on Tail Risks in Macroeconomics

Ignacio Garrón Vedia

2023

PhD in Economics | Ignacio Garrón Vedia

ERSITAT DE
CELONA

UNIVERSITAT DE
BARCELONA

PhD in Economics

Essays on Tail Risks in Macroeconomics

Ignacio Garrón Vedia

UNIVE
BARC

PhD in Economics

Thesis title:

Essays on Tail Risks in Macroeconomics

PhD candidate:
Ignacio Garrón Vedia

Advisors:
Helena Chuliá Soler
Jorge M. Uribe Gil

Date:
April 2023

UNIVERSITAT DE BARCELONA

Dedication

A las luces de mi vida:
mi familia,
Valeria y Lucas;
mis padres,
Adolfo y Sonia;
mis hermanos,
Adolfo y Mattias.

A la memoria de mis abuelos:
Hernán, Elva, Leoncio, y Elina.

Acknowledgments

For the greater glory of God. From the moment I committed my life and work to Him, He has taken my hand and led me out of the shadows. Against all odds, I have been able to travel forward on my journey, and I have promised to make my life worthwhile.

This thesis is the epilogue to a story of calamity and love. A year before I decided to pursue this PhD in Economics, I was diagnosed with a potentially life-threatening illness. At that time, I had a stable, well-paid job, a one-year-old son, and a family. This was to be the turning point in my life. I was unable to go outside, I couldn't play tennis or football, I couldn't even go and meet my loved ones, and my career prospects had suddenly been snatched away from me. What, up to that point, had been my primary focus in life had vanished and I was left devastated. To compound matters further, this all coincided with the outbreak of the Covid-19 pandemic. Yet, I was neither finished nor afraid; I could still rely on the love of my family and friends. It was at this moment that I asked myself, if I'm not going to be here tomorrow, what can I do with myself today? What can I offer my son that I cannot give him now? I delved deep into my heart and recalled that, as I had always loved to conduct research, it had long been my ambition to complete a PhD. Although at that moment, it seemed quite impossible, I knew it was something worth giving to my son – this was the dream I had to follow. And so I set out on a different life journey, one based not on money, nor on pride, nor on comfort, but on love. I am grateful to my supervisors, family, and friends for accompanying me on this journey and for being there through both calm and storm.

I would like to express my deepest gratitude to my supervisors, Professors Helena Chuliá and Jorge Uribe, for their guidance and support throughout this journey. Their insightful advice has helped me at every stage of my research. I am especially appreciative of the support they provided when I was applying for the PREDOC-UB scholarship during the first year and, later, when trying to present my work at conferences. Also, they provided me with invaluable technical insights and suggestions at various stages of my thesis. I wish to thank them for their willingness to meet up and work through the different drafts of this thesis with me. I am also deeply indebted to them for their understanding and support during those difficult moments when, for personal reasons, my spirits were low.

I would also like to express my deepest gratitude to all the academics and administrative staff at the Universitat de Barcelona. My sincere thanks to Jordi Roca from the Universitat de Barcelona School of Economics for his support with administrative matters and his constant goodwill throughout this journey. His excellent support when I sought entry to the job market was vital. I would also like to thank Elisabet Viladecans, Ció Patxot, Jerbashian Vahagn, Oriol Tejada, Carles Maño, and Rafael Serrano for providing me with such rigorous job market training. I wish to acknowledge the work of Iain Robinson (UB Serveis Lingüístics) who kindly reviewed the English of the different chapters that make up this thesis. I am grateful for the financial support provided by the PREDOC-UB scholarship from the Universitat de Barcelona, which has enabled me to complete this thesis. Without this scholarship, it would have been impossible for me and my family to stay in Barcelona. Many thanks to Jose Peres Cajías and Augusto Blanc for their support and friendship during the last part of the thesis. And, finally, I would wish to thank Montserrat Guillen, Luis Ortiz Gracia, Manuela Alcañiz, and María José Gallego, for the supportive friendly atmosphere they create at all times in my Department.

Words cannot express my gratitude to my son, Lucas, and my wife, Valeria. I embarked on this journey with them, knowing that it would be difficult, but that there could be no room for fear. They willingly sacrificed all their comforts and left the ones they love behind in Bolivia during the Covid-19 pandemic, just so that I could follow my dream. Having you here changed my life: it made me wiser, braver, more empathetic and a better person in every way. Suddenly, everything in my life made sense. Without you, I definitely wouldn't have been able to face this challenge. Valeria, thank you for putting your career on hold for the time being to support mine and for taking care of Lucas. Your dreams are no less than mine, and I hope to support you now in fulfilling them. I have promised to love you through the good times and the bad. Lucas, may this small act of courage on the part of your father serve as an example to help you follow your dreams. I want you to know that you were the first and foremost reason I had for undertaking this project. Even when the odds appear to be stacked against you, I want you to learn from my example and to never give up chasing your dream. Let no one tell you that you can't do something; I love you infinitely.

I am deeply indebted to my father (Adolfo), mother (Sonia), brothers (Adolfo and Mattias), uncles and aunts (Waldo, Gualberto, Rosario, Héctor (R.I.P.), Alicia, Xavier), cousins (Marcela, Patricia, Cecilia, Ana, Martin, Daniel, Waldo, Horacio), sister-in-law (Mirna) and nephews and nieces (Sebastián, Sabrina, Catalina, Mattias, Gael). The love I feel for you all is beyond words and I thank you for being with me in the good times, but especially when things were not always going as expected. Dad, my hero, you were always by my side in the most important moments,

holding my hand and giving me security. Mom, my strength, and my guidance in my decisions, you showed me what true love means. Thanks to you two, I feel an immense joy to be with my son, just like you did with me. My brothers, Adolfo and Mattias, who have played the role of older brothers, protecting me, and always setting a good example. If I hadn't followed in your steps, I would not be here. Thank you for being the best brothers. Mirna, you are the sister I never had, thank you for your support. Nephews, your uncle will always be here for you. Thank you for bringing so much joy in to my life. I must also thank my parents-in-law, Osvaldo and María, and my uncles-in-law, Gonzalo and Fernando, for their support and the wonderful conversations we had while I was working on my thesis.

Finally, I would like to extend my sincerest thanks to my friends, especially to Ha, Wilma, and Grace on the PhD program in Economics, with whom we have shared so many memories during the last few years. Ha, we have been friends since day one. We have survived the difficult times and seen our way out to better days, we have shared tears and laughter, but we have always stayed firmly on track. I will forever be grateful for your support and friendship on this journey together. Wilma, the other Bolivian PhD in our cohort, you are a great friend, economist, and human being. Thanks for showing me that I can be a better person. Grace, many thanks for your advice and for being so kind to me and my family, it has meant so much to us. Also, many thanks to Ricardo, David, Gökhan, Taha, Mariona, Eduardo, Sabuhi, Witson, Renzo, Hamza, Ji Chang, Lluvia and the rest of the PhD students and faculty members who I have met and shared many special moments with. I would like to express my special thanks to Javier Aliaga, who has been my boss, professor, friend, and an inspiration in my pursuit of a PhD. I am grateful to Maria Jose Roa for encouraging me to pursue a PhD back in 2017, when I was an Economist at the Center of Latin American Monetary Studies in Mexico. I would also like to thank my friends in the Analysis Department at the Banco Central de Bolivia, who trained me and instilled in me a love for macro-finance and central banking. I remain grateful to Oscar Díaz for introducing me very early in my career on the research in macro-finance topics and for his constant support. Oswaldo, Tatiana, Rolando, Martín, Marco, Patricia, Tamara, Sergio, Renán, Carlos, and Andrés, I thank you for the many lessons and the inspiration during the years I worked there. Last but not least, I want to thank my friends with whom I have shared years of friendship, Fernando Paz, Juan Pablo Rowert, Alejandra Cordova, Mariela Fernandez, Eduardo Flores, Martín Velazco, Javier Nemer, Jose Luis Pérez, Sebastián Cadavid, Gabriela Palacios, Giovanni Pérez, Rodrigo Leyton, Luis Aliaga, Luis Aparicio, Gabriel Zalles, Fabio Moreira, Diego Suarez, Fraddy Torrico, Pablo Agramont, and Alejandro Tamayo.

This thesis is a testament to your unconditional love and encouragement.

Contents

List of Tables

List of Figures

1 Introduction

> *Given our inevitably incomplete knowledge about key structural aspects of an ever-changing economy and the sometimes asymmetric costs or benefits of particular outcomes, a central bank needs to consider not only the most likely future path for the economy, but also the distribution of possible outcomes about that path.* (Greenspan, 2004, p. 37)

Central banks and international organizations forecast relevant economic variables to guide their policy decisions. Traditionally, these estimates have focused on the central moment of the distribution of variables, for example, the future expected value of GDP growth or inflation conditional on the available information set. However, as the former Governor of the Federal Reserve (FED), Alan Greenspan, pointed out, the conduct of monetary policy has, at its core, crucial elements of risk management (Greenspan, 2004). Such a conceptual framework highlights the need to study the sources of risk and uncertainty (including the Knightian view), quantifying them, and assessing their associated costs. In general, policy decisions should not only take into account the economy's expected path, but also the distribution of outcomes associated with that path, e.g., downside or upside risks.

In recent years, policy has focused on tail risks related to economic variables, such as output, unemployment, and prices, and this has motivated the development of new statistical tools to evaluate the likelihood of distress scenarios. One of the most influential tools used by regulators and policy makers in this regard is the growth-at-risk approach, pioneered by Giglio et al. (2016) and Adrian et al. (2019), which echoes the concept of value at risk, which has been widely used and understood by regulators and practitioners for at least two decades. Globally, there are a number of institutions, including the Federal Reserve System, the International Monetary Fund, and central banks, that publish and discuss output growth and inflation probability distributions (Sánchez and Röhn, 2016; Prasad et al., 2019).

This thesis contributes to our understanding of tail risks in macroeconomics. The general objective is to develop new tools to improve the measurement of tail risks for forecasting purposes, and to study the factors that explain tail risks across funding markets and economic variables (i.e. credit, stocks, output growth, inflation, and unemployment), for a specific economy or a broader set of countries. Two main ap-

proaches are used to understand tail risks, which reflect the need to analyze the mechanisms via which risks are transmitted and to improve the forecasting performance of tools currently used in the literature. The first of these approaches relates financial shocks originating from the United States to global funding markets, using a quantile regression framework (Adrian et al., 2019). This approach is further supported by a body of literature that reports that external shocks, such as changes in US financial conditions, including monetary policy rates, could affect domestic credit in other regions (e.g. Kalemli-Özcan, 2019; Bräuning and Ivashina, 2020b; Di Giovanni et al., 2022). The second approach builds on the idea that despite the popularity of the framework developed by Adrian et al. (2019), its forecasting performance has not been extensively studied for many settings, including real-time nowcasting (Ferrara et al., 2022; Carriero et al., 2022), point versus density forecasts (e.g. Adrian et al., 2019; Brownlees and Souza, 2021), other macroeconomic variables (unemployment rate and inflation) (Kiley, 2021; Adams et al., 2021), and for a wide range of countries (Brownlees and Souza, 2021).

This thesis comprises four original chapters that seek to address two problems identified in the literature: i) How do US financial conditions impact funding markets (credit and stocks) in a large set of countries around the world under different scenarios of macro-financial distress?; and ii) what role can be played by high-frequency data, real variables, and machine learning techniques in improving the forecasting performance of macroeconomic tail risk measures? To answer these questions, the various chapters of this thesis extend the framework developed by Adrian et al. (2019) to study different economic phenomena – specifically, credit growth, stock returns, GDP growth, unemployment, and inflation – using different methods, either to make inferences about parameters, or to produce point or density forecasts, for a specific economy or a broader set of countries. Chapter 2 specifically addresses the first question, while Chapters 3-5 deal with the second. Thus, in Chapter 2, I document vulnerable funding episodes around the world. In Chapters 3 and 4, I analyze the role of high-frequency data and real variables in forecasting tail risks, while in Chapters 3 and 5 I also explore new machine learning techniques. Finally, Chapter 3 focuses on point forecasts, while Chapters 4 and 5 concern themselves with density forecasts.

International propagation of US financial shocks in funding markets under stress

In Chapter 2, entitled "Vulnerable Funding in the Global Economy", I study the propagation of financial conditions in the United States to global financial markets. Unlike previous studies examining the effect of financial conditions on real eco-

nomic activity (e.g. Adrian et al., 2019), I focus on a crucial intermediate step: that is, how financial conditions in the United States impact funding markets (credit and stocks) in a large set of countries around the world, especially during scenarios of macro-financial distress. This distinction is important from a policy perspective, as policies that seek to safeguard the financial stability of domestic economies would expect to mitigate the adverse effects of large, negative financial shocks from the US at this intermediate financial level. I also acknowledge that financial conditions must be understood in a broader sense that includes changes in the first and second moments of financial conditions (see Ludvigson et al., 2021). Lastly, I examine what is the most likely reason for a given country's vulnerability to changes in US financial conditions, testing whether this vulnerability is due to the size or depth of a country's financial market or the strength of its financial connectedness with the US (e.g. Alfaro et al., 2004; Kalemli-Özcan, 2019). My results show that the answer depends on whether I am dealing with credit or stock markets, and, by so doing, I provide fresh insights into this stream of the literature.

Forecasting macroeconomic risks

In the second part of my dissertation, I tackle the problem of producing accurate, out-of-sample tail forecasts for output growth, unemployment and inflation. In Chapter 3, entitled "Daily growth-at-risk: financial or real drivers", I propose a daily growth-at-risk approach, based on high-frequency financial and real indicators, for monitoring downside risks in the US economy. This Chapter makes three contributions to the literature. First, I show that the informational content of daily financial and real economy indicators differs across time. Thus, in certain circumstances, forecasting accuracy depends heavily on such financial indicators as the equity market volatility index or credit spreads; however, in other circumstances, real economic indicators, such as the Aruoba-Diebold-Scotti business conditions index (Aruoba et al., 2009), are better for improving forecasts. Here, the results clearly point to the time-varying importance of real and financial variables. Second, I contribute to the literature by using high-frequency financial and real indicators. Unlike most studies that employ either quarterly (e.g. Adrian et al., 2019; Brownlees and Souza, 2021) or weekly indicators (Carriero et al., 2022) to forecast tail risk to output growth, I estimate different models using daily predictors. Finally, I use a battery of new shrinkage, regularization and dimensionality reduction techniques, such as those afforded by LASSO (Belloni and Chernozhukov, 2011), elastic net (Zou and Hastie, 2005), the adaptive sparse group LASSO (Mendez-Civieta et al., 2021), and targeted predictors based on principal components analysis (Bai and Ng, 2008; Lima et al., 2020), to produce tail forecasts and compare them with past

candidates in the literature.

In Chapter 4, entitled "Daily Unemployment at Risk", I further exploit the high-frequency framework developed in Chapter 3 to produce unemployment density forecasts. Although this chapter is fairly brief, its insights nonetheless are powerful. The study reported contributes to the unemployment-at-risk literature (Kiley, 2021; Adams et al., 2021), by providing real-time daily unemployment nowcasts to inform policymakers at the highest possible frequency about the tail-risks surrounding current or near-future unemployment. This approach shows that a simple mixed data sampling quantile model using the daily indicator of real economic activity developed by Aruoba et al. (2009) can provide more precise density estimates than the financial indicators hitherto used in the literature.

Finally, in Chapter 5, entitled "Forecasting Inflation Risk Around the Globe", I address the problem of forecasting density forecasts for a large panel of countries ($n = 75$). By using a broader set of countries and employing state-of-the-art machine learning techniques, I make three contributions to the field. First, unlike previous studies (e.g. Banerjee et al., 2020; Lopez-Salido and Loria, 2022; Queyranne et al., 2022), I compute inflation density forecasts for a larger panel of countries using a set of global factors as predictors corresponding to five regions. This provides evidence that, in general, global inflation factors improve the accuracy of density forecasts, while the previous literature has tended to focus on point estimates (e.g. Ciccarelli et al., 2015; Kamber and Wong, 2020; Medeiros et al., 2021, 2022). This eclectic approach is largely supported by evidence that inflation is largely a global phenomenon. Second, while most studies in the literature only employ the quantile framework developed by Adrian et al. (2019) to produce density forecasts, I use both quantile regressions and random forest estimators (Athey et al., 2019). I show that the latter provide superior predictive performance, as also documented in the recent literature (Medeiros et al., 2021, 2022; Goulet Coulombe et al., 2022). Third, I construct two inflation risk measures, namely the probability of high and low inflation, across regions (see Lopez-Salido and Loria, 2022; Garratt and Petrella, 2022). In this sense, I provide novel heterogeneous patterns of these measures across regions.

The working paper versions of Chapters 2-4 of this thesis can be found in:

- Chuliá, H., Garrón, I., & Uribe, J. M. (2021). Vulnerable Funding in the Global Economy. Documents de Treball (IREA), (6), 1.
- Chuliá, H., Garrón, I., & Uribe, J. M. (2022). Daily Growth at Risk: financial or real drivers? The answer is not always the same. Documents de Treball (IREA), (8), 1.
- Chuliá, H., Garrón, I., & Uribe, J. M. (2022). Monitoring daily unemploy-

ment at risk. Documents de Treball (IREA), (11), 1.

At the moment of depositing this thesis, two chapters have been submitted to journals and are under "revise and resubmit": Chapter 2 in the Journal of Banking and Finance, and Chapter 3 in the International Journal of Forecasting. The results of Chapters 4 and 5 are preliminary and could be further improved in the future.

2 Vulnerable Funding in the Global Economy

2.1 Introduction

An influential set of recent studies has documented the significant predictive power of financial conditions on real economic activity during distressed macroeconomic scenarios, that is, on the left (and negative) tail of the GDP growth distribution. This literature, pioneered by the works of Giglio et al. (2016) and Adrian et al. (2019, 2021), has coined the term Growth at Risk (GaR), which echoes the concept of Value at Risk, widely used and understood by regulators and practitioners around the world for at least the last two decades.[1] In fact, the indicator has gained popularity among international regulators to the point of becoming part of the toolkit of central banks and financial supervisors for monitoring financial stability. Hence, estimating and reporting the lowest quantiles of the GDP distribution, predicted by financial conditions, one or several quarters ahead, has become standard practice (Prasad et al., 2019). This practice, which originated as a domestic economy exercise, in which the aim is to predict the GDP of the US with an index of the financial conditions of the same country, usually the National Financial Conditions Index (NFCI)[2], quickly became global in practice. Therefore, the ability of financial conditions to predict the left tail of economic activity in a relatively large set of different countries has also been examined and evaluated (e.g. Brownlees and Souza, 2021; Arrigoni et al., 2020).

We contribute to this literature in three ways. i) First, unlike previous studies that examine the effect of financial conditions on international real economic activity, we focus on a crucial intermediate step: We study how financial conditions in the US impact funding markets (credit and stocks) in a large set of countries around the world, under macro-financial distress scenarios. In other words, we focus on

[1] See as well on the vulnerable growth literature the works by Kiley (2021), Adrian et al. (2021), Loria et al. (2023), Figueres and Jarociński (2020), and Delle Monache et al. (2021).

[2] The NFCI calculated by Chicago's Fed captures financial risk, leverage, and credit quality within a single indicator. It offers a comprehensive view of US financial conditions in money debt and equity markets alongside both traditional and shadow banking systems.

vulnerable funding instead of vulnerable growth. This intermediate step is crucial because financial shocks do not transit directly, or in a vacuum, from the US to the global economic activity. On the contrary, US financial conditions mainly impact global economic activity by deteriorating funding opportunities for households and firms around the world. This distinction is also important from a policy perspective because it is at this intermediate financial level where policies that seek to safeguard the financial stability of domestic economies can expect to mitigate in some way the adverse effects of the large, negative financial shocks that may emerge from the United States market. In this respect, we document that US Financial conditions have a larger and more significant impact on the lowest quantiles of credit and stock prices on a global scale than on the central quantiles. $ii)$ Second, also unlike the previous literature, we acknowledge that financial conditions must be understood in a broader sense that includes not only changes in the first moment of financial conditions (as measured by the NFCI) but also changes in the second moment of financial conditions (which are better approximated by the index of financial uncertainty proposed by Ludvigson et al. (2021)).

First and second moment shocks impact global funding differently. On one hand, credit growth largely responds to first moment shocks in US financial conditions four quarters after they originated, which is consistent with a reduction in international funding sources for financing domestic investment, and therefore with the international credit view for the transmission of financial shocks to different countries. On the other hand, stock markets react more sensitively and rapidly (mainly within a quarter) to second moment shocks. This latter effect is more consistent with an expectation channel of the transmission of shocks, which in turn is associated with probable portfolio rebalancing by international portfolio holders, following an increase in US financial uncertainty. We empirically show that the two channels, the credit view and the portfolio view are complementary, and both are necessary to understand how financial conditions in the US spillover into the rest of the world. $iii)$ Third, we examine what is the most likely reason for a given country's vulnerability to changes in US financial conditions. Namely, we test whether such vulnerability can be explained by the size or depth of a country's financial market as it can be inferred from previous studies (e.g. Alfaro et al., 2004; Kalemli-Özcan, 2019), or if the explanation is rooted in the strength of the financial connectedness of a given country with the US. We show that the answer depends on whether we focus on credit or stock markets. In the case of credit markets, the most persistent and negative outcomes in terms of vulnerability are clearly more associated with the size or depth of the market while, in the case of stock markets, vulnerable funding episodes are associated with the financial closeness to the US. This result sheds new light on the problem compared to the previous literature, which does not employ the large

number of countries that we consider, and also does not focus on macro financially-distressed scenarios when funding is vulnerable.

To achieve our objectives we analyze vulnerable funding around the world. Vulnerable funding consists of two indicators: Credit at Risk (CaR) and Equity at Risk (EaR). CaR refers to the impact of US financial conditions (including financial uncertainty) on the lowest quantiles of real credit growth, and EaR refers to the impact of stock market prices on the lowest quantiles. Loans and shares are the two main funding sources used by corporations to finance their operations, especially their investments (Parsons and Titman, 2008; Fama and French, 2012). Therefore, evaluating the impact of the financial conditions of the world's largest economy on the lowest quantiles of the growth of credit and stock prices of the rest of the world is a crucial gap in the literature that we aim to fill. Our approach intends to be comprehensive, thus we include more than 40 countries in our estimations, with information spanning six decades (from 1960 to 2019) in most cases. Our data set consists of economies in all stages of development and comprises all sorts of recessionary and non-recessionary periods. To the best of our knowledge no previous article within the vulnerable growth literature has used such a large data set to back-up its claims.

Methodologically speaking, thanks to the multinational point of view of our research, we are able to circumvent two controversial issues regarding the estimation of effects in the vulnerable growth literature. The first issue is related to the lack of relevant controls on economic activity at the national level, which are required to assess the effect of financial conditions on future growth. The second issue is related to the presence of global macroeconomic and financial cycles that need to be considered when the propagation of shocks on a global scale is estimated. Regarding the first issue, Reichlin et al. (2020) and Plagborg-Møller et al. (2020) emphasize that the predictive power of financial conditions seems to disappear once the model controls for (enough) real-economy variables. Therefore, the deterioration of financial conditions might be more of an endogenous response of the system than of an exogenous shock that deteriorates future real economic activity. In other words, by not having enough controls on real variables, the vulnerable growth literature might be overstating the true impact of financial conditions on future economic activity. This identification issue is related to the problem of identifying the effects of real and financial uncertainty on the real economy (Ludvigson et al., 2021; Carriero et al., 2020), and also to the extensive controversy in the macroeconomics literature on the extent to which we can isolate the effects of policy variables, like the interest rate, on the real economy series[3], which is of course an unsolved problem.

[3]See Nakamura and Steinsson (2018) for a recent summary on the non-neutrality of monetary

To estimate the effects of US financial conditions on global credit and equity markets, we follow a conservative path. We assume that shocks to US financial conditions do not come from the domestic variables of each individual country in our sample, although they may be influenced by common shocks to all markets external to the US economy. In other words, US financial conditions are not influenced by a small shock to the credit market in the Netherlands or Mexico, but they may be influenced by sufficiently large shocks that affect many economies simultaneously. This assumption is backed-up by recent literature that documents the dominant role of the US economy in relation to other countries, and in particular its monetary policy, which significantly influences the commonality of business and financial cycles around the world (Ammer et al., 2016; Jordà et al., 2019; Miranda-Agrippino and Rey, 2020a,b). At the same time, by controlling for global factors, we emphasize that US shocks might be correlated with global financial and economic activity shocks, which cannot be ruled out by only stressing the dominance of the US economy. This point has been explored for instance by Chudik and Pesaran (2015) and Cesa-Bianchi et al. (2021). Lacking control for these common factors will probably lead to a bias of omitted-variables in the estimated effects on a domestic level. Thus, in short, while we assume that domestic economic variables in each country are not the origination of the financial conditions shocks to the US, we acknowledge the presence of common factors in the global economy which are not caused by UF financial conditions and indeed can influence them. This strategy can be followed only within an international framework as ours, and in this way, it moves away from the debate of the identification of financial conditions effects on real and nominal variables within a single economy that we mentioned before.

Our study is also related to the large corpus of theoretical and empirical literature that has expanded the credit-channel to international grounds. It has therefore contributed to explaining the transmission of financial shocks across the world economy (Peek and Rosengren, 1997; Cetorelli and Goldberg, 2012; Ivashina et al., 2015; Bruno and Shin, 2015; Choi, 2018; Choi et al., 2018; Baskaya et al., 2017; Gete and Melkadze, 2018; Bräuning and Ivashina, 2020b; Di Giovanni et al., 2022, among others). We revise this literature and connect it with our contributions in the next section, which, in short, aim to help regulators foresee future risks to funding opportunities for domestic investment and consumption, and therefore to economic activity after a financial shock to the US economy has been observed (as occurred for instance during the Great Recession). We also aim to document the main way in which vulnerable growth occurs, which is precisely through the propagation of financial shocks across the global financial markets, i.e., via vulnerable funding.

policy.

The rest of this document is organized as follows: Section 2.2 briefly revises two perspectives in the literature that can explain the transmission of US financial conditions to the international funding markets, namely the credit view and the portfolio view, and also revise the two main explanations underlying vulnerable funding, market depth and market connectedness. Section 2.3 outlines our methodology. Section 2.4 describes our data and sources, and presents details about the construction of our macroeconomic and financial global factors. Section 2.5 contains our main empirical results and discussion. Section 2.6 concludes.

2.2 The international spread of US financial conditions

In addition to the vulnerable growth literature summarized in the introduction, our study is related to two different sets of studies: Those which emphasize the channels through which financial shocks transit from a central economy (generally the US) to the rest of the global markets, and those which examine the macroeconomic determinants of financial vulnerability to external shocks. Both sets of studies are too rich to be summarized in this subsection, so we focus on those studies that directly provide a baseline for understanding our main results. In the former group of studies we find a subset of articles that highlight the role of credit in the international propagation of financial shocks, which we label as the credit view, and a second subset that emphasizes the transmission of financial shocks through expectations, which we include in the portfolio view of the transmission of shocks.

In the second group of studies we find a great majority of articles that point to the size and depth of the financial markets as the main determinants of financial vulnerability to external shocks, we have therefore labeled them as the financial development determinant. There is also a second subset that stresses the importance of financial connectedness across the global financial markets as the main explanatory factor, which we have labeled the financial connectedness determinant. Both channels and determinants are important for our different definitions of financial conditions, based on first and second moment indicators. The classification does not claim to be either exhaustive or exclusive. Indeed, in referenced studies the channels and determinants are closely examined. For instance, as highlighted by Alfaro et al. (2004), the role of local financial markets is crucial in enabling foreign direct investment. The more developed the local financial markets, the easier it is for credit-constrained entrepreneurs to start their own business. Large varieties of intermediate goods imply positive spillovers to the final goods sector and, as a consequence, financial markets allow the backward linkages between foreign and

domestic firms to turn into FDI spillovers.

Hence, our revision is more oriented towards serving as a starting point for understanding the empirical results in the next section, as well as how these relate to our working hypothesis explained in the introduction about the existence of vulnerable funding episodes following first and second moment shocks to financial conditions in the US.

2.2.1 The channels

A. The international credit view

According to this literature, external factors, such as US interest rates and global financial conditions, are key determinants of capital flows, especially in the short run. Which is important because, as highlighted by Kalemli-Özcan et al. (2020), there is evidence of a strong association between capital flows, GDP volatility, and financial crises. This general view consists in understanding that international creditors may react to a change in financial conditions, including monetary policy stances in their original economies, by reducing their exposition to foreign markets, to satisfy risk-taking constraints on their international credit portfolio holdings. Thus, as emphasized by Bräuning and Ivashina (2020b), some intended consequences of the US monetary policy within its domestic economy, may end up having intended consequences on a global basis (i.e. spillover of "prudent risk-taking" or "productive risk-taking").

In these lines, Bruno and Shin (2015) highlight the role of financing costs of banks, which are closely linked to the reference policy rate chosen by the central bank. If funding costs affect decisions on how much exposure to take on, monetary policy will then affect the economy through greater risk-taking by the banking sector. Di Giovanni et al. (2022) also document that an easing in global financial conditions leads to lower borrowing costs and an increase in local lending. The shocks on credit can potentially transit via international banks, as in Cetorelli and Goldberg (2012), via foreign banks lending elsewhere, as in Bräuning and Ivashina (2020a) and Ivashina et al. (2015), via domestic banks borrowing from foreign banks and global investors over the global financial cycle, as in Baskaya et al. (2017), or even via credit trade by multinational establishments (Lin and Ye, 2018).

B. The international portfolio view

Even if we abstract from the direct link that provides lending, it could also be the case that if a peak of uncertainty in the US associated with a worsening of financial conditions is interpreted as a signal of future higher domestic vulnerability in

other countries, this increase may lead to higher precautionary savings which do not remain within the domestic economies but instead flow abroad, reducing domestic demand (Fernández-Villaverde et al., 2011). Similarly, it could lead to a contraction in banks' credit supply after facing greater uncertainty, which can be rationalized by the arguments explored by Bordo et al. (2016), Alessandri and Mumtaz (2019), Alessandri and Bottero (2020).

We contribute to the previous literature on the transmission channels in two ways: first, we focus on the most vulnerable market scenarios, automatically identified by estimating Credit at Risk and Equity at Risk statistics, which has not been done before (all the aforementioned literature focuses on the average scenarios, and most studies center on a small number or individual countries). Therefore, we acknowledge the non-linear dimension emphasized by the consensus of the macroeconomic literature in recent years, which is necessary for explaining economic collapses (Isohätälä et al., 2016; Brunnermeier and Sannikov, 2016; Gertler and Gilchrist, 2018). Second, we jointly analyze the impacts of first moment shocks proxied by the NFCI, and second moment financial conditions proxied by the index of financial uncertainty of Ludvigson et al. (2021). Thus we are able to disentangle the entire effect of financial conditions on the global economy. Our results emphasize the role of the portfolio view for the propagation of second moment financial condition shocks and of the credit view for understanding the propagation of first moment financial conditions shocks.

2.2.2 The determinants

A. Size and depth of the domestic financial market

The previous literature reports that global financial conditions have an asymmetric impact on the economic activity of emerging and advanced economies. For example, Carrière-Swallow and Céspedes (2013) find that in comparison to the US and other developed countries, emerging economies suffer much more severe falls in investment and private consumption following an exogenous uncertainty shock. They present evidence on the correlation between the dynamics of investment and consumption and the depth of financial markets. The authors emphasize the role of financial institutions and argue that the lack of development of local financial markets can limit the economy's ability to take advantage of potential FDI spillovers. Alfaro et al. (2004) evaluate the various links among the FDI, financial markets, and economic growth. They conclude that FDI alone plays an unclear role in economic growth, and that it is well-developed financial markets and institutions that enable a country to take advantage of increases in foreign investment. Kalemli-Özcan (2019)

shows that changes in US monetary policy affect capital flows in and out of emerging markets more than they do in advanced economies, since the capital flows of emerging markets are more risk sensitive, and US policy affects the risk sentiments of global investors.

Other authors such as Bräuning and Ivashina (2020b) document that global bank flows driven by US monetary policy affect credit conditions in emerging markets, at the firm level, which confirms that global banks contracting credit is not compensated by an increase in credit by local banks. On the contrary, it leads to a general credit contraction, an increase in interest rate spreads, and finally to a lower probability of refinancing.

The same narrative can be tracked in the previous literature regarding the transmission of international stock market shocks to domestic economies across the world. For instance, Bhattacharya et al. (2019) document that unanticipated changes in US uncertainty have significant effects on financial and macroeconomic emerging market economies. The transmission is traced back to a depreciation of the local currency of domestic economies, which leads to a decline in local stock markets and increases long-term interest rate spreads in relation to the US. This is followed by a decrease in capital inflows into the domestic economies.

B. Financial connectedness with the US

It is important to think of this literature as a complement of the studies in subsection A, which emphasizes the role played by the size and depth of the domestic markets that receive the shock, instead of as an alternative explanation. To illustrate this point, Fink and Schüler (2015) emphasize the importance of financial linkages with the US rather than via bilateral trade to explain the propagation of financial condition shocks across the global economy. However, precisely for this reason the transmission to emerging market economies (EME) may occur to a different extent than the transmission to advanced economies. Fink and Schüler (2015) find that, indeed, an adverse shock to the overall US financial system dries up capital flows from the US to the EME and that this decline in cross-border lending results in tighter financing conditions for the EME.

Alfaro and Chen (2012) use granular data to research the way in which multinationals around the world responded to the 2008 crisis compared to local firms. They explore three channels through which FDI affects establishment performance: production linkages, financial linkages, and multinational networks. These authors' results show that FDI flows played an important although heterogeneous role in explaining the performance of multinational firms during the Global Financial Crisis. They emphasized both the role of FDI linkages in the international transmission

of shocks and the important interaction of the various facets that determine these transmissions, from considerations of financial constraints to the engagement of some firms with vertical production linkages.

Lin and Ye (2018) explore a trade credit channel through which FDI firms can propagate global liquidity shocks to host countries, despite these host countries implementing tight controls on portfolio flows. This is important because, in practice, while many developing countries impose tight restrictions on non-FDI flows, they are significantly open to FDI inflows. These authors show that indeed a positive global liquidity shock eases raising international funds for FDI firms. This in turn, strengthens the advantage of FDI firms in providing trade credit to local downstream firms. In short, there is a trade credit channel through which FDI firms can propagate global liquidity shocks to host economies despite the presence of tight controls on non-FDI financial flows.

In terms of contributions, our multi-country and comprehensive approach allows us to test which factor best explains the heterogeneous dynamic of Credit at Risk and Equity at Risk indicators that we estimate for the cross-section of countries. We find that the vulnerability of credit markets is better explained by the size or depth of credit markets, while financial connectedness to the US, measured as the relative importance of US direct foreign investment to a country's GDP, better explains the vulnerability of stock markets.

2.3 Methodology

To avoid the criticisms mentioned in the introduction regarding the possible endogeneity of financial first and second moment shocks with respect to credit and stock markets within a single economy, we estimate multi-country factor augmented quantile-regression models. Our models consider directly the influence of common real and financial factors of a global nature, on the domestic economic series. Thus, they allow us to better isolate the causal effects of financial conditions on funding markets around the world.

Our base-line specification for each country i is given by Equation (2.1):

$$Q_{\tau}(y_{i,t+h}) = \alpha_{0i}(\tau) + \beta_{0i}(\tau)\, y_{i,t} + \beta_{1i}(\tau)\, us.fc_t + \delta_i(\tau)' X_t, \tag{2.1}$$

where, $i = 1, \ldots, N$, refers to the country, $h = \{0, 1, 4\}$, to the forecasting horizon, and $\tau = \{0.05, 0.10.0.20, 0.50\}$ to the quantile of the dependent variable. $y_{i,t+h}$ is either the quarterly change of real credit growth in logarithms (Credit at Risk) or the quarterly change of the stock price index in logarithms (Equity at Risk), at time horizon $t+h$. On its side, $us.fc_t$ is the US financial condition indicator, which can

be either the NFCI of Chicago's Fed or the Financial Uncertainty Index provided by Ludvigson et al. (2021), publicly available on the webpage of the authors. X_t consists of a global macroeconomic factor and a global financial factor. $\alpha_{0i}, \beta_{0i}, \beta_{1i}$ and $\delta(\tau)$ denote the parameters corresponding to the τ-th quantile.

We emphasize that $Q_\tau(y_{i,t+h})$ is a conditional quantile of the response variable, and for this reason there is not a random term in Equation (2.1). In other words, $Q_\tau(y_{i,t+h})$ characterizes $y_{i,t+h}$ but it is deterministic in nature. Nevertheless, we can present Equation (2.1) alternatively in the following way:

$$y_{i,t+h} = \alpha_{0i}(\tau) + \beta_{0i}(\tau) y_{i,t} + \beta_{1i}(\tau) us.fc_t + \delta_i(\tau)' X_t + \varepsilon_{i,t}, \tag{2.2}$$

where $\varepsilon_{i,t}$ is a random noise that is assumed to follow the following quantile-restriction $P[\varepsilon_{i,t} \leq 0 | \alpha_{0i}(\tau) + \beta_{0i}(\tau) y_{i,t} + \beta_{1i}(\tau) us.fc_t + \delta_i(\tau)' X_t] = \tau$. The presentation of the model in Equation (2.2) emphasizes the factor structure of the CaR and EaR statistics. The model for each country is estimated using individual conditional quantile regressions as proposed by Koenker and Bassett (1978), but $y_{i,t+h}$ in all countries is a function of common factors, $us.fc_t$ and X_t, which do not have crosssectional variation but only vary over time, via a country-specific intercept α_{0i} and countryspecific slope coefficients ($\beta_{0i}, \beta_{1i}, \delta_i$). All the variables were normalized before estimation to have zero mean and unitary variance. In this way, we are able to compare the magnitude of the effects across different countries.

The model in Equation (2.1) expands a traditional conditional mean regression, in the sense that it explains the whole conditional time-series distribution of credit growth and stock returns. In particular, the parameters are estimated by solving the following optimization problem:

$$\hat{\Theta}(\tau) = argmin_{\Theta(\tau)} E\left[\rho_\tau\left(y_{i,t+h} - Q_\tau(y_{i,t+h})\right)\right], \tag{2.3}$$

where $\Theta(\tau) = [\alpha_{0i}(\tau), \beta_{0i}(\tau), \beta_{1i}(\tau), \delta_i]\prime$ are the parameters, and ρ_τ is a loss function given by $\rho_\tau = (1-\tau)1(\{\varepsilon_{i,t+h} < 0\})|\varepsilon_{i,t+h}| + \tau 1(\{\varepsilon_{i,t+h} > 0\})|\varepsilon_{i,t+h}|$, where $\varepsilon_{i,t+h}$ is the error term and with $1(\{\varepsilon_{i,t+h} < 0\})$ taking the value of 1 when the subscript is true and 0 otherwise. As it is well known, the mathematical formulation in Equation (2.3) leads to the solution of a linear programming optimization problem that we have omitted here. Its basic structure and the counterpart algorithm solution can be found in Koenker (2005).

Quantile regressions have been employed in the factor models literature since at least Ando and Tsay (2011). We estimate the global factors using PCA, following the tradition of the factor literature, as described for example by Bai and Ng (2008, 2020) and Stock and Watson (2012), and also the approach of aforementioned studies on GaR. An alternative to Equation (2.1) would be to incorporate the global

factors, as Chudik and Pesaran (2015) did, using the crosssectional means for the variables in the data set. This would result in a quantile factor model in the form of Harding et al. (2020). Both these authors' approaches and our approach are inspired by the necessity to incorporate common factors to model the dynamics of the cross-sectional units. These are fundamental when multinational comparisons are carried out in order to reduce the risk of omitting relevant confounding variations. Note as well that we do not have a balanced panel (and we do not require it). Our approach is more flexible than that because our factors use all the available cross-sectional units at each period in the sample. However, the country-specific estimates depend on the number of timeseries units available for each country, which in most cases run from 1960Q1 to 2019Q4, and only in three cases consist of shorter samples (which are indicated in the results).

2.4 Data

Our dataset includes a set of macroeconomic and financial variables for advanced and emerging economies and US data on financial conditions. Specifically, we use a long quarterly data panel constructed and provided by Monnet and Puy (2019), which covers real Gross Domestic Product (GDP), credit, consumer prices, nominal stock prices, and sovereign bond yields for advanced and emerging countries over the whole post-war period. Compared to other similar sources, such as the Organization for Economic Cooperation and Development (OECD) or the Bank of International Settlements (BIS), the coverage gains for these data are around 20% to 30% for advanced economies, and more than 100% for emerging economies. More specifically, real GDP is available for 37 countries, real credit for 45 countries, consumer prices for 48, nominal stock prices for 25 countries and bond yields for 18, with a sample size that ranges between 1950Q1 and 2019Q4 per country.[4] We restrict our sample to starting in 1960-1Q because of poor data quality for the earlier periods (we observed very extreme values and large volatility). For the purposes of our analysis, we transform our variables to achieve stationarity before estimation. Table 2.A2 in the Appendix shows the transformations applied to each series and Figure 2.A1 plots both the untransformed and transformed series with their associated unit root tests.[5]

Similarly to US data on financial conditions, we use either the National Financial Condition Index[6]or the financial uncertainty indicator proposed by Ludvigson et al.

[4]See Table 2.A1 in the Appendix for details on data availability, Table 2.A2 for details on transformations of the variables, and Table 2.A3 for details on summary statistics.

[5]We test for unit roots using the Augmented Dickey-Fuller (ADF).

[6]The NFCI is constructed and published by the Federal Reserve Bank of Chicago and it is

(2021)[7]. On one hand, following the seminal work of Adrian et al. (2019), NFCI is considered to be one of the most relevant predictors of the lower conditional quantiles of output growth for the US (e.g. Arrigoni et al., 2020; Brownlees and Souza, 2021; Beutel et al., 2020). Based on Brave et al. (2011), the NFCI is a weighted average of 105 measures of financial activity, each scaled to have zero mean and one standard deviation. Positive NFCI values imply that US financial conditions are tighter than average. Since the NFCI has weekly periodicity, for our analysis we aggregated it by taking the quarter averages for the overall sample, starting at 1971Q1. This implies that for our econometric estimations that include this variable, the sample is reduced to around 200 observations. On the other hand, the financial uncertainty index is constructed by Ludvigson et al. (2021) using a rich dataset of variables that fully characterize US financial markets. The authors of the index estimate a factor model for the large dataset, and predict each variable using their latent factor structure. Then, they estimate the time-varying conditional volatility of the residuals of each series and determine the average across all of them to obtain the financial uncertainty indicator.

As stated above, in our estimations we include a global macroeconomic factor and a global financial factor to control for the commonality of business and financial cycles previously emphasized by the literature. The central idea of our approach is to summarize fluctuations in macroeconomic and financial variables for a large and heterogeneous panel of advanced and emerging economies by using factor models. In particular, we estimate two global factors: the first factor, which we refer to as the global financial factor ($N = 89; T = 240$, from 1960Q1 to 2019Q4) contains real credit growth, stock returns and changes in sovereign bond yields; and the second factor, which we refer to as the global macroeconomic factor ($N = 174; T = 240$, from 1960Q1 to 2019Q4), also includes real GDP growth and inflation on top of the abovementioned variables.

We estimate these common factors by a two-step procedure that combines first-step estimation via Principal Component Analysis (PCA)[8] with the Kalman filter, where the latter is used to compute recursively the expected value of the common factors, which is iterated until convergence of the Expected-Maximization (EM) algorithm (Doz et al., 2012). This procedure is especially relevant for our work as we deal with some missing data for specific countries at the end of the sample. We compute the factors from the stationary variables and assume they can be repre-

available at: https://www.chicagofed.org/publications/nfci/index.

[7]The Financial Uncertainty indicator is available for the US on the web page of one of its authors, at: https://www.sydneyludvigson.com/macro-and-financial-uncertainty-indexes.

[8]In order to estimate principal components in the first stage, missing values are imputed by the average of respective country-specific variables.

sented by a VAR(1) process. However, the two factors (global macroeconomic and financial) estimated using the two-steps algorithm are very similar to the factors computed by direct estimation via PCA. Therefore, we opt for reporting only the latter in our results (see Table 2.A4).

Figure 2.1 plots the NFCI jointly with the global macroeconomic and financial factors over the sample period. Consistent with Miranda-Agrippino and Rey (2020b), we find that our global factors point to the existence of a global cycle that is linked to the US recession periods as identified by the NBER (red shaded areas). These global factors, the NFCI and the financial uncertainty index share a pronounced contemporaneous common component, especially around the global financial crisis. In this period, we notice a sharp movement of the global factors and a tightening in US financial conditions. This suggests that, in order to explore the international transmission of financial fragility in the US to the conditional distribution of global credit markets and stock markets, we should control for the contemporaneous global and financial cycles. Thus, we should focus on the additional "marginal" information provided by the indicator of financial fragility in the US. We also observe that the NFCI and the financial uncertainty index share some common spikes, e.g. around the 1973-1975 recession due to the oil crisis coupled with the stock market crash, and during the global financial crisis, but appear to be capturing different aspects of US financial fragility. In particular, the NFCI is more volatile and moved up notably during the recession periods in the early 80s, while the uncertainty index stayed subdued over the same period. However, the opposite happened in the late 1990s and during the collapse of the speculative dot-com bubble in the early 2000s. Moreover, during 2018-2019 the uncertainty index rose significantly while the NFCI remained stable.

Finally, to assess cross-country heterogeneity, we construct three variables related to the size of credit and stock markets, respectively, and financial interconnection with the US. Specifically, we measure the size of credit markets by the annual average of the credit to GDP ratio for each country and the size of stock markets by the annual average of the market capitalization to GDP ratio. This data has been collected from the World Bank database[9] and, in both cases, the time span is from 1960 to 2019. Financial interconnection with the US is measured by the total direct investment of the US as a percentage of the country's GDP (for the sample period, 1989 to 2019). To this end, we compute for each country the maximum value of US investment inflows relative to its GDP.[10] We use historical data on US direct

[9]Credit refers to financial resources (loans, securities, and other claims) provided to the private sector by banks. Market capitalization is the share price times the number of shares outstanding for listed domestic companies.

[10]Results are robust when we use the average instead of the maximum value.

investment abroad from the National Bureau of Economic Research and nominal GDP from the International Monetary Fund statistics.[11]

Figure 2.1: Global factors and US financial conditions

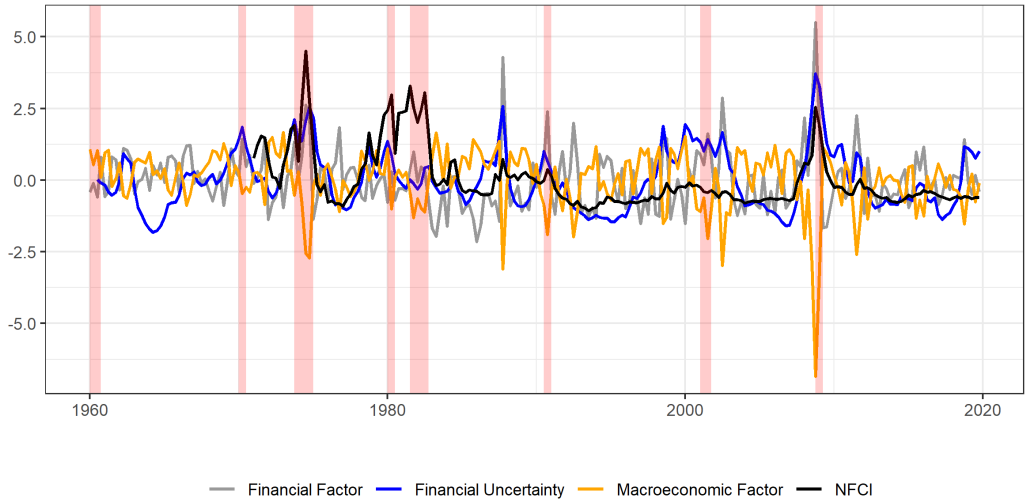

Sources: Chicago National Financial Condition Index (NFCI) and author's computation.
Note: Standardized variables. Time span 1960Q1 to 2019Q4. Red shaded area represents NBER recessions at the end of the period.

2.5 Results

First, we present our estimation results of the impact of shocks due to US financial conditions on credit growth and stock returns. We distinguish between changes in the first moment of financial conditions (as measured by the NFCI) and changes in the second moment of financial conditions (as measured by the index of financial uncertainty proposed by Ludvigson et al. (2021)). We then assess the heterogeneity on the vulnerability of credit and stock markets to US financial conditions across countries. First, we graphically show our results sorting the countries according to different measures related to the size of credit and stock markets, and the relative importance of US foreign investment for each country. Finally, we carry out cross-sectional regressions that use as input the quantile slopes of CaR and EaR estimated in the first round of regressions, and as explanatory variables the ones mentioned above.

[11] See Table 2.A5 in the Appendix for information on these variables.

2.5.1 Impact of NFCI shocks on global markets

Table 2.1 summarizes the estimation results for real credit growth as the dependent variable for quantiles $\tau = \{0.05, 0.10.0.20, 0.50\}$ and for forecasting horizons $h = \{0, 1, 4\}$. We run two different regressions. The first one only includes the NFCI while the second one controls for the global financial and macroeconomic factors. The table reports the following information: the first and last quartiles of the distribution of estimated coefficients (q25-q75), the proportion of countries for which the variable is statistically significant at a 90% confidence level (Sig.), and, for the NFCI, it is also shown the proportion of countries that display negative and significant quantile slope coefficients (Sig. < 0).

Three main findings emerge from the results in Table 2.1. First, the impact of the NFCI on real credit growth is more frequently (and significantly) negative on the lower quantiles than on the central quantiles of credit growth. In other words, the proportion of countries for which the effect is significant, is much higher in the lower quantiles. This result suggests that US financial fragility is an important predictor of downside risks to real credit growth in the global economy. Second, our results hold when we control for global financial and macroeconomic factors, i.e., the performance of the model including the global factors is basically indistinguishable from the model including only the NFCI. Third, the results also hold irrespective of the forecasting horizon $(h = \{0, 1, 4\})$ but the highest percentage of countries for which the impact of NFCI on the quantile at $\tau = 0.05$ (0.10) of real credit growth is statistically significant and negative is obtained when $h = 4$, with 27% (30%) for 44 countries. This suggests that the global economy requires one year to fully transmit most of the first moment shocks of US financial conditions to the rest of the credit markets in the world, which is consistent with a credit view explanation of the transmission of shocks, i.e., deterioration of financial conditions seems to generate a reduction in international funding sources for financing domestic investment, which fully materializes one year after the shock.

Interestingly, the forecasting power of NFCI on the conditional distribution of credit is more heterogeneous than the effect of the other covariates in all our specifications. That is, US financial conditions clearly impact the negative tail of credit growth of a higher number of countries than in the case of the average quantiles, while the other variables, whether they are global common factors or idiosyncratic characteristics, exert a more homogeneous effect across the conditional distribution of credit.

From Table 2.1 we also see that the impact of financial conditions in the United States is very heterogeneous across countries. While it is a relevant predictor of negative credit dynamics at least four quarters ahead for around $25 - 30\%$ of our

sample, it is not for the rest of the countries. Moreover, the impact of the three global factors, namely, two global factors and the US financial conditions index, vary greatly across countries. That is, in most of the cases the effects contained between the first and the third quartiles of the cross-sectional distribution of countries include both positive and negative magnitudes, meaning that global factors impact credit creation around the world heterogeneously.

Table 2.2 summarizes the estimation results for stock returns as the dependent variable. Again, we run two models for each quantile of the dependent variable ($\tau = \{0.05, 0.10.0.20, 0.50\}$) and forecasting horizon ($h = \{0, 1, 4\}$). The first model only includes the NFCI while the second also considers controls for the global financial and macroeconomic factors. The table reports the following information: the first and last quartiles of the distribution of estimated coefficients (q25-q75), the proportion of countries for which the variable is statistically significant at a 90% confidence level (Sig.); for the NFCI, the proportion of countries that are associated with negative and significant coefficients is also shown (Sig. < 0). The results show that the highest impact of US financial conditions on the left tail of conditional stock returns is observed when $h = 0$, i.e., NFCI significantly explains downside risk in stock markets in a contemporaneous fashion. This key result is observed even if we control for global financial and macroeconomic factors, as the percentage of countries for which the NFCI coefficient is statistically significant goes from 32% ($\tau = 0.05$ quantile) to 48% ($\tau = 0.10$ quantile), out of 25 countries. Interestingly, the contemporaneous impact at the median is significant for a larger proportion of countries (60%), but this percentage drops to 12% when we control for the global factors. At horizons $h = 1$ and $h = 4$, the effects of NFCI on stock markets are less pronounced, both at the lower tail and at the central quantiles.

An interesting pattern that confirms that the US is the probable origin of shocks to the global economy can also be seen in Table 2.2. This pattern agrees with previous literature on global cycles, and also validates our multinational approach. Namely, at $h = 1$, local financial conditions in the United States exert a significant impact in around 4-12% of the countries of our sample, for quantiles between $\tau = 0.05$ and 0.20, while the global financial factors impact the same quantiles for 12-16% of the countries and the global macroeconomic factors for 0-12%. In contrast, when $h = 4$, the impact of the US domestic financial conditions only exert a significant influence in 4-12% of the countries, while the global financial and macroeconomic factors have gained in significance to affect 40-52% and 28-64% of countries, respectively. This would be the case if one year after the US shock, this original shock has been fully transmitted to the global economy, and the non-linear amplification mechanisms operating in financial markets on a global scale are responsible for the newest sources of financial fragility in the global economy.

Once again, the effects across countries at the lowest quantiles of the stock market growth are heterogeneous. That is, the interquartile range of the cross-sectional distribution of countries includes both positive and negative values, not only for the financial condition index, but also in the case of macroeconomic and financial global factors, indicating heterogeneous risksharing across countries. While a large fraction of the countries react negatively to a deterioration of either the financial conditions in the US or the two global factors, most of them do not react or even react positively to the shock.

One way in which the transmission of shocks may occur across countries is through spillover effects of the "prudent risk-taking" or "productive risk-taking" channel of monetary policy. This is a channel that leads to increased risk-taking by banks in response to monetary policy easing, which is consistent with traditional portfolio allocation models. Namely, lower policy rates make riskier investments more attractive.

Importantly, the largest effects of US financial fragility on credit markets are observed one year after the realization of the shock, suggesting that US financial conditions can be used as a predictor of the future vulnerability of domestic credit conditions by regulators and central banks around the globe. On the contrary, the effects on stock markets are mainly contemporaneous, which prevents this indicator being used to forecast future prices or as an early warning indicator that alerts about future limitation of internal (equity) funding.

Table 2.1: Quantile regressions, Impact of NFCI on real credit growth (CaR)

		$\tau = 0.05$	$\tau = 0.10$	$\tau = 0.20$	$\tau = 0.50$
Regressions for $h = 0$					
US financial conditions indicator					
$NFCI_t$	q25-q75	[-0.32;0.07]	[-0.22;0.02]	[-0.14;0.05]	[-0.05;0.08]
	Sig.<0	0.25	0.16	0.14	0.07
US financial conditions indicator + Global factors					
$NFCI_t$	q25-q75	[-0.25;0.02]	[-0.24;0.01]	[-0.16;0.02]	[-0.06;0.07]
	Sig.<0	0.18	0.14	0.25	0.07
$GFIN_t$	q25-q75	[0.02;0.56]	[0.00;0.56]	[0.03;0.52]	[0.13;0.52]
	Sig.	0.25	0.34	0.45	0.5
$GMACRO_t$	q25-q75	[-0.08;0.63]	[-0.1;0.52]	[-0.05;0.53]	[0.11;0.54]
	Sig.	0.27	0.3	0.45	0.5
Regressions for $h = 1$					
US financial conditions indicator					
y_{it}	q25-q75	[0.05;0.32]	[0.07;0.36]	[0.06;0.35]	[0.09;0.43]
	Sig.	0.30	0.48	0.59	0.70
$NFCI_t$	q25-q75	[-0.28;-0.02]	[-0.24;-0.06]	[-0.19;-0.01]	[-0.08;0.02]
	Sig.<0	0.23	0.25	0.30	0.07
US financial conditions indicator + Global factors					
y_{it}	q25-q75	[0.06;0.30]	[0.05;0.35]	[0.09;0.37]	[0.09;0.43]
	Sig.	0.36	0.48	0.57	0.68
$NFCI_t$	q25-q75	[-0.26;-0.02]	[-0.24;-0.03]	[-0.17;-0.05]	[-0.06;0.06]
	Sig.<0	0.16	0.27	0.25	0.02
$GFIN_t$	q25-q75	[-0.45;0.37]	[-0.27;0.23]	[-0.16;0.17]	[-0.08;0.19]
	Sig.	0.30	0.23	0.25	0.30
$GMACRO_t$	q25-q75	[-0.4;0.40]	[-0.24;0.23]	[-0.11;0.26]	[0.00;0.27]
	Sig.	0.30	0.23	0.27	0.39
Regressions for $h = 4$					
US financial conditions indicator					
y_{it}	q25-q75	[0.24;0.57]	[0.32;0.55]	[0.34;0.56]	[0.33;0.62]
	Sig.	0.61	0.80	0.89	0.98
$NFCI_t$	q25-q75	[-0.41;0.02]	[-0.28;-0.02]	[-0.22;0.00]	[-0.09;0.02]
	Sig.<0	0.25	0.20	0.34	0.18
US financial conditions indicator + Global factors					
y_{it}	q25-q75	[0.29;0.56]	[0.27;0.60]	[0.33;0.58]	[0.34;0.60]
	Sig.	0.68	0.77	0.84	0.98
$NFCI_t$	q25-q75	[-0.32;-0.01]	[-0.31;-0.02]	[-0.22;-0.02]	[-0.07;0.04]
	Sig.<0	0.27	0.30	0.3	0.14
$GFIN_t$	q25-q75	[-0.48;0.11]	[-0.32;0.19]	[-0.18;0.20]	[-0.05;0.15]
	Sig.	0.16	0.09	0.20	0.16
$GMACRO_t$	q25-q75	[-0.49;0.05]	[-0.37;0.15]	[-0.23;0.16]	[-0.03;0.16]
	Sig.	0.16	0.20	0.20	0.18

Note: Sig. denotes proportion of countries for which the variable is statistically significant at 90% confidence level; q25-q75 shows the first and third quartiles of the estimated coefficients. Intercepts are omitted in the table. Standard errors are based on bootstrapping with 1000 replications. Sample: 1971Q1 to 2019Q4 for 44 countries, except for Bolivia (to 2019Q3), Iceland (to 2018Q4) and Taiwan (to 2018Q4).

Table 2.2: Quantile regressions, Impact of NFCI on stock markets (EaR)

		$\tau = 0.05$	$\tau = 0.10$	$\tau = 0.20$	$\tau = 0.50$
Regressions for $h = 0$					
US financial conditions indicator					
$NFCI_t$	q25-q75	[-0.65;-0.24]	[-0.47;-0.2]	[-0.37;-0.08]	[-0.24;-0.08]
	Sig.<0	0.36	0.56	0.68	0.60
US financial conditions indicator + Global factors					
$NFCI_t$	q25-q75	[-0.34;0.00]	[-0.24;0.02]	[-0.15;-0.01]	[-0.05;0.04]
	Sig.<0	0.32	0.48	0.36	0.12
$GFIN_t$	q25-q75	[-0.79;-0.41]	[-0.85;-0.42]	[-0.83;-0.39]	[-0.78;-0.35]
	Sig.	0.60	0.68	0.76	0.88
$GMACRO_t$	q25-q75	[-0.09;0.25]	[-0.1;0.26]	[-0.14;0.23]	[-0.06;0.21]
	Sig.	0.20	0.08	0.40	0.24
Regressions for $h = 1$					
US financial conditions indicator					
y_{it}	q25-q75	[0.18;0.51]	[0.19;0.47]	[0.18;0.41]	[0.26;0.37]
	Sig.	0.56	0.64	0.80	0.92
$NFCI_t$	q25-q75	[-0.23;0.01]	[-0.2;0.00]	[-0.18;-0.02]	[-0.1;0.01]
	Sig.<0	0.12	0.16	0.16	0.16
US financial conditions indicator + Global factors					
y_{it}	q25-q75	[-0.01;0.29]	[0.08;0.33]	[0.15;0.37]	[0.16;0.38]
	Sig.	0.08	0.32	0.48	0.56
$NFCI_t$	q25-q75	[-0.21;0.05]	[-0.18;0.01]	[-0.15;0.00]	[-0.07;0.01]
	Sig.<0	0.12	0.04	0.08	0.16
$GFIN_t$	q25-q75	[-0.35;0.09]	[-0.53;-0.07]	[-0.41;-0.09]	[-0.24;-0.01]
	Sig.	0.12	0.12	0.16	0.00
$GMACRO_t$	q25-q75	[-0.20;0.40]	[-0.31;0.03]	[-0.26;-0.09]	[-0.18;-0.03]
	Sig.	0.08	0.00	0.12	0.00
Regressions for $h = 4$					
US financial conditions indicator					
y_{it}	q25-q75	[-0.10;0.29]	[0.00;0.17]	[-0.02;0.10]	[-0.09;0.03]
	Sig.	0.20	0.16	0.08	0.08
$NFCI_t$	q25-q75	[-0.28;0.14]	[-0.14;0.09]	[-0.09;0.06]	[-0.06;0.04]
	Sig.<0	0.04	0.04	0.04	0.12
US financial conditions indicator + Global factors					
y_{it}	q25-q75	[-0.07;0.16]	[-0.13;0.17]	[-0.11;0.12]	[-0.10;0.04]
	Sig.	0.00	0.04	0.08	0.08
$NFCI_t$	q25-q75	[-0.18;0.21]	[-0.17;0.13]	[-0.08;0.09]	[-0.07;0.06]
	Sig.<0	0.04	0.12	0.04	0.08
$GFIN_t$	q25-q75	[-0.96;-0.33]	[-0.79;-0.46]	[-0.64;-0.34]	[-0.36;-0.08]
	Sig.	0.40	0.52	0.52	0.36
$GMACRO_t$	q25-q75	[-0.82;-0.36]	[-0.88;-0.36]	[-0.62;-0.40]	[-0.38;-0.11]
	Sig.	0.28	0.56	0.64	0.52

Note: Sig. denotes proportion of countries for which the variable is statistically significant at 90% confidence level; q25-q75 shows the first and third quartiles of the estimated coefficients. Intercepts are omitted in the table. Standard errors are based on bootstrapping with 1000 replications. Sample: 1971Q1 to 2019Q4 for 25 countries.

2.5.2 Impact of US financial uncertainty (FUN) shocks on global markets

Global credit markets

Similar to Table 2.1, Table 2.3 summarizes the estimation results for credit growth as the dependent variable but this time bringing into play the US financial uncertainty index instead of the NFCI.

We observe that the impact of financial uncertainty on the lower quantiles of real credit growth is negative and higher in absolute value than on the central quantiles. However, the proportion of countries for which the effect is significant is similar across quantiles. These results hold when we control for global financial and macroeconomic factors. This time, the highest effects of financial uncertainty are recorded well in advance of $h = 4$. Indeed, the impact is quite similar across all forecasting horizons ($h = \{0, 1, 4\}$). Importantly, on $h = 4$, first moment financial shocks on credit growth (Table 2.1) exert an economically and statistically significant effect for a greater number of countries compared to other horizons. This is in accordance with first moment shocks associated with credit tightness and which consistently take more time to spillover to global markets, therefore supporting the credit view of the spread. As with NFCI, we can see that the impact of financial uncertainty in the US is very heterogeneous across countries, not only because it is a relevant predictor of negative credit dynamics for around 16-25% of our sample of countries but not for the rest, but also because these effects can be positive or negative. If we focus on the global factors, we observe that global factors impact credit creation around the world heterogeneously. In general, these covariates impact the average quantiles of credit growth of a higher number of countries than in the case of the negative tail. In addition, the effects of these global factors include a wide range of values, often showing high positive values even in the lowest quantiles.

Similar to Table 2.2, Table 2.4 summarizes the estimation results for stock returns as the dependent variable but using the US financial uncertainty index instead of the NFCI as our financial conditions indicator.

The results show that at horizons $h = 0$ and $h = 1$, the impact of financial uncertainty at the lower tail of the distribution of conditional stock returns is very high. At horizon $h = 4$, the effects of financial uncertainty are much less pronounced. This key result is observed even if we control for global financial and macroeconomic factors, as the percentage of countries for which the financial uncertainty coefficient is statistically significant goes from 60% ($\tau = 0.05$ quantile) to 76% ($\tau = 0.10$ quantile) out of 25 countries. This fast and strong response of global stock markets to US financial uncertainty is consistent with portfolio rebalancing by international

investors following an increase in US financial uncertainty, and thus, with the portfolio view of transmission.

As with NFCI, we observe that financial uncertainty impacts the lower quantiles of stock markets more frequently and significantly than the average quantiles, while the impact of global common factors (financial and macroeconomic) is higher on the average quantiles. Interestingly, we observe a less heterogeneous response across countries than in the case of NFCI. That is, financial uncertainty is a relevant predictor of stock price declines for a larger percentage of countries than NFCI, and, in addition (in all cases), the effect documented for the lowest quartiles ($\tau = 0.05$ and $\tau = 0.1$) is negative.

Overall, our results confirm that both first and second moment shocks to US financial conditions convey powerful signals on downside risks to funding markets. Our findings suggest that, like the vulnerable growth episodes documented in the previous literature, there is also vulnerable funding periods of a global scale, originating from financial fragility in the US. These results highlight the importance of funding for the transmission of recessionary shocks. In addition, our results emphasize the role of the portfolio view for the propagation of financial uncertainty (largely through the stock market), and of the credit view to understand the propagation of first moment financial conditions shocks (largely through the credit market). The two mechanisms are complementary and help to better understand the propagation of US financial conditions across global markets.

Table 2.3: Quantile regressions, Impact of Financial Uncertainty on real credit growth (CaR)

		$\tau = 0.05$	$\tau = 0.10$	$\tau = 0.20$	$\tau = 0.50$
Regressions for $h = 0$					
US financial uncertainty indicator					
FUN_t	q25-q75	[-0.23;0.05]	[-0.2;0.02]	[-0.13;0.02]	[-0.07;0.02]
	Sig.<0	0.14	0.20	0.25	0.23
US financial uncertainty indicator + Global factors					
FUN_t	q25-q75	[-0.29;0.02]	[-0.21;-0.02]	[-0.15;0.00]	[-0.1;0.05]
	Sig.<0	0.16	0.25	0.25	0.20
$GFIN_t$	q25-q75	[-0.15;0.57]	[0.07;0.54]	[0.05;0.61]	[0.17;0.64]
	Sig.	0.36	0.48	0.57	0.68
$GMACRO_t$	q25-q75	[-0.13;0.48]	[-0.09;0.52]	[0.00;0.62]	[0.10;0.67]
	Sig.	0.32	0.50	0.55	0.64
Regressions for $h = 1$					
US financial uncertainty indicator					
y_{it}	q25-q75	[0.00;0.25]	[-0.03;0.28]	[0.09;0.30]	[0.13;0.41]
	Sig.	0.30	0.39	0.64	0.73
FUN_t	q25-q75	[-0.22;0.04]	[-0.17;0.01]	[-0.1;0.00]	[-0.09;-0.02]
	Sig.<0	0.18	0.20	0.23	0.25
US financial uncertainty indicator + Global factors					
y_{it}	q25-q75	[-0.09;0.25]	[-0.01;0.26]	[0.05;0.27]	[0.09;0.36]
	Sig.	0.30	0.43	0.57	0.73
FUN_t	q25-q75	[-0.22;0.06]	[-0.14;0.04]	[-0.12;0.00]	[-0.07;0.03]
	Sig.<0	0.16	0.18	0.23	0.14
$GFIN_t$	q25-q75	[-0.31;0.21]	[-0.33;0.16]	[-0.14;0.23]	[0.01;0.29]
	Sig.	0.27	0.25	0.34	0.30
$GMACRO_t$	q25-q75	[-0.21;0.28]	[-0.23;0.25]	[-0.18;0.27]	[0.07;0.31]
	Sig.	0.25	0.27	0.39	0.34
Regressions for $h = 4$					
US financial uncertainty indicator					
y_{it}	q25-q75	[0.22;0.57]	[0.24;0.55]	[0.29;0.57]	[0.34;0.61]
	Sig.	0.61	0.70	0.89	0.98
FUN_t	q25-q75	[-0.23;0.03]	[-0.17;0.01]	[-0.11;-0.01]	[-0.1;0]
	Sig.<0	0.18	0.23	0.18	0.23
US financial uncertainty indicator + Global factors					
y_{it}	q25-q75	[0.21;0.56]	[0.26;0.56]	[0.31;0.57]	[0.33;0.58]
	Sig.	0.59	0.75	0.89	0.98
FUN_t	q25-q75	[-0.24;-0.02]	[-0.20;0.01]	[-0.13;-0.03]	[-0.09;0.01]
	Sig.<0	0.18	0.23	0.20	0.18
$GFIN_t$	q25-q75	[-0.38;0.20]	[-0.26;0.25]	[-0.15;0.19]	[0.02;0.18]
	Sig.	0.27	0.20	0.27	0.23
$GMACRO_t$	q25-q75	[-0.44;0.12]	[-0.30;0.18]	[-0.19;0.14]	[0.02;0.21]
	Sig.	0.32	0.30	0.18	0.25

Note: Sig. denotes proportion of countries for which the variable is statistically significant at 90% confidence level; q25-q75 shows the first and third quartiles of the estimated coefficients. Intercepts are omitted in the table. Standard errors are based on bootstrapping with 1000 replications. Sample: 1971Q1 to 2019Q4 for 44 countries, except for Bolivia (to 2019Q3), Iceland (to 2018Q4) and Taiwan (to 2018Q4).

Table 2.4: Quantile regressions, Impact of Financial Uncertainty on stock markets (EaR)

		$\tau = 0.05$	$\tau = 0.10$	$\tau = 0.20$	$\tau = 0.50$
Regressions for $h = 0$					
US financial uncertainty indicator					
FUN_t	q25-q75	[-0.64;-0.36]	[-0.57;-0.30]	[-0.44;-0.23]	[-0.27;-0.16]
	Sig.<0	0.88	0.88	0.92	0.88
US financial uncertainty indicator + Global factors					
FUN_t	q25-q75	[-0.31;-0.04]	[-0.22;-0.02]	[-0.13;-0.03]	[-0.05;0.01]
	Sig.<0	0.48	0.48	0.32	0.12
$GFIN_t$	q25-q75	[-0.89;-0.17]	[-0.84;-0.29]	[-0.80;-0.38]	[-0.66;-0.32]
	Sig.	0.56	0.68	0.88	0.88
$GMACRO_t$	q25-q75	[-0.21;0.36]	[-0.15;0.24]	[-0.16;0.17]	[0.00;0.23]
	Sig.	0.28	0.28	0.36	0.4
Regressions for $h = 1$					
US financial uncertainty indicator					
y_{it}	q25-q75	[0.09;0.45]	[0.11;0.37]	[0.18;0.33]	[0.23;0.34]
	Sig.	0.52	0.56	0.72	0.96
FUN_t	q25-q75	[-0.58;-0.33]	[-0.42;-0.26]	[-0.25;-0.12]	[-0.13;-0.02]
	Sig.<0	0.88	0.76	0.56	0.24
US financial uncertainty indicator + Global factors					
y_{it}	q25-q75	[-0.02;0.36]	[-0.04;0.38]	[0.11;0.33]	[0.21;0.39]
	Sig.	0.32	0.32	0.60	0.72
FUN_t	q25-q75	[-0.64;-0.26]	[-0.46;-0.21]	[-0.27;-0.12]	[-0.11;-0.03]
	Sig.<0	0.6	0.76	0.6	0.24
$GFIN_t$	q25-q75	[-0.27;0.28]	[-0.27;0.18]	[-0.24;0.02]	[-0.24;-0.02]
	Sig.	0.20	0.20	0.16	0.12
$GMACRO_t$	q25-q75	[-0.19;0.37]	[-0.18;0.13]	[-0.25;0.04]	[-0.18;-0.08]
	Sig.	0.20	0.04	0.08	0.16
Regressions for $h = 4$					
US financial uncertainty indicator					
y_{it}	q25-q75	[-0.16;0.21]	[-0.05;0.12]	[-0.03;0.05]	[-0.07;0.06]
	Sig.	0.04	0.08	0.12	0.12
FUN_t	q25-q75	[-0.29;-0.09]	[-0.22;-0.08]	[-0.13;0]	[-0.04;0.04]
	Sig.<0	0.12	0.08	0.16	0.04
US financial uncertainty indicator + Global factors					
y_{it}	q25-q75	[-0.18;0.16]	[-0.15;0.15]	[-0.11;0.06]	[-0.12;0.09]
	Sig.	0.04	0.12	0.08	0.16
FUN_t	q25-q75	[-0.27;-0.07]	[-0.19;-0.04]	[-0.11;-0.04]	[-0.08;0.00]
	Sig.<0	0.08	0.12	0.12	0.04
$GFIN_t$	q25-q75	[-0.48;-0.02]	[-0.50;-0.11]	[-0.42;-0.17]	[-0.40;-0.11]
	Sig.	0.12	0.16	0.52	0.64
$GMACRO_t$	q25-q75	[-0.56;-0.09]	[-0.55;-0.08]	[-0.49;-0.22]	[-0.37;-0.25]
	Sig.	0.20	0.36	0.60	0.72

Note: Sig. denotes proportion of countries for which the variable is statistically significant at 90% confidence level; q25-q75 shows the first and third quartiles of the estimated coefficients. Intercepts are omitted in the table. Standard errors are based on bootstrapping with 1000 replications. Sample: 1971Q1 to 2019Q4 for 25 countries.

2.5.3 Cross-country heterogeneity

Graphical analysis

To examine which is the most likely reason for a given country's vulnerability to changes in US financial conditions, first, we relate the size of each country's credit and stock market responses to two classical determinants of the international spread of financial shocks, namely, the size of credit (stock) markets, and the relative importance of US foreign investment for each country. We measure the size of credit markets by the annual average of the credit to GDP ratio for each country, the size of stock markets by the annual average of the market capitalization to GDP ratio and, financial interconnection by the total direct investment of the US as a percentage of the country's GDP. To this end, we calculate, for each country, the maximum value of US investment inflows relative to its GDP.[12]

In both cases, credit and stock markets, we show the results for the horizon and the ordering measure that provides the clearest pattern. This translates into showing the results for horizon $h = 0$ and sorting the countries by the size or depth of the market in the case of credit markets and by their financial closeness to the US in the case of stock markets.[13]

Figure 2.2 shows the impact of NFCI over the entire distribution of credit growth of the countries in the sample (for forecasting horizon $h = 0$), ordered according to their credit to GDP ratio. Interestingly, we find that there is a cluster in the lower left-hand corner of the heat map, suggesting that the economies with lower credit to GDP ratios are more sensitive to a first moment shock to US financial conditions and that the response is stronger in the left tail (lower quantiles) of the distribution. However, the response of economies with higher credit to GDP ratios is much weaker, or inexistent. That is, the smaller the credit market, the more likely that country will experience vulnerable funding episodes. In turn, credit market size is associated with market development, which suggests an asymmetric impact of first moment shocks of financial conditions on emerging and advanced economies. This result implies that when we focus on shocks to the first moment of the financial conditions, vulnerable funding is clearly associated with the size or depth of a country's credit market. This is consistent with the view advanced, for instance, by Alfaro et al. (2004) and Kalemli-Özcan (2019).

Figure 2.3 shows the impact of the NFCI over the entire distribution of stock returns (for forecasting horizon $h = 0$) of the countries in the sample ordered by their degree of financial interconnection with the US. We find a cluster in the upper left-hand corner of the heat maps, suggesting that the sensitivity of the effect of the

[12] The results are robust when we use the average instead of the maximum value.
[13] Results for horizons $h = 1$ and $h = 4$ are available upon request.

Figure 2.2: Impact of the NFCI over the distribution of real credit growth

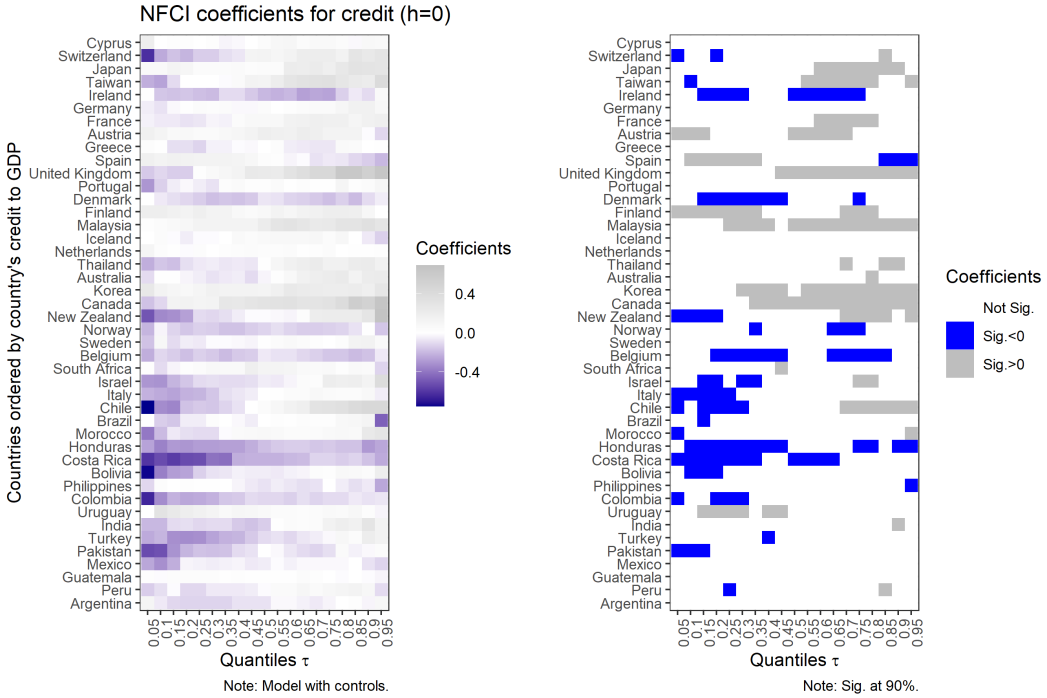

Note: The left-hand panel shows the NFCI coefficients for $\tau = 0.05 - 0.95$ in 0.05 intervals, for all 44 countries. The right-hand panel presents the statistical significance of the NFCI coefficients as well as the sign of the estimated coefficient. The blue (grey)-shaded areas are defined as being negatively (positively) statistically significant at the 90 % level of confidence, whereas the white-shaded area corresponds to insignificant coefficients associated with the NFCI.

NFCI in the lower part of the distribution of stock returns is related to the relative importance of US investment for a given country. This suggests that stock markets of economies that share stronger financial links with the US are more severely affected by a tightening in US financial conditions than economies with weaker financial ties with the US.

Interestingly, most of the countries showing larger stock market responses to first moment shocks in US financial conditions are developed markets. It seems that the relative importance of US foreign flows to a country does determine to a great extent how domestic share values will react following a deterioration of US financial conditions, and indeed in general, how these values react to global financial factors. While FDI flows are more volatile for emerging countries, as past literature has documented, the stock markets of advanced economies, such as Ireland, Switzerland, the Netherlands, Canada and the United Kingdom (which are the five top receivers of direct US foreign investment), are also among the countries most affected in our sample by a deterioration in US financial conditions. This can be observed by

Figure 2.3: Impact of NFCI over the distribution of current stock returns

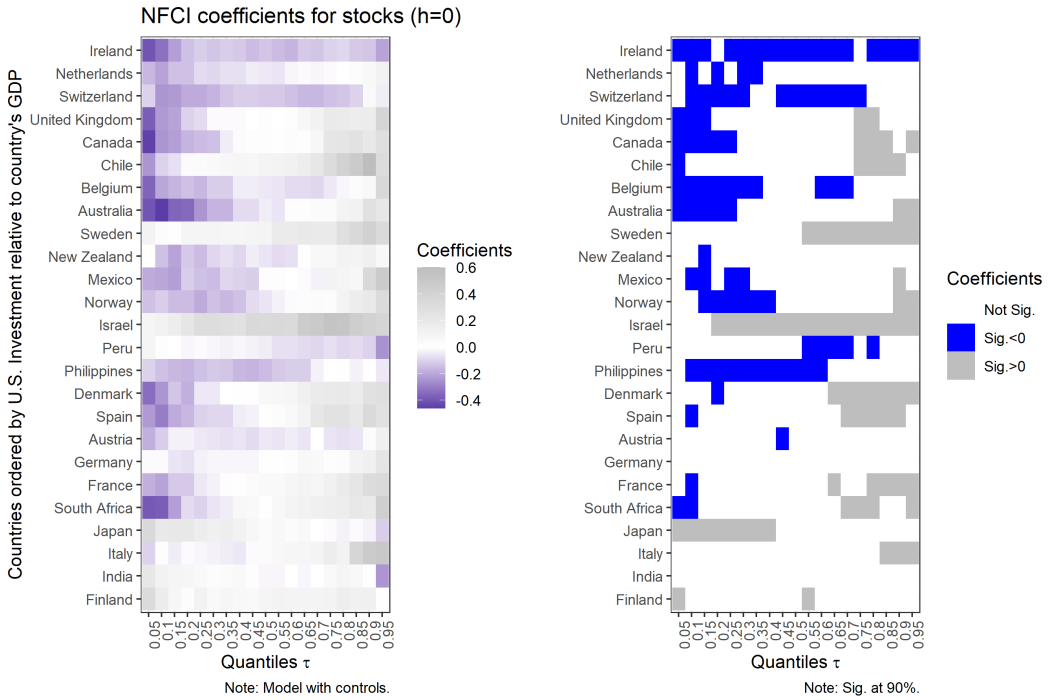

Note: The left-hand panel shows the NFCI coefficients for $\tau = 0.05 - 0.95$ in 0.05 intervals, for all 25 countries. The right-hand panel presents the statistical significance of the NFCI coefficients as well as the sign of the estimated coefficient. The blue (grey)-shaded areas are defined as being negatively (positively) statistically significant at the 90 % level of confidence, whereas the white-shaded area corresponds to insignificant coefficients associated with the NFCI.

looking at the significance of the estimated effects for the five countries (right-hand side plot) as well as the darker color in the heat map associated with the quantile slope that measures the effect of NFCI in each market (left hand side plot) of Figure 2.3. Thus, the depth and liquidity of the local stock market may prevent the impact of the external shock on the real economy from being dramatic; however, in any case, the local funding opportunities reduce the impact of the deterioration of US financial conditions, as expected. These results show the vulnerability of local financial markets to external imbalances and credit restrictions, given the high degree of interconnectedness of current global finance.

Figure 2.4 shows the impact of US financial uncertainty over the entire distribution of credit growth (for forecasting horizon $h = 0$) of the countries in the sample, ordered according to size or depth of the market. As with first moment shocks to US financial conditions, we observe that the size or depth of the credit markets is important for explaining credit vulnerability to financial uncertainty and that most of the countries showing higher responses are emerging market economies. Again,

the smaller the size of the credit market, the more likely a country will experience vulnerable funding episodes. This result is consistent with Carrière-Swallow and Céspedes (2013) who find that in comparison with the US and other developed countries, emerging economies suffer much more severe falls in investment and private consumption following an exogenous uncertainty shock. Bhattacharya et al. (2019) also document that unanticipated changes in US uncertainty have significant effects on emerging market economies.

We also find that, although in general the effect is more negative in the lower quantiles than in the central ones, the proportion of countries for which the effect is significant is relatively similar across the entire distribution.

Figure 2.4: Impact of the Financial Uncertainty index over the distribution of real credit growth

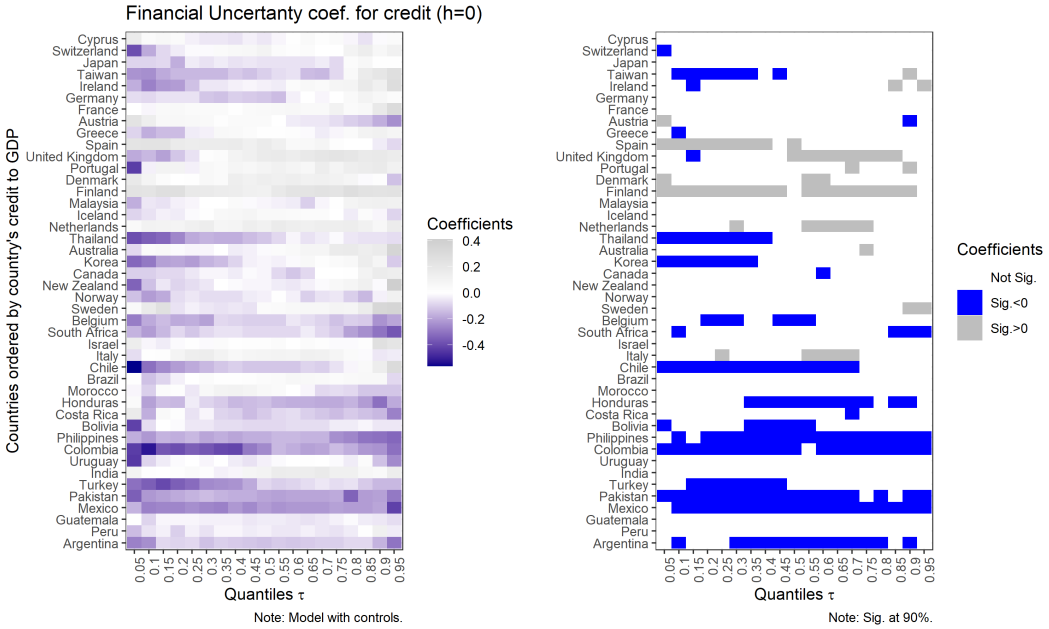

Note: The left-hand panel shows the financial uncertainty coefficients for $\tau = 0.05 - 0.95$ in 0.05 intervals, for all 44 countries. The right-hand panel presents the statistical significance of the financial uncertainty coefficients as well as the sign of the estimated coefficient. The blue (grey)-shaded areas are defined as being negatively (positively) statistically significant at the 90% level of confidence, whereas the white-shaded area corresponds to insignificant coefficients associated with the financial uncertainty index.

Finally, Figure 2.5 shows the impact of US financial uncertainty over the entire distribution of the stock return (for forecasting horizon $h = 0$) of the countries in the sample, ordered according to the strength of their financial links with the US. Now, we observe graphically that the impact of financial uncertainty at the left tail of the conditional distribution of stock returns is very large for a high percentage of coun-

tries. As with first moment shocks, we find a cluster in the upper left-hand corner of the heat map, suggesting that the sensitivity of the effect of financial uncertainty on the lower part of the distribution of stock returns is related to the degree of US investment abroad. Again, the stock markets of advanced economies are among the countries most affected in our sample after a shock to financial uncertainty in the US.

Overall, we find that the heterogeneous dynamic of Credit at Risk episodes is better explained by the size or depth of the credit market, while in the case of Equity at Risk episodes, heterogeneity is more related to the financial interconnections with the US. This result holds for both first moment shocks and financial uncertainty shocks.

Figure 2.5: Impact of the Financial Uncertainty index over the distribution of current stock returns

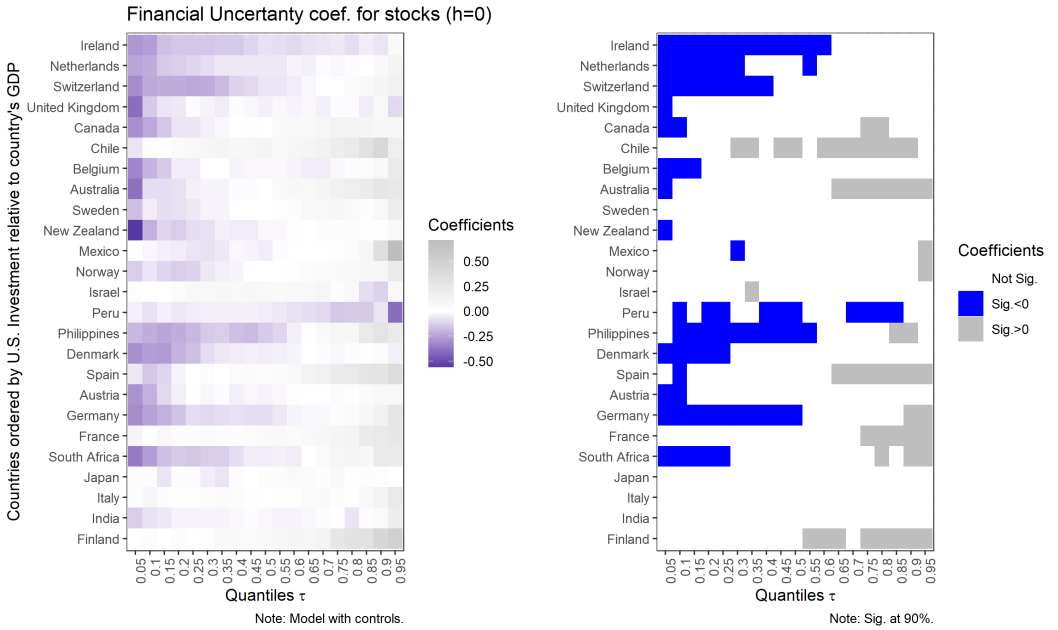

Note: The left-hand panel shows the financial uncertainty coefficients for $\tau = 0.05 - 0.95$ in 0.05 intervals, for all 25 countries. The right-hand panel presents the statistical significance of the financial uncertainty coefficients as well as the sign of the estimated coefficient. The blue (grey)-shaded areas are defined as being negatively (positively) statistically significant at the 90% level of confidence, whereas the white-shaded area corresponds to insignificant coefficients associated with the financial uncertainty index.

Cross-sectional analysis

In this subsection we present the results of our exploratory regressions that measure the association between financial vulnerability and the two classical determinants

of the international spreading of financial shocks. We used as our right-hand-side variable the slope coefficients of CaR and EaR at various quantiles, and as left-hand-side variables both the ratio of US direct investment to the GDP of each country and the ratio of credit (market capitalization) to GDP of each country. We estimate these latter variables using the average of the yearly indicators across the sample period (1960Q1- 2019Q4) and using the annual maximum across the sample (to emphasize the most extreme scenarios). Table 2.5 to 2.8 present the results using the maxima version, which are virtually the same as using the averages (which are available upon request). Table 2.5 and 2.6 focus on the credit market and Table 2.7 and 2.8 on the stock market.

Table 2.5: Cross-sectional determinants of vulnerable credit (first moment shock)

	$\tau = 0.05$	$\tau = 0.10$	$\tau = 0.20$	$\tau = 0.50$	$\tau = 0.80$	$\tau = 0.90$	$\tau = 0.95$
				Regressions for $h = 0$			
US inv./GDP (%)	0.000200	-0.000584	-0.000856	-0.00101	-0.00118*	-0.000904	0.000164
	(0.00104)	(0.000800)	(0.000615)	(0.000776)	(0.000675)	(0.000715)	(0.000798)
Credit/GDP (%)	**0.00249****	**0.00175****	**0.00144****	**0.00138*****	0.00124*	0.00120*	0.00172*
	(0.00109)	(0.000777)	(0.000584)	(0.000445)	(0.000656)	(0.000679)	(0.000911)
Constant	-0.317***	-0.213***	-0.158***	-0.0596*	0.0301	0.0330	-0.0210
	(0.0813)	(0.0615)	(0.0472)	(0.0297)	(0.0412)	(0.0493)	(0.0665)
				Regressions for $h = 1$			
US inv./GDP (%)	-0.000358	-0.000884	-0.00125	**-0.000886*****	-0.000679*	-0.000343	-0.000486
	(0.000936)	(0.00112)	(0.00108)	(0.000267)	(0.000361)	(0.000879)	(0.000866)
Credit/GDP (%)	0.00193*	0.00111	0.000585	0.000496	**0.000961****	0.000534	0.00121
	(0.00102)	(0.000662)	(0.000462)	(0.000468)	(0.000431)	(0.000541)	(0.000939)
Constant	-0.280***	-0.196***	-0.126***	-0.0183	0.0192	0.0907**	0.0722
	(0.0813)	(0.0527)	(0.0304)	(0.0260)	(0.0287)	(0.0382)	(0.0625)
				Regressions for $h = 4$			
US inv./GDP (%)	-0.00284	-0.00236	-0.00161*	**-0.00198*****	-0.000739	-0.00132	-0.00135
	(0.00218)	(0.00149)	(0.000853)	(0.000429)	(0.000771)	(0.00145)	(0.00108)
Credit/GDP (%)	**0.00244****	0.000960	-0.000108	**0.000800****	0.000561	-0.000139	-0.000281
	(0.00114)	(0.000755)	(0.000443)	(0.000309)	(0.000465)	(0.000621)	(0.00100)
Constant	-0.303***	-0.201***	-0.0792**	-0.0429*	0.0420	0.142***	0.160**
	(0.0935)	(0.0661)	(0.0376)	(0.0239)	(0.0281)	(0.0444)	(0.0630)
N	44	44	44	44	44	44	44

Note: Robust standard errors in parentheses $^{*}p < 0.10, ^{**}p < 0.05, ^{***}p < 0.01$.

From a general reading of Table 2.5 when $h = 0$, we see that market size significantly explains the transmission of NFCI shocks. The effect is that expected according to the theory and is in agreement with previous studies, namely, the larger the market the lower the negative effect of US financial conditions on that market. When $h = 1$ and $h = 4$, market size loses its significance in most of the cases as it only remains significant at the lowest quantiles (0.05) and the median of the distribution. Financial closeness to the US helps to explain the central quantiles when $h = 1$ $(\tau = 0.8)$ and $h = 4$ $(\tau = 0.5)$ but not the vulnerable funding episodes associated with the lowest quantiles. The same narrative can be seen in Table 2.6,

namely market size helps to explain the propagation of financial uncertainty across the world credit markets when $h = 0$, while at other horizons and especially for the lowest quantiles the explanation escapes from these two traditional determinants.

Table 2.6: Cross-sectional determinants of vulnerable credit (second moment shock)

	$\tau = 0.05$	$\tau = 0.10$	$\tau = 0.20$	$\tau = 0.50$	$\tau = 0.80$	$\tau = 0.90$	$\tau = 0.95$
				Regressions for $h = 0$			
US inv./GDP (%)	-0.000269	-0.000502	-0.000436	0.000299	0.000801*	0.000584*	0.00170***
	(0.000905)	(0.00123)	(0.000972)	(0.000582)	(0.000430)	(0.000324)	(0.000410)
Credit/GDP (%)	0.00138	0.00146**	0.000987**	0.000936*	0.00140**	0.00178**	0.00242**
	(0.000837)	(0.000549)	(0.000487)	(0.000536)	(0.000642)	(0.000797)	(0.000962)
Constant	-0.206***	-0.193***	-0.124***	-0.0844**	-0.104**	-0.118**	-0.177***
	(0.0601)	(0.0390)	(0.0362)	(0.0341)	(0.0423)	(0.0524)	(0.0643)
				Regressions for $h = 1$			
US inv./GDP (%)	-0.00177	-0.000651	-0.000769	0.0000613	0.000471*	0.000766**	0.000461
	(0.00183)	(0.000984)	(0.000751)	(0.000478)	(0.000267)	(0.000347)	(0.00139)
Credit/GDP (%)	-0.000280	0.000302	0.000504	0.000586	0.000659	0.00110	0.00250*
	(0.000923)	(0.000491)	(0.000419)	(0.000401)	(0.000538)	(0.000714)	(0.00127)
Constant	-0.0672	-0.0713*	-0.0756**	-0.0572*	-0.0366	-0.0585	-0.148**
	(0.0841)	(0.0398)	(0.0353)	(0.0293)	(0.0341)	(0.0487)	(0.0724)
				Regressions for $h = 4$			
US inv./GDP (%)	-0.000462	-0.00135	-0.00109**	-0.00110***	0.000539*	0.000190	0.000662
	(0.00141)	(0.000864)	(0.000507)	(0.000380)	(0.000294)	(0.000447)	(0.000554)
Credit/GDP (%)	0.00103	-0.000441	-0.000644**	0.000369	0.000225	0.000322	0.0000929
	(0.000758)	(0.000510)	(0.000258)	(0.000285)	(0.000615)	(0.000780)	(0.00118)
Constant	-0.192***	-0.0627*	-0.0249	-0.0482**	-0.00561	0.0371	0.0458
	(0.0501)	(0.0353)	(0.0186)	(0.0180)	(0.0342)	(0.0466)	(0.0801)
N	44	44	44	44	44	44	44

Note: Robust standard errors in parentheses $^{*}p < 0.10, ^{**}p < 0.05, ^{***}p < 0.01$.

When we turn our attention to the stock markets, a different landscape emerges. In Table 2.7 we can observe that when $h = 0$ the relative size of US investment (market closeness to the US) significantly explains the transmission of NFCI shocks. The effect is that expected according to the theory: the markets closest to the US (i.e. those that have a larger relative reception of US annual investment as a percentage of local GDP) are the most affected (independently of the size of the market), which can be rationalized with the portfolio view operating on the global transmission of US financial conditions. This time the size of the market does not offer explanatory power for the vulnerable funding episodes (or even for the transmission in the highest quantiles).

When we move from $h = 0$ to $h = 1$ and $h = 4$, financial closeness keeps its explanatory power for the central quantiles but not for the lowest. Moreover, for

the central cases the market size gains some statistical power, which nevertheless is accompanied by a negative sign, meaning that advanced economies are more susceptible to receiving shocks from the US than emerging economies. A very similar panorama arises when we move to the last table of our estimations (Table 2.8). This table focuses on the effect of second moment shocks (financial uncertainty) on the stock markets. Again it is financial closeness instead of market size which offers significant explanatory power of vulnerable funding episodes. The size of the stock market only matters four quarters after the shock has occurred. Our cross-sectional regressions tell us that market size and financial closeness to the US explain vulnerable funding episodes, at least contemporaneously. Nevertheless, the explanation depends on the market. Credit markets react according to market size, while stock markets react according to financial closeness. There are no notable differences in this case between the explanatory power of the first and second moment shocks of these two variables.

Table 2.7: Cross-sectional determinants of vulnerable equity (first moment shock)

	$\tau = 0.05$	$\tau = 0.10$	$\tau = 0.20$	$\tau = 0.50$	$\tau = 0.80$	$\tau = 0.90$	$\tau = 0.95$
				Regressions for $h = 0$			
US inv./GDP (%)	-0.00206**	-0.00172***	-0.000933**	-0.00102***	-0.00154***	-0.00205***	-0.00208*
	(0.000889)	(0.000542)	(0.000361)	(0.000255)	(0.000337)	(0.000592)	(0.00107)
Market Cap./GDP (%)	-0.00124	-0.00129*	-0.000317	-0.000117	0.000412	0.000103	0.000128
	(0.00106)	(0.000713)	(0.000415)	(0.000366)	(0.000887)	(0.000773)	(0.00121)
Constant	-0.00952	-0.0128	-0.0351	0.0324	0.117*	0.217***	0.216**
	(0.0766)	(0.0554)	(0.0395)	(0.0360)	(0.0647)	(0.0650)	(0.0906)
				Regressions for $h = 1$			
US inv./GDP (%)	-0.000509	-0.0000444	-0.000627**	-0.000906***	-0.000740**	-0.0000370	0.000994
	(0.000816)	(0.000462)	(0.000225)	(0.000246)	(0.000342)	(0.000395)	(0.00106)
Market Cap./GDP (%)	-0.00144	-0.000531	-0.000890**	-0.0000682	0.00182*	0.00275***	0.00237***
	(0.00119)	(0.000933)	(0.000424)	(0.000437)	(0.000888)	(0.000791)	(0.000772)
Constant	-0.0116	-0.0382	-0.00695	-0.00529	-0.0441	-0.0617	-0.0108
	(0.1000)	(0.0714)	(0.0371)	(0.0354)	(0.0579)	(0.0676)	(0.0705)
				Regressions for $h = 4$			
US inv./GDP (%)	-0.000400	-0.000130	-0.00130***	-0.000229	-0.000937**	-0.0000656	-0.000329
	(0.00177)	(0.000544)	(0.000434)	(0.000495)	(0.000375)	(0.000623)	(0.000711)
Market Cap./GDP (%)	-0.00199	-0.00240**	-0.00145**	-0.000563	0.0000627	0.00117	0.000862
	(0.00127)	(0.000895)	(0.000611)	(0.000483)	(0.000817)	(0.00118)	(0.00114)
Constant	0.178	0.167*	0.122**	0.0469	0.0791	0.0915	0.205**
	(0.109)	(0.0869)	(0.0533)	(0.0516)	(0.0725)	(0.0748)	(0.0850)
N	25	25	25	25	25	25	25

Note: Robust standard errors in parentheses $^{*}p < 0.10, ^{**}p < 0.05, ^{***}p < 0.01$.

Table 2.8: Cross-sectional determinants of vulnerable equity (second moment shock)

	$\tau = 0.05$	$\tau = 0.10$	$\tau = 0.20$	$\tau = 0.50$	$\tau = 0.80$	$\tau = 0.90$	$\tau = 0.95$
Regressions for $h = 0$							
US inv./GDP (%)	-0.00109**	-0.00124***	-0.000714***	-0.000578***	-0.00108***	-0.00147***	-0.00102**
	(0.000431)	(0.000277)	(0.000191)	(0.000140)	(0.000294)	(0.000414)	(0.000486)
Market Cap./GDP (%)	-0.00103	-0.000489	-0.000257	0.0000940	0.000817**	0.000897	-0.000184
	(0.000684)	(0.000605)	(0.000444)	(0.000326)	(0.000373)	(0.000591)	(0.00102)
Constant	-0.107	-0.0684	-0.0467	-0.00853	0.0265	0.105*	0.201*
	(0.0678)	(0.0489)	(0.0331)	(0.0223)	(0.0326)	(0.0547)	(0.104)
Regressions for $h = 1$							
US inv./GDP (%)	-0.00316**	-0.00142***	-0.000857*	-0.000213	-0.000283	0.000396	0.0000253
	(0.00130)	(0.000404)	(0.000437)	(0.000176)	(0.000185)	(0.000346)	(0.000389)
Market Cap./GDP (%)	-0.00195*	-0.000895	-0.000746*	-0.000278	0.000753*	0.00162***	0.00126
	(0.00100)	(0.000730)	(0.000389)	(0.000397)	(0.000379)	(0.000528)	(0.000753)
Constant	-0.271***	-0.248***	-0.124***	-0.0477*	-0.0195	-0.0333	0.0816
	(0.0795)	(0.0590)	(0.0367)	(0.0264)	(0.0285)	(0.0360)	(0.0595)
Regressions for $h = 4$							
US inv./GDP (%)	0.000271	0.000310	-0.000418*	-0.000448	-0.000262	-0.000353	0.000387
	(0.000509)	(0.000283)	(0.000202)	(0.000327)	(0.000412)	(0.000330)	(0.000549)
Market Cap./GDP (%)	-0.00212***	-0.00166**	-0.000471	-0.000232	0.000436	0.00112	0.00136
	(0.000677)	(0.000681)	(0.000495)	(0.000299)	(0.000448)	(0.000904)	(0.00114)
Constant	-0.0346	-0.0297	-0.0368	-0.00249	0.00279	0.00531	0.0163
	(0.0715)	(0.0456)	(0.0339)	(0.0253)	(0.0334)	(0.0565)	(0.0632)
N	25	25	25	25	25	25	25

Note: Robust standard errors in parentheses $^{*}p < 0.10, ^{**}p < 0.05, ^{***}p < 0.01$.

2.6 Conclusions

We systematically document vulnerable funding episodes in the world economy. That is, financial conditions in the United States have significant predictive power in the lowest quantiles of credit growth and stock market prices around the global economy. However, the established effects are very heterogeneous in several dimensions. Vulnerable funding depends on the country, the funding market, i.e., credit or stock, and the type of shock, i.e., mean-shock to financial conditions or second-moment uncertainty shock. We also show that vulnerable funding can be explained, mainly contemporaneously, by the relative market size in the case of credit markets and by the financial links with the US (measured by the total direct investment of the US as a percentage of the country's GDP) in the case of the stock market.

Our methodological approach uses quantile regressions, following the emphasis of the Growth at Risk literature, which allows us to examine the impact of US financial conditions on the entire conditional distribution of credit and stock market prices around the world, and hence to document the asymmetric impacts summarized above. We complement our model specification with global economic and

financial factors that we construct using a rich data set that comprises more than 40 countries, in most cases with information spanning almost six decades. Our results are robust to including both a global macroeconomic factor and a global financial factor.

The impact of US financial conditions on global stock markets is immediate, so that the strongest effects are observed in the same period when the shock occurs. This reduces the possibility of using the indicator of US financial conditions as a measure of future market performance, or as an early warning indicator foreseeing future limited funding by corporations. The opposite occurs in the case of credit markets, the larger effects are observed, according to our results, one year after the shock occurs. This means that US financial conditions may serve as a predicting variable of future vulnerability of domestic credit markets. These two effects put together emphasize the importance of funding for the transmission of recessionary shocks throughout the global economy, as well as the need to monitor funding variables and their relationship with global financial shocks in financial stability exercises conducted by central banks and regulators around the world on a regular basis.

The policy implications of our results are clear. We show that international funding markets are a source of persistence and amplification of financial conditions shocks across the global economy. This means that a deterioration of US financial conditions calls for policy actions in other economies around the world. For instance, an increase in market uncertainty that is associated with lower global liquidity and credit availability might worsen the fall in investment (and slow down the economic recovery) observed after an international shock to US financial conditions. Under these scenarios it may be determinant, on the part of domestic fiscal and monetary authorities, to foster internal demand by reducing the cost of financing and providing liquidity to companies that look to invest once uncertainty has returned to its normal levels. We show that this line of reasoning is more general than the previous literature has indicated, because the deterioration of funding opportunities, either via credit or the stock market, is observed in all types of economies regardless of the size of their financial markets. Indeed, such differentiation does not matter at all for stock markets, and although it is important for credit markets, in the sense that larger markets are less prone to vulnerable funding episodes than smaller markets, according to our estimation results, vulnerable funding is also a concern for developed economies.

2.A Appendix A

Table 2.A1: Availability of information for each country and variable in Monnet and Puy (2019) macro-financial dataset

Country	Variable	Start	End	T
Argentina	CPI	1950 Q1	2019 Q4	280
Argentina	Real credit	1950 Q1	2019 Q4	280
Argentina	Real GDP	1957 Q1	2019 Q4	252
Australia	CPI	1950 Q1	2019 Q4	280
Australia	Real credit	1950 Q1	2019 Q4	280
Australia	Real GDP	1957 Q1	2019 Q4	252
Australia	Nominal stock prices	1950 Q1	2019 Q4	280
Australia	Bond Yield	1955 Q1	2019 Q4	260
Austria	CPI	1950 Q1	2019 Q4	280
Austria	Real credit	1950 Q1	2019 Q4	280
Austria	Real GDP	1950 Q1	2019 Q4	280
Austria	Nominal stock prices	1950 Q1	2019 Q4	280
Belgium	CPI	1950 Q1	2019 Q4	280
Belgium	Real credit	1950 Q4	2019 Q4	277
Belgium	Real GDP	1950 Q1	2019 Q4	280
Belgium	Nominal stock prices	1951 Q1	2019 Q4	276
Belgium	Bond Yield	1957 Q1	2017 Q4	244
Bolivia	CPI	1950 Q4	2019 Q4	277
Bolivia	Real credit	1950 Q4	2019 Q3	276
Brazil	CPI	1950 Q4	2019 Q4	277
Brazil	Real credit	1950 Q4	2019 Q4	277
Brazil	Real GDP	1957 Q1	2019 Q4	252
Canada	CPI	1950 Q1	2019 Q4	280
Canada	Real credit	1950 Q1	2019 Q4	280
Canada	Real GDP	1950 Q1	2019 Q4	280
Canada	Nominal stock prices	1950 Q1	2019 Q4	280
Canada	Bond Yield	1950 Q1	2017 Q2	270
Chile	CPI	1950 Q1	2019 Q4	280
Chile	Real credit	1950 Q4	2019 Q4	277
Chile	Real GDP	1950 Q1	2019 Q4	280
Chile	Nominal stock prices	1953 Q1	2019 Q4	268
Colombia	CPI	1952 Q4	2019 Q4	269

Colombia	Real credit	1952 Q4	2019 Q4	269
Costa Rica	CPI	1950 Q4	2019 Q4	277
Costa Rica	Real credit	1950 Q4	2019 Q4	277
Cyprus	CPI	1957 Q1	2019 Q4	252
Cyprus	Real credit	1958 Q1	2019 Q4	248
Denmark	CPI	1950 Q1	2019 Q4	280
Denmark	Real credit	1950 Q1	2019 Q4	280
Denmark	Real GDP	1950 Q1	2019 Q4	280
Denmark	Nominal stock prices	1950 Q1	2019 Q4	280
Denmark	Bond Yield	1955 Q1	2019 Q4	260
El Salvador	CPI	1957 Q1	2019 Q4	252
Finland	CPI	1950 Q1	2019 Q4	280
Finland	Real credit	1950 Q4	2019 Q4	277
Finland	Real GDP	1950 Q1	2019 Q4	280
Finland	Nominal stock prices	1951 Q1	2019 Q4	276
France	CPI	1950 Q1	2019 Q4	280
France	Real credit	1950 Q1	2019 Q4	280
France	Real GDP	1950 Q1	2019 Q4	280
France	Nominal stock prices	1950 Q1	2019 Q4	280
France	Bond Yield	1955 Q1	2017 Q2	250
Germany	CPI	1950 Q1	2019 Q4	280
Germany	Real credit	1950 Q1	2019 Q4	280
Germany	Real GDP	1950 Q1	2019 Q4	280
Germany	Nominal stock prices	1953 Q1	2019 Q4	268
Germany	Bond Yield	1957 Q1	2017 Q2	242
Greece	CPI	1950 Q1	2019 Q4	280
Greece	Real credit	1953 Q4	2019 Q4	265
Greece	Real GDP	1950 Q2	2019 Q4	279
Guatemala	CPI	1950 Q1	2019 Q4	280
Guatemala	Real credit	1950 Q4	2019 Q4	277
Honduras	CPI	1950 Q4	2019 Q4	277
Honduras	Real credit	1950 Q4	2019 Q4	277
Iceland	CPI	1955 Q1	2019 Q4	260
Iceland	Real credit	1955 Q1	2018 Q4	256
Iceland	Real GDP	1957 Q2	2019 Q4	251
India	CPI	1950 Q1	2019 Q4	280
India	Real credit	1950 Q1	2019 Q4	280
India	Real GDP	1950 Q1	2019 Q4	280
India	Nominal stock prices	1950 Q1	2019 Q4	280

Ireland	CPI	1950 Q1	2019 Q4	280
Ireland	Real credit	1950 Q1	2019 Q4	280
Ireland	Real GDP	1950 Q1	2019 Q4	280
Ireland	Nominal stock prices	1955 Q1	2019 Q4	260
Ireland	Bond Yield	1957 Q1	2017 Q2	242
Israel	CPI	1951 Q4	2019 Q4	273
Israel	Real credit	1951 Q4	2019 Q4	273
Israel	Real GDP	1957 Q1	2019 Q4	252
Israel	Nominal stock prices	1955 Q1	2019 Q4	260
Italy	CPI	1950 Q1	2019 Q4	280
Italy	Real credit	1950 Q1	2019 Q4	280
Italy	Real GDP	1950 Q1	2019 Q4	280
Italy	Nominal stock prices	1950 Q1	2019 Q4	280
Italy	Bond Yield	1955 Q1	2019 Q4	260
Japan	CPI	1950 Q1	2019 Q4	280
Japan	Real credit	1950 Q1	2019 Q4	280
Japan	Real GDP	1950 Q1	2019 Q4	280
Japan	Nominal stock prices	1950 Q1	2019 Q4	280
Japan	Bond Yield	1950 Q1	2017 Q2	270
Korea	CPI	1950 Q1	2019 Q4	280
Korea	Real credit	1951 Q4	2019 Q4	273
Korea	Real GDP	1957 Q1	2019 Q4	252
Luxembourg	CPI	1950 Q1	2019 Q4	280
Luxembourg	Real GDP	1950 Q1	2019 Q4	280
Malaysia	CPI	1950 Q1	2019 Q4	280
Malaysia	Real credit	1952 Q4	2019 Q4	269
Malta	CPI	1957 Q1	2019 Q4	252
Mexico	CPI	1950 Q1	2019 Q4	280
Mexico	Real credit	1950 Q1	2019 Q4	280
Mexico	Real GDP	1950 Q1	2019 Q4	280
Mexico	Nominal stock prices	1950 Q1	2019 Q4	280
Morocco	CPI	1957 Q1	2019 Q4	252
Morocco	Real credit	1959 Q1	2019 Q4	244
Morocco	Real GDP	1957 Q1	2019 Q4	252
Netherlands	CPI	1950 Q1	2019 Q4	280
Netherlands	Real credit	1950 Q1	2019 Q4	280
Netherlands	Real GDP	1950 Q1	2019 Q4	280
Netherlands	Nominal stock prices	1950 Q1	2019 Q4	280
Netherlands	Bond Yield	1955 Q1	2019 Q2	258

New Zealand	CPI	1950 Q1	2019 Q4	280
New Zealand	Real credit	1950 Q1	2019 Q4	280
New Zealand	Real GDP	1957 Q1	2019 Q4	252
New Zealand	Nominal stock prices	1950 Q1	2019 Q4	280
New Zealand	Bond Yield	1957 Q1	2019 Q4	252
Norway	CPI	1950 Q1	2019 Q4	280
Norway	Real credit	1950 Q1	2019 Q4	280
Norway	Real GDP	1950 Q1	2019 Q4	280
Norway	Nominal stock prices	1950 Q1	2019 Q4	280
Norway	Bond Yield	1957 Q1	2019 Q4	252
Pakistan	CPI	1950 Q1	2019 Q4	280
Pakistan	Real credit	1950 Q4	2019 Q4	277
Pakistan	Real GDP	1950 Q1	2019 Q4	280
Peru	CPI	1950 Q4	2019 Q4	277
Peru	Real credit	1950 Q4	2019 Q4	277
Peru	Nominal stock prices	1950 Q1	2019 Q4	280
Philippines	CPI	1950 Q4	2019 Q4	277
Philippines	Real credit	1950 Q4	2019 Q4	277
Philippines	Real GDP	1963 Q1	2019 Q4	228
Philippines	Nominal stock prices	1953 Q1	2019 Q4	268
Portugal	CPI	1950 Q1	2019 Q4	280
Portugal	Real credit	1950 Q1	2019 Q4	280
Portugal	Real GDP	1955 Q1	2019 Q4	260
Portugal	Bond Yield	1955 Q1	2017 Q2	250
South Africa	CPI	1950 Q1	2019 Q4	280
South Africa	Real credit	1950 Q4	2019 Q4	277
South Africa	Real GDP	1957 Q1	2019 Q4	252
South Africa	Nominal stock prices	1950 Q1	2019 Q4	280
South Africa	Bond Yield	1955 Q1	2019 Q4	260
Spain	CPI	1950 Q1	2019 Q4	280
Spain	Real credit	1953 Q4	2019 Q4	265
Spain	Real GDP	1950 Q1	2019 Q4	280
Spain	Nominal stock prices	1950 Q1	2019 Q4	280
Sweden	CPI	1950 Q1	2019 Q4	280
Sweden	Real credit	1950 Q1	2019 Q4	280
Sweden	Real GDP	1950 Q1	2019 Q4	280
Sweden	Nominal stock prices	1950 Q1	2019 Q4	280
Sweden	Bond Yield	1955 Q1	2017 Q2	250
Switzerland	CPI	1950 Q1	2019 Q4	280

Switzerland	Real credit	1950 Q1	2019 Q4	280
Switzerland	Real GDP	1955 Q1	2019 Q4	260
Switzerland	Nominal stock prices	1950 Q1	2019 Q4	280
Switzerland	Bond Yield	1955 Q1	2019 Q4	260
Taiwan	CPI	1957 Q1	2019 Q4	252
Taiwan	Real credit	1957 Q1	2018 Q4	248
Taiwan	Real GDP	1957 Q1	2019 Q4	252
Thailand	CPI	1950 Q1	2019 Q4	280
Thailand	Real credit	1950 Q4	2019 Q4	277
Turkey	CPI	1950 Q4	2019 Q4	277
Turkey	Real credit	1950 Q4	2019 Q4	277
Turkey	Real GDP	1957 Q1	2019 Q4	252
United Kingdom	CPI	1950 Q1	2019 Q4	280
United Kingdom	Real credit	1950 Q1	2019 Q4	280
United Kingdom	Real GDP	1950 Q1	2019 Q4	280
United Kingdom	Nominal stock prices	1950 Q1	2019 Q4	280
United Kingdom	Bond Yield	1955 Q1	2019 Q4	260
United States	CPI	1950 Q1	2019 Q4	280
United States	Real credit	1950 Q1	2019 Q4	280
United States	Real GDP	1950 Q1	2019 Q4	280
United States	Nominal stock prices	1950 Q1	2019 Q4	280
United States	Bond Yield	1953 Q2	2019 Q4	267
Uruguay	CPI	1950 Q4	2019 Q4	277
Uruguay	Real credit	1950 Q4	2019 Q4	277
Uruguay	Real GDP	1957 Q1	2019 Q4	252

Table 2.A2: Variables and transformations

Original	Transformation	Definition
Real GDP ($\boldsymbol{x1_t}$)	$\Delta \log(x1_t)$	Real GDP growth (q-o-q)
CPI ($\boldsymbol{x2_t}$)	$\Delta^2 \log(x2_t)$	Inflation growth (q-o-q)
Credit ($\boldsymbol{x3_t}$)	$\Delta \log(x3_t/x2_t)$	Real credit growth (q-o-q)
Stock price ($\boldsymbol{x4_t}$)	$\Delta \log(x4_t)$	Stock returns (q-o-q)
Bond yield ($\boldsymbol{x5_t}$)	$\Delta(x5_t)$	Bond yield change (q-o-q)

Table 2.A3: Descriptive statistics of the variables after transformations

Country	Variable	Mean	Sd	Min	Max
Argentina	Real credit	0.01	0.11	-0.91	0.61
Argentina	Real GDP	0.01	0.02	-0.08	0.08
Argentina	CPI	0.00	0.16	-1.52	0.94
Australia	Real credit	0.02	0.01	-0.02	0.06
Australia	Real GDP	0.01	0.01	-0.02	0.04
Australia	CPI	0.00	0.01	-0.04	0.05
Australia	Nominal stock prices	0.01	0.08	-0.49	0.2
Australia	Bond yield	-0.02	0.48	-1.65	1.83
Austria	Real credit	0.01	0.02	-0.04	0.08
Austria	Real GDP	0.01	0.01	-0.02	0.04
Austria	CPI	0.00	0.02	-0.13	0.08
Austria	Nominal stock prices	0.01	0.09	-0.61	0.45
Belgium	Real credit	0.01	0.02	-0.07	0.1
Belgium	Real GDP	0.01	0.01	-0.02	0.04
Belgium	CPI	0.00	0.01	-0.02	0.02
Belgium	Nominal stock prices	0.01	0.07	-0.37	0.21
Belgium	Bond yield	-0.02	0.34	-1.39	1.09
Bolivia	Real credit	0.02	0.10	-0.58	0.71
Bolivia	CPI	0.00	0.13	-1.04	0.69
Brazil	Real credit	0.02	0.07	-0.41	0.34
Brazil	Real GDP	0.01	0.02	-0.08	0.07
Brazil	CPI	0.00	0.11	-1.15	0.49
Canada	Real credit	0.01	0.02	-0.03	0.08
Canada	Real GDP	0.01	0.01	-0.02	0.03
Canada	CPI	0.00	0.01	-0.03	0.02
Canada	Nominal stock prices	0.01	0.07	-0.37	0.19
Canada	Bond yield	-0.01	0.47	-2.19	2.15
Chile	Real credit	0.03	0.08	-0.34	0.54
Chile	Real GDP	0.01	0.02	-0.14	0.11
Chile	CPI	0.00	0.07	-0.45	0.39
Chile	Nominal stock prices	0.07	0.16	-0.38	0.88
Colombia	Real credit	0.01	0.04	-0.19	0.13
Colombia	CPI	0.00	0.04	-0.22	0.22
Costa Rica	Real credit	0.01	0.04	-0.18	0.13
Costa Rica	CPI	0.00	0.02	-0.11	0.06

Cyprus	Real credit	0.02	0.03	-0.16	0.13
Cyprus	CPI	0.00	0.02	-0.06	0.05
Denmark	Real credit	0.01	0.01	-0.03	0.07
Denmark	Real GDP	0.01	0.01	-0.08	0.06
Denmark	CPI	0.00	0.01	-0.04	0.04
Denmark	Nominal stock prices	0.02	0.08	-0.39	0.3
Denmark	Bond yield	-0.03	0.63	-3.34	2.75
El Salvador	CPI	0.00	0.02	-0.05	0.05
Finland	Real credit	0.01	0.02	-0.05	0.14
Finland	Real GDP	0.01	0.01	-0.07	0.05
Finland	CPI	0.00	0.01	-0.04	0.04
Finland	Nominal stock prices	0.02	0.10	-0.35	0.42
France	Real credit	0.01	0.02	-0.04	0.08
France	Real GDP	0.01	0.01	-0.05	0.08
France	CPI	0.00	0.01	-0.02	0.01
France	Nominal stock prices	0.01	0.08	-0.33	0.23
France	Bond yield	-0.02	0.42	-1.62	1.81
Germany	Real credit	0.01	0.01	-0.02	0.05
Germany	Real GDP	0.01	0.01	-0.05	0.04
Germany	CPI	0.00	0.01	-0.02	0.03
Germany	Nominal stock prices	0.01	0.08	-0.32	0.23
Germany	Bond yield	-0.03	0.37	-1.37	1.07
Greece	Real credit	0.01	0.03	-0.07	0.10
Greece	Real GDP	0.01	0.02	-0.05	0.08
Greece	CPI	0.00	0.03	-0.07	0.07
Guatemala	Real credit	0.01	0.11	-1.44	0.58
Guatemala	CPI	0.00	0.02	-0.08	0.09
Honduras	Real credit	0.02	0.03	-0.10	0.12
Honduras	CPI	0.00	0.02	-0.06	0.05
Iceland	Real credit	0.01	0.05	-0.15	0.28
Iceland	Real GDP	0.01	0.02	-0.09	0.10
Iceland	CPI	0.00	0.03	-0.15	0.12
India	Real credit	0.02	0.04	-0.11	0.15
India	Real GDP	0.01	0.02	-0.07	0.09
India	CPI	0.00	0.03	-0.13	0.09
India	Nominal stock prices	0.02	0.11	-0.64	0.37
Ireland	Real credit	0.01	0.03	-0.10	0.11
Ireland	Real GDP	0.01	0.02	-0.06	0.21
Ireland	CPI	0.00	0.01	-0.07	0.04

Ireland	Nominal stock prices	0.02	0.09	-0.49	0.35
Ireland	Bond yield	-0.02	0.66	-2.19	2.40
Israel	Real credit	0.03	0.05	-0.17	0.45
Israel	Real GDP	0.01	0.02	-0.12	0.10
Israel	CPI	0.00	0.04	-0.30	0.23
Israel	Nominal stock prices	0.05	0.14	-0.84	0.61
Italy	Real credit	0.01	0.03	-0.05	0.09
Italy	Real GDP	0.01	0.01	-0.03	0.10
Italy	CPI	0.00	0.01	-0.05	0.04
Italy	Nominal stock prices	0.01	0.10	-0.30	0.35
Italy	Bond yield	-0.02	0.56	-2.30	2.34
Japan	Real credit	0.01	0.02	-0.07	0.08
Japan	Real GDP	0.01	0.01	-0.05	0.03
Japan	CPI	0.00	0.01	-0.04	0.05
Japan	Nominal stock prices	0.01	0.08	-0.36	0.22
Japan	Bond yield	-0.03	0.35	-1.22	1.50
Korea	Real credit	0.03	0.04	-0.13	0.19
Korea	Real GDP	0.02	0.02	-0.07	0.08
Korea	CPI	0.00	0.03	-0.13	0.17
Luxembourg	Real GDP	0.01	0.02	-0.05	0.06
Luxembourg	CPI	0.00	0.01	-0.03	0.02
Malaysia	Real credit	0.03	0.04	-0.07	0.24
Malaysia	CPI	0.00	0.01	-0.06	0.03
Malta	CPI	0.00	0.02	-0.04	0.05
Mexico	Real credit	0.01	0.06	-0.31	0.28
Mexico	Real GDP	0.01	0.02	-0.06	0.08
Mexico	CPI	0.00	0.03	-0.22	0.09
Mexico	Nominal stock prices	0.05	0.15	-0.72	0.7
Morocco	Real credit	0.02	0.04	-0.13	0.12
Morocco	Real GDP	0.01	0.03	-0.14	0.17
Morocco	CPI	0.00	0.02	-0.07	0.04
Netherlands	Real credit	0.01	0.02	-0.04	0.08
Netherlands	Real GDP	0.01	0.01	-0.05	0.06
Netherlands	CPI	0.00	0.01	-0.06	0.04
Netherlands	Nominal stock prices	0.01	0.08	-0.42	0.17
Netherlands	Bond yield	-0.02	0.37	-1.23	1.31
New Zealand	Real credit	0.01	0.04	-0.12	0.17
New Zealand	Real GDP	0.01	0.02	-0.08	0.11
New Zealand	CPI	0.00	0.01	-0.06	0.05

New Zealand	Nominal stock prices	0.01	0.08	-0.44	0.23
New Zealand	Bond yield	-0.02	0.61	-2.33	4.35
Norway	Real credit	0.01	0.02	-0.05	0.08
Norway	Real GDP	0.01	0.01	-0.03	0.04
Norway	CPI	0.00	0.01	-0.05	0.06
Norway	Nominal stock prices	0.02	0.10	-0.51	0.34
Norway	Bond yield	-0.01	0.37	-1.45	1.56
Pakistan	Real credit	0.02	0.06	-0.21	0.24
Pakistan	Real GDP	0.01	0.02	-0.05	0.09
Pakistan	CPI	0.00	0.02	-0.10	0.11
Peru	Real credit	0.02	0.08	-0.52	0.34
Peru	CPI	0.00	0.15	-1.56	1.23
Peru	Nominal stock prices	0.08	0.35	-0.47	3.37
Philippines	Real credit	0.02	0.05	-0.23	0.13
Philippines	Real GDP	0.02	0.11	-0.10	1.62
Philippines	CPI	0.00	0.03	-0.12	0.11
Philippines	Nominal stock prices	0.01	0.13	-0.36	1.09
Portugal	Real credit	0.01	0.03	-0.07	0.07
Portugal	Real GDP	0.01	0.01	-0.03	0.06
Portugal	CPI	0.00	0.02	-0.08	0.06
Portugal	Bond yield	0.00	0.72	-3.76	3.07
South Africa	Real credit	0.01	0.02	-0.04	0.09
South Africa	Real GDP	0.01	0.01	-0.02	0.05
South Africa	CPI	0.00	0.01	-0.04	0.03
South Africa	Nominal stock prices	0.02	0.09	-0.26	0.24
South Africa	Bond yield	0.02	0.61	-2.07	3.39
Spain	Real credit	0.01	0.02	-0.07	0.08
Spain	Real GDP	0.01	0.01	-0.03	0.04
Spain	CPI	0.00	0.01	-0.04	0.04
Spain	Nominal stock prices	0.01	0.09	-0.28	0.36
Sweden	Real credit	0.01	0.02	-0.06	0.06
Sweden	Real GDP	0.01	0.01	-0.04	0.03
Sweden	CPI	0.00	0.01	-0.04	0.03
Sweden	Nominal stock prices	0.02	0.09	-0.29	0.33
Sweden	Bond yield	-0.02	0.45	-1.76	2.06
Switzerland	Real credit	0.01	0.01	-0.05	0.05
Switzerland	Real GDP	0.01	0.01	-0.05	0.03
Switzerland	CPI	0.00	0.01	-0.02	0.03
Switzerland	Nominal stock prices	0.01	0.07	-0.34	0.16

Switzerland	Bond yield	-0.02	0.27	-0.82	0.87
Taiwan	Real credit	0.02	0.03	-0.14	0.12
Taiwan	Real GDP	0.02	0.02	-0.05	0.08
Taiwan	CPI	0.00	0.02	-0.16	0.08
Thailand	Real credit	0.02	0.03	-0.09	0.13
Thailand	CPI	0.00	0.02	-0.06	0.08
Turkey	Real credit	0.02	0.06	-0.25	0.18
Turkey	Real GDP	0.01	0.02	-0.11	0.07
Turkey	CPI	0.00	0.04	-0.20	0.14
United Kingdom	Real credit	0.01	0.02	-0.04	0.07
United Kingdom	Real GDP	0.01	0.01	-0.03	0.05
United Kingdom	CPI	0.00	0.01	-0.08	0.04
United Kingdom	Nominal stock prices	0.02	0.08	-0.27	0.35
United Kingdom	Bond yield	-0.02	0.54	-1.88	1.76
United States	Real credit	0.01	0.02	-0.04	0.04
United States	Real GDP	0.01	0.01	-0.02	0.04
United States	CPI	0.00	0.01	-0.04	0.02
United States	Nominal stock prices	0.02	0.06	-0.36	0.19
United States	Bond yield	-0.01	0.46	-2.45	1.54
Uruguay	Real credit	0.00	0.07	-0.31	0.22
Uruguay	Real GDP	0.01	0.02	-0.07	0.09
Uruguay	CPI	0.00	0.04	-0.17	0.18

Table 2.A4: Correlations between global factors

Coefficient of correlation	Financial factor (PC1)	Financial factor (2 stage)	Macroeconomic factor (PC1)	Macroeconomi factor (2 stage)
Financial factor (PC1)	1	0.98	-0.88	-0.98
Financial factor (2 stage)	0.98	1	-0.89	-0.99
Macroeconomic factor (PC1)	-0.88	-0.89	1	0.93
Macroeconomic factor (2 stage)	-0.98	-0.99	0.93	1

Table 2.A5: Cross-section variables

Country	Credit/ GDP (%)		Market Cap./GDP (%)		US inv./GDP (%)	
	Mean	N	Mean	N	Max	N
Argentina	16.44	58	10.86	43	10.04	31
Australia	65.1	60	79.36	41	13.25	30
Austria	90.24	19	17.74	45	4.43	31
Belgium	61.95	19	46.02	44	13.27	31
Bolivia	29.15	60			6.1	31
Brazil	41.07	60	49.3	20	6.2	31
Canada	64.04	49	108.49	41	23.26	31
Chile	44.14	60	95.97	29	14.83	31
Colombia	28.23	60	45.84	15	4.45	31
Costa Rica	30	60	6.45	18	15.21	31
Cyprus	193	19	25.72	14	23.48	30
Denmark	81.41	54	29.21	30	5.4	30
El Salvador	34.73	55			17.58	31
Finland	81.15	19	63.67	22	1.39	30
France	90.71	19	48.45	44	3.37	31
Germany	92.08	19	32.13	45	3.84	31
Greece	89.29	19	37.06	19	0.79	31
Guatemala	19.18	60			4.61	31
Honduras	30.03	60			8.61	31
Iceland	72.1	60			3.4	14
India	26.94	60	76.27	17	1.75	30
Ireland	98.38	19	51.83	22	135.64	31
Israel	52.25	60	49.75	41	7.98	31
Italy	50.44	30	45.69	10	2.05	31
Japan	119.36	60	70.48	45	2.59	31
Korea	65.03	60	47.69	40	2.63	31
Luxembourg	56.23	30	104.14	45	1095.82	31
Malaysia	78.15	60	132.34	39	7.74	31
Malta	57.2	26	43.01	20	21.5	18
Mexico	21.12	60	21.19	44	9.34	31
Morocco	31.49	56	55.38	10	0.7	31
Netherlands	71.03	30	66.59	43	111.54	31
New Zealand	63.4	60	38.94	35	10.6	31
Norway	62.94	60	40.37	39	8.5	31

Pakistan	22.24	60	21.94	24	0.96	30
Peru	18.04	60	37.78	23	7.47	31
Philippines	28.47	60	58.04	24	7.34	31
Portugal	81.5	30	23.07	42	2.3	30
Singapore	77.43	60	166.79	41	85.84	31
South Africa	52.37	59	167.8	45	2.88	31
Spain	84.2	30	48.1	44	5.37	31
Sweden	62.66	60	48.19	29	11.29	31
Switzerland	126.4	57	142.54	45	37.09	31
Taiwan	110.16	35			5.09	30
Thailand	70.51	60	66.1	31	5.79	31
Turkey	25.24	60	24.86	27	0.82	31
United Kingdom	83.1	60	86.3	34	30.54	31
Uruguay	27.63	60	4.06	2	5.09	30

Note: N denotes the annual non-missing sample size available for each indicator. The time spam for Credit/ GDP and Market Cap./GDP is 1960 to 2019, and for US inv./GDP it is 1989 to 2019.

Figure 2.A1: Original series, transformed series and unit root tests

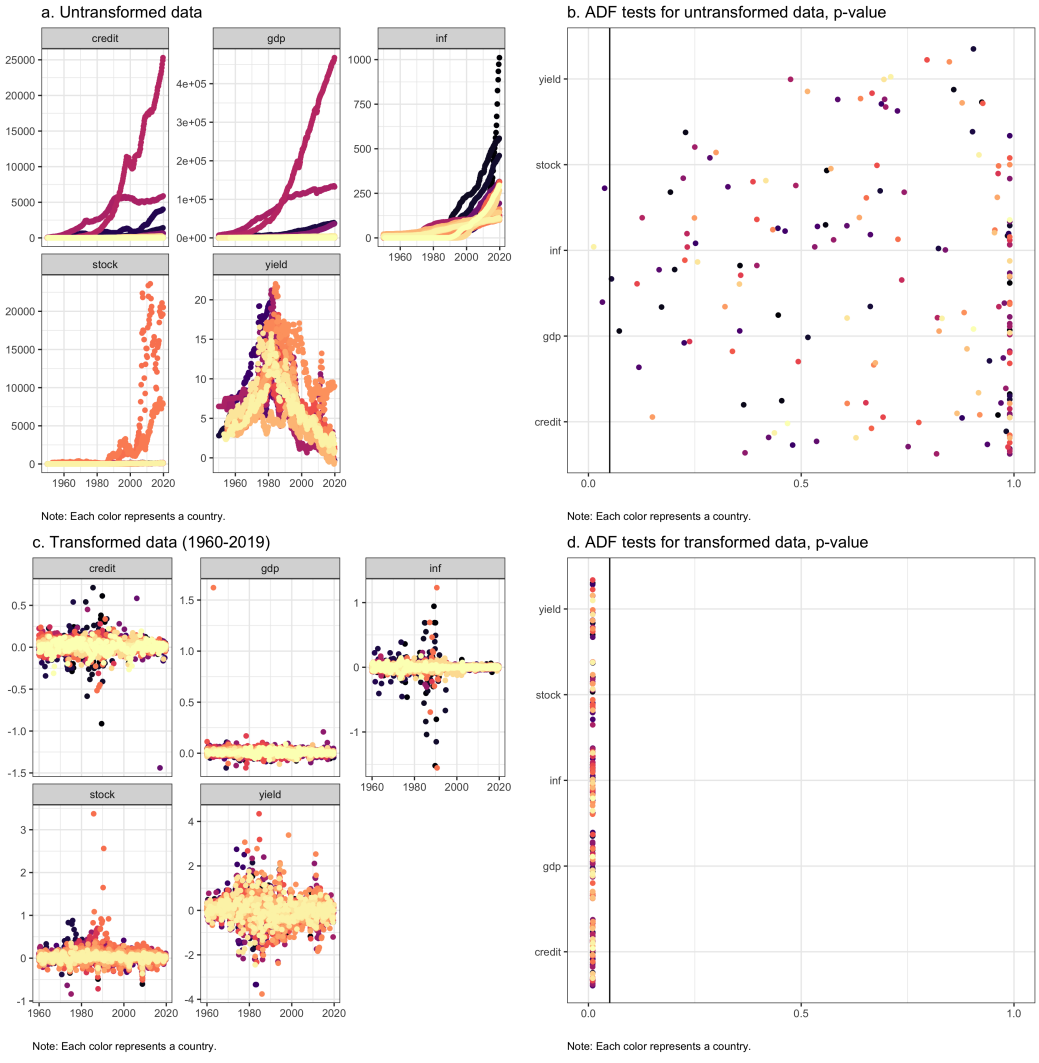

3 Daily growth-at-risk: financial or real drivers? The answer is not always the same

3.1 Introduction

Many recent studies have analyzed the predictive power of financial variables as indicators of real economic activity in times of crisis. One stream of this literature has emphasized the significant role played by financial indicators in forecasting low quantiles of the real GDP growth rate (e.g., Giglio et al., 2016; Adrian et al., 2019), while another reports that, having controlled for real variables, financial indicators have little to add to the mix (e.g., Reichlin et al., 2020; Plagborg-Møller et al., 2020). And yet, at the same time, a number of studies actually make the opposite claim and conclude that after financial variables have been incorporated into the forecasting equation, real variables have little to add (see Carriero et al., 2022).

This lack of consensus arises because forecasting real economic activity (or any part of the growth distribution, for that matter) using financial variables is a uniquely challenging problem: first, because financial and real variables are generally sampled at different frequencies, the former at a considerably higher frequency than the latter, and, second, because quantifying just how much financial variables add in terms of forecasting power seems to be as much a causal question as a predictive one, inseparable in this regard from the recurring controversy in economics concerning the dichotomy between nominal and real variables, and how (and the extent to which) the former influence the latter. Furthermore, this second concern highlights the tension between what can be considered tasks of pure "prediction" and pure "causal" inference in the social sciences, in general, and in economics, in particular (Athey, 2017). This theoretical distinction is far from clear when it comes to undertaking macroeconomic studies that are, out of necessity, observational and in which forecasting can generally be improved by using domain knowledge that is causal. Moreover, forecasting exercises are generally expected to improve our understanding of the causal mechanisms at work in the economy. In short, we tend

to trust forecasts more than we can actually fathom.

Given the complexity of this relationship and the multiplicity of aims that a researcher or policy maker may have when making a forecast, we recommend an eclectic approach be adopted. In so doing, both financial and real variables should ideally be used for forecasting episodes of economic crisis, while the data should be allowed to highlight the relative importance of each set of variables on a time-varying basis. By adhering to such an approach, we are able to make two major contributions to the field. First, we show that the informational content of daily financial and real economy indicators differs across time. Thus, in certain circumstances, forecasting accuracy depends heavily on such financial indicators as the equity market volatility (VXO) index or credit spreads; however, in other circumstances, real economic indicators, such as the Aruoba-Diebold-Scotti business conditions (ADS) index (Aruoba et al., 2009), are better at enhancing forecasts. Here, our results clearly point to the time-varying importance of real and financial variables. We compute the optimal weights that our nowcasting growth-at-risk (GaR) models assign to the ADS index or to financial variables when combining forecasts and we show that in periods such as the aftermath of the Global Financial Crisis (GFC), financial indicators play a far more relevant role than the ADS index, while the opposite holds true for the recent Covid-19 crisis. This finding is in agreement with the general consensus reached by the macrofinancial literature which highlights the financial nature of the GFC, during which financial markets and intermediaries acted as amplifiers of systemic shocks (Isohätälä et al., 2016; Brunnermeier and Sannikov, 2016; Gertler and Gilchrist, 2018). It is also in agreement with studies claiming that the Covid-19 crisis was simply a product of the supply restrictions imposed to contain the pandemic, which were real and supply-side in nature, albeit with repercussions for aggregate demand (Guerrieri et al., 2022). Thus, it is apparent that understanding the mechanisms underpinning a crisis is a purely causal task that can enable researchers to interpret the results of the forecasting exercise and, to improve the actual forecast.

Second, we also contribute to the GaR literature, as pioneered by Adrian et al. (2019), by using high-frequency financial and real indicators. Unlike most of the literature that employs either quarterly (e.g., Adrian et al., 2019; Brownlees and Souza, 2021) or weekly indicators (Carriero et al., 2022) to forecast tail risk to GDP growth, we estimate our models using daily right-hand side variables. This means our results are based on more real-time information than is usually the case in the extant literature. Exceptions exist - most notably Ferrara et al. (2022) and De Santis and Van der Veken (2020) - however, in the cited instances, real variables are neglected and the number of financial indicators included is limited. Thus, our results are supported by richer cross-sectional information at the intended frequency

than is the case in previous studies and so we present models of considerably greater accuracy.

One significant concern that needs to be addressed when working with daily predictors, yet without excluding any variables (financial or real) a priori, is the rate at which the number of parameters to be estimated increases. In this instance, shrinkage, regularization and dimensionality reduction techniques, such as those afforded by LASSO, elastic net (EN), the adaptive sparse group LASSO or principal components analysis (PCA), become essential. Here, we introduce these methods into mixed data sampling (MIDAS)-Quantile models for estimating GaR and use quantile regression for high-dimensional spaces, as proposed by Belloni and Chernozhukov (2011), and PCA to reduce the dimensions of our problem even further. In line with the warnings reported by Lima et al. (2020) and Lima and Meng (2017), parameterreduction techniques are critical when operating at such high frequencies. The LASSO-Quantile (LASSO-Q) model is described as outperforming other alternatives proposed in the literature, for example, traditional MIDAS quantile regression, where the vector of high-frequency terms takes an arbitrary form, estimated by either frequentist (Ghysels et al., 2016) or Bayesian methods (Mogliani and Simoni, 2021; Ferrara et al., 2022), both in- and out-of-sample. In addition, in line with Stock and Watson (2004), Andreou et al. (2013), and Ferrara et al. (2022), we show that combined forecasts using all indicators are more accurate, especially out-of-sample.

We validate our conclusions using a battery of statistics drawn from different fields of forecasting and quantitative risk management. Here, rather than relying on a single statistic taken from the forecasting literature which, for instance, may not take into account when the value at risk (VaR) of a series is estimated (low or high conditional quantile), we seek to ensure two properties: unconditional coverage and independence (Christoffersen, 1998). This is important because, as shown by Brownlees and Souza (2021) in a multi-country setting, original indicators of GaR frequently fail to pass basic tests designed in finance to measure the precision of VaR estimates. This, in turn, can call into question the utility of the whole enterprise.

We show that this is not the case for our indicators. In fact, on the vast majority of occasions, daily financial information together with daily information on real activity are especially useful for anticipating adverse scenarios for GDP growth. Moreover, we show that our GaR statistics are adequate and satisfy expectations in terms of performance.

The rest of this paper is organized as follows. Sections 3.2 and 3.3 present our data and methodology, respectively. Section 3.4 presents our main results, while section 3.5 concludes.

3.2 Data

Here, we seek to nowcast the conditional tail of the distribution of real GDP growth (or GNP for some of the sample period[1]) on a pseudo real-time basis. To do this, we use the quarterly real-time data set reported by the Federal Reserve Bank of Philadelphia (FRBP) spanning the period from 1986Q1 to 2020Q4. Specifically, this dataset captures the advance estimate for the previous quarter, released towards the end of the month of the current quarter.[2]

In the case of our high-frequency variables, we include 12 daily predictors to make the GaR forecasts (11 financial and 1 real variable). Of this set, eight series are the same as those employed by Pettenuzzo et al. (2016): i) the ADS daily business cycle index designed by Aruoba et al. (2009), which comes from a dynamic factor model at daily frequency; ii) the interest rate spread between the 10-year government bond rate and the federal fund rate (ISPREAD); iii) the change in the effective Federal Funds rate (EFFR); iv) the BAA-AAA-rated corporate bond yield credit spread (CSPREAD); v) the excess return on the market (RET); vi) the returns on the portfolio of small minus big stocks (SMB); vii) the returns on the portfolio of high minus low book-tomarket ratio stocks (HML); and $viii$) the returns on a winner minus loser momentum spread portfolio (MOM). In addition, we include four financial indicators: the equity market volatility index (VXO), which has previously been used as a risk indicator;[3] the spread between the yield of 10-year constant maturity Treasury bonds and 3-month Treasury bills (TERM), as a predictor of US recessions;[4] the spread between the 3-month LIBOR based on US dollars and the 3-month Treasury bill spread (TED), as a proxy of credit risk;[5] and the Composite Indicator of Systemic Stress (CISS) for the US, which is a systemic risk measure based on 15 raw market indicators, following a computation analogous to the CISS for the Euro Area (Holló et al., 2012). This last variable is used as a benchmark indicator in our models, as the standard GaR framework considers a composite financial condition index (Adrian et al., 2019; Figueres and Jarociński, 2020). Again, our data sample spans the period from 1986Q1 to 2020Q4 and is restricted by the

[1] In December 1991, the Bureau of Economic Analysis switched from reporting GNP to reporting GDP as its output measure. Later, in January 1996, they also switched from calculating GDP using fixed-weight aggregation to chain-weight methods.

[2] Faust et al. (2013) use this dataset to forecast real-time measures of economic activity using Bayesian model averaging with a large number of real and financial indicators.

[3] Rey (2015) shows that this indicator comoves with global capital flows, global credit growth, and global asset prices. Longstaff et al. (2011) also document that the price of sovereign risk is strongly correlated with VXO.

[4] Estrella and Mishkin (1998) and the subsequent literature have shown the forecasting power of the term spread for recessions.

[5] Gunay (2020) shows that the TED spread is superior to credit default swap indexes as an early warning indicator for the credit market.

availability of data for all indicators.

The ADS index is used in our nowcasting exercise with weekly vintages starting 30 November 2008. Although this approach reduces uncertainty at the sample endpoints (Amburgey and McCracken, 2022), uncertainty remains due to the estimation of the ADS index in a previous step. Maldonado and Ruiz (2021) emphasize the importance of measuring this type of uncertainty accurately in empirical applications. This means, for instance, that favourable economic conditions (i.e. better than average) can only be confidently asserted if both the point estimate of the ADS index and its confidence intervals are positive. This uncertainty is, therefore, inherent in our GaR models, given that they use the ADS index as an input variable, and may, as such, produce overstated results (i.e. providing estimates that appear more precise than what they actually are). This limitation applies to all nowcasting exercises that use an index estimated in a prior step (and not only the ADS index), and needs to be acknowledged. We include up to one year of daily lags of the high-frequency indicator in all our specifications. A detailed description of these indicators is provided in Table 3.1.

Table 3.1: Detailed description of variables

Variable	Frequency	Sample	Lags	Description	Source
ADS	Daily	Jan. 1, 1986, to Dec. 31, 2020	1 year	ADS index weekly vintages collected in real-time from 30 November 2008	Federal Reserve Bank of Philadelphia
ISPREAD	Daily	Jan. 1, 1986, to Dec. 31, 2020	1 year	Interest rate spread between the 10-year government bond rate and the federal fund rate	Federal Reserve Bank of St. Louis
EFFR	Daily	Jan. 1, 1986, to Dec. 31, 2020	1 year	Effective Federal Funds rate, first difference	Federal Reserve Bank of St. Louis
CSPREAD	Daily	Jan. 1, 1986, to Dec. 31, 2020	1 year	BAA-AAA-rated corporate bond yield credit spread	Federal Reserve Bank of St. Louis
RET	Daily	Jan. 1, 1986, to Dec. 31, 2020	1 year	Excess return on the market, value-weight return of US stocks	Fama and French (1993)
SMB	Daily	Jan. 1, 1986, to Dec. 31, 2020	1 year	The average return on the three small portfolios minus the average return on the three big portfolios	Fama and French (1993)
HML	Daily	Jan. 1, 1986, to Dec. 31, 2020	1 year	The average return on the two value portfolios minus the average return on the two growth portfolios	Fama and French (1993)
MOM	Daily	Jan. 1, 1986, to Dec. 31, 2020	1 year	The average return on the two high prior return portfolios minus the average return on the two low prior return portfolios	Fama and French (1993)
VXO	Daily	Jan. 1, 1986, to Dec. 31, 2020	1 year	Option-based implied volatility measure of S&P100	Federal Reserve Bank of St. Louis
TERM	Daily	Jan. 1, 1986, to Dec. 31, 2020	1 year	Spread between the yield of 10-year constant maturity Treasury bonds and of 3-month Treasury bills	Federal Reserve Bank of St. Louis
TED	Daily	Jan. 1, 1986, to Dec. 31, 2020	1 year	Spread between 3-Month LIBOR based on US dollars and 3-month Treasury bills	Federal Reserve Bank of St. Louis
CISS	Daily	Jan. 1, 1986, to Dec. 31, 2020	1 year	Daily systemic risk measure based on Holló et al. (2012)	European Central Bank
GDP growth	Quarterly	Q1, 1986, to Q4, 2020	1 quarter	Real GDP or Gross National Product, percent change from preceding period, quarterly, seasonally adjusted	Federal Reserve Bank of Philadelphia

3.3 Methodology

To nowcast tail risks in GDP growth, we extend Adrian et al's (2019) formulation to account for high-frequency (daily) predictors. In this section, we show briefly how we adapt the standard GaR to incorporate daily financial and real indicators using mixed data sampling. To this end, we compare the respective performances of a traditional MIDAS (with Almon lag polynomials), Bayesian MIDAS, LASSO, EN, adaptive sparse group LASSO, and soft and hard thresholding methods. We also show how we combine forecasts, an approach that has been shown to improve forecast accuracy. Finally, we present the tools used to evaluate tail risk forecasts. A quick note for notation: bold letters and symbols refer to multivariate objects such as vectors and matrices.

3.3.1 Growth-at-risk framework

As in the standard framework of quarterly GaR pioneered by Giglio et al. (2016) and Adrian et al. (2019), we rely on quantile regressions (Koenker and Bassett, 1978). Specifically, we assess the combined effect of past GDP growth (y_{t-h}) and a given financial condition indicator (x_{t-h}) at quarter t and forecast horizon h on current output growth (y_t). At this point it is important to recall that even though x_{t-h} is observed daily, it is aggregated to quarterly frequency by simple averaging.

The baseline quantile regression is given by:

$$y_t = \beta_0(\tau) + \beta_1(\tau) y_{t-h} + \beta_2(\tau) x_{t-h} + \epsilon_t \tag{3.1}$$

where $\boldsymbol{\beta}(\tau) = (\beta_0(\tau), \beta_1(\tau), \beta_2(\tau))'$ denotes the vector of parameters corresponding to the τ-th quantile, and ϵ_t is a random noise.

The parameters in Eq. (3.1) are estimated by minimizing the tick loss (TL) function:

$$TL_\tau = \frac{1}{T} \sum_{t=h+1}^{T} \left[\rho_\tau \left(y_t - Q_\tau \left(y_t \mid y_{t-h}, x_{t-h} \right) \right) \right] \tag{3.2}$$

where $\rho_\tau(\epsilon_t) = (1-\tau)1(\epsilon_t < 0)|\epsilon_t| + \tau 1(\epsilon_t > 0)|\epsilon_t|$, with $1(\epsilon_t < 0)$ taking a value of 1 when the subscript is true and 0 otherwise. The mathematical formulation in Eq. (3.2) leads to the solution of a linear programming optimization problem that we have not included here. Its basic structure and the counterpart algorithm solution can be found in Koenker (2005).

The predicted value from Eq. (3.1) is the quantile of $y_{T|T-h}$, which is conditional on the information available up to $T-h$,

$$Q_\tau\left(y_T \mid y_{T-h}, x_{T-h}\right) = \beta_0(\tau) + \beta_1(\tau) y_{t-h} + \beta_2(\tau) x_{t-h}. \tag{3.3}$$

Koenker and Bassett (1978) further prove that $Q_\tau(y_T|y_{T-h}, x_{T-h})$ is a consistent linear estimator of the conditional quantile function of y_t. In this setting, we are particularly interested in the GaR(10%) measure defined as the conditional 10% quantile forecast (see, Figueres and Jarociński, 2020; Ferrara et al., 2022; Carriero et al., 2022), namely $Q_{\tau=10\%}(y_T|y_{T-h}, x_{T-h})$.[6]

This last equation can be interpreted as the 10% quantile of GDP growth, which is conditional on the information set available up to $T-h$ for the predictors. On the one hand, a vast literature documents that financial conditions constitute strong predictive information for the lower quantiles of future GDP growth (see, e.g., Adrian et al., 2019; Prasad et al., 2019; Brownlees and Souza, 2021; Figueres and Jarociński, 2020; Ferrara et al., 2022); however, on the other, Plagborg-Møller et al. (2020) and Reichlin et al. (2020) state that controlling for real factors is necessary to measure accurately the real-time effect of financial indicators on real activity. We take these two results into account in the framework we develop here by incorporating, as a high-frequency indicator of the real sector, the Aruoba et al's ADS daily business cycle index (2009), in addition to the financial indicators. We then adopt a combination approach, aimed at producing a better point forecast, and we verify the optimal weights of individual high-frequency predictors by following the literature in this field (see Stock and Watson, 2004; Andreou et al., 2013; Pettenuzzo et al., 2016; Ferrara et al., 2022).

3.3.2 Adapting the standard GaR approach to high-frequency indicators

The handicap of the formulation as stated in Eq. (3.1) is that by aggregating the high-frequency indicator, the model cannot respond to daily shocks. Thus, in line with Ferrara et al. (2022), we adapt it so as to account for the daily information flow of the high-frequency indicator up to the latest available observation (minus h_d days), based on the following regression:

$$y_t = \beta_0(\tau) + \beta_1(\tau) y_{t-1} + \boldsymbol{X}^{D\prime}_{t-h_d} \boldsymbol{\phi}(\tau) + \epsilon_t \tag{3.4}$$

where $\boldsymbol{\phi}(\tau)$ is a $p \times 1$ vector of daily parameters and $\boldsymbol{X}^D_t = \left(x^0_t, x^1_t, \ldots, x^{p-1}_t\right)'$ is a $p \times 1$ vector of the high-frequency variable available on a daily basis, with

[6] Alternatively, Adrian et al. (2019) use the 5% quantile forecast as the measure of tail risk. However, due to our shorter sample period, we opt to use the 10% quantile.

$x_t^j, j = (0,1,2,\ldots,p-1)$, which is updated d times between quarter t and $t-1$. In this setup, we consider y_t as being affected by up to one year ($q = 4$ quarters) of past daily shocks and past GDP growth, giving a total number of parameters (including the constant) approximately equal to $K = q*d+2 = 4*60+2 = 242$, assuming a five-day working week ($d = 60$ days); that is, $\boldsymbol{X}_{t-h_d}^D = \left(x_t^0, x_{t-\frac{1}{60}}^1, \ldots, x_{t-\frac{239}{60}}^{239}\right)'$, with $x_{t-h_d}^j$. Notice that in this formulation, the forecast horizon is expressed in high-frequency terms, that is, $h_d = (0,1/d,2/d,\ldots,(p-1)/d)$.

Our estimation window is wider than that employed by Ferrara et al. (2022), the latter considering a 60-day lag window for the high-frequency indicator. This enables the model to capture up to one year's worth of daily information. In our case, the number of parameters K is relatively higher than the total number of observations T, so we are faced with a parameter proliferation problem, which invalidates the standard estimation procedure of the quantile regression. Thus, in what follows, we discuss the four alternative methods used in our results section to estimate the above regression.

3.3.3 MIDAS-Q

The MIDAS-Quantile model (MIDAS-Q) offers an effective solution for incorporating highfrequency indicators into Eq. (3.4), relying on a restriction of the form in which the distributed lags of the high-frequency variable are included in the regression. Specifically, we introduce the high-frequency lagged vector $\boldsymbol{X}_{t-h_d}^D$ in a quantile regression for the low-frequency dependent variable y_t as follows:

$$y_t = \beta_0(\tau) + \beta_1(\tau) y_{t-1} + \sum_{j=0}^{p-1} b(j;\boldsymbol{\theta}(\tau)) L_d^j x_{t-h_d}^j + \epsilon_t \tag{3.5}$$

where $b(j;\boldsymbol{\theta}(\tau)) = \sum_{i=0}^{c} \theta_{i,j}(\tau) j^i$ is the Almon lag polynomial weighting function, which depends on the vector of parameters $\boldsymbol{\theta}(\tau)$, where $j = (0,1,2,\ldots,p-1)$, and the order of the Almon lag polynomial is given by c. While Ghysels et al. (2016) propose the Beta lag polynomial function for the quantile weighting function, we consider the Almon lag polynomial as in other more recent works (Lima et al., 2020; Mogliani and Simoni, 2021; Ferrara et al., 2022). Under the so-called "direct method", Eq. (3.5) can be reparameterized as follows:

$$y_t = \beta_0(\tau) + \beta_1(\tau) y_{t-1} + \widetilde{\boldsymbol{X}}_{t-h_d}^{D\prime} \boldsymbol{\phi}(\tau) + \epsilon_t \tag{3.6}$$

where $\widetilde{\boldsymbol{X}}_{t-h_d}^D := \boldsymbol{Q} \times \boldsymbol{X}_{t-h_d}^D$ is a $(c+1)\times 1$ vector representing the transformed highfrequency predictor, $\boldsymbol{Q}$ is a $((c+1)\times p)$ weighting matrix with the $(i-th+1)$

row element of $\boldsymbol{Q}$ equal to $\left(0^i, 1^i, 2^i, \ldots, (p-1)^i\right)$ for $i = 0, \ldots, c$. Following Ferrara et al. (2022), we set $c = 3$ (third degree Almon lag) and impose two end-point zero restrictions on the slope and the value of the lag polynomial $(r = 2)$, such as $b(p-1;\theta_j(\tau)) = 0$ and $\nabla_j b(j;\theta_j(\tau))|_{j=p-1} = 0$, as in Mogliani and Simoni (2021). This causes the weighting structure to slowly reduce to zero. Consequently, the number of parameters of the high-frequency indicator to be estimated is reduced from $(c+1)$ to $(c+1-r)$ parameters.

3.3.4 BMIDAS-Q

The Bayesian version of the MIDAS-Quantile model (BMIDAS-Q), based on the asymmetric Laplace distribution (ALD) estimation pioneered by Yu and Moyeed (2001), offers a convenient alternative for estimating Eq. (3.6). This approach is adopted by Ferrara et al. (2022) to nowcast GaR for the Eurozone when using high-frequency financial indicators. Yu and Moyeed (2001) showed that the minimization problem of quantile regressions (see Eq. (3.6)) is equivalent to maximizing the likelihood function using the ALD for the error term ϵ_t. Here, we use the Gibbs sampling method as implemented by Kozumi and Kobayashi (2011), alongside their mixture representation of ALD. In this framework, the error term ϵ_t in Eq. (3.6) can be represented as a location-scale mixture of normal distributions in which the mixing distribution follows an exponential distribution (see Kozumi and Kobayashi, 2011). This implies that Eq. (3.6) can be expressed as:

$$y_t = \beta_0(\tau) + \beta_1(\tau) y_{t-1} + \widetilde{\boldsymbol{X}}^{D\prime}_{t-h_d} \boldsymbol{\phi}(\tau) + \varphi_1(\tau) v_t + \varphi_2(\tau) \sqrt{\sigma v_t} u_t \tag{3.7}$$

where φ_1 and φ_2 are fixed parameter functions of the quantile τ, $v_t = \sigma z_t$ follows a standard exponential function, and u_t is a standard normal function. This leads to the following likelihood function (to simplify assume $\boldsymbol{X}_t$ contains all covariates):

$$f\left(y_t \mid \boldsymbol{X}_t' \boldsymbol{\phi}(\tau), v_t, \sigma\right) \propto \exp\left(-\sum_{t=1}^{T} \frac{\left(y_t - \boldsymbol{X}_t' \boldsymbol{\phi}(\tau) - \varphi_1(\tau) v_t\right)^2}{2\varphi_2(\tau)^2 \sqrt{\sigma v_t}}\right) \prod_{t=1}^{T} \frac{1}{\sqrt{\sigma v}} \tag{3.8}$$

with posterior densities for $\boldsymbol{\phi}, v$ and σ given by:

$$\boldsymbol{\phi} \mid \boldsymbol{X}, v, \sigma, \tau \sim N(\widetilde{\boldsymbol{\beta}}, \widetilde{\boldsymbol{V}}),$$

$$v \mid \boldsymbol{X}, \boldsymbol{\phi}, \sigma, \tau \sim GiG\left(\frac{1}{2}, \frac{\left(y_t - \boldsymbol{X}_t' \boldsymbol{\phi}(\tau)\right)^2}{\sigma \varphi_2(\tau)^2}, \frac{2}{\sigma} + \frac{\varphi_1(\tau)^2}{\sigma \varphi_2(\tau)}\right),$$

$$\sigma \mid \boldsymbol{X}, v, \boldsymbol{\phi}, \tau \sim \text{Inv-Gamma}(a, b),$$

where

$$\widetilde{\boldsymbol{\beta}} = \widetilde{\boldsymbol{V}} \left(\sum_{t=1}^{T} \frac{\boldsymbol{X}_t \left(y_t - \varphi_1(\tau) v_t \right)}{\varphi_2(\tau)^2 \sigma v_t} \right) \text{ and } \widetilde{\boldsymbol{V}}^{-1} = \sum_{t=1}^{T} \frac{\boldsymbol{X}_t' \boldsymbol{X}_t}{\varphi_2(\tau)^2 \sigma v_t} + \widetilde{\boldsymbol{V}}_0^{-1}$$

and a and b are shape and scale parameters of the inverse gamma distribution, respectively. In our framework, as in that employed by Carriero et al. (2022), we are interested in using the posterior mean of the coefficient vector $\boldsymbol{\phi}(\tau)$ to produce point forecasts.

3.3.5 Soft thresholding: LASSO-Q and EN-Quantile (EN-Q)

One caveat of the restricted MIDAS approach presented above is that the predetermined choice of the weighting function might result in a lag structure for the high-frequency predictor that fails to maximize forecast accuracy. Thus, as an alternative, we propose estimating GaR by using either the LASSO or EN regularization for choosing a lag structure for the high-frequency predictors (Bai and Ng, 2008; Lima et al., 2020).

Accordingly, we select the lags of the high-frequency variable, based on the LASSO-Q algorithm proposed by Belloni and Chernozhukov (2011). The model can be summarized as follows,

$$\begin{aligned} \min_{\beta,\phi} E[\rho_\tau(y_t - \beta_0(\tau) - \beta_1(\tau) y_{t-1} - \boldsymbol{X}_{t-\mathrm{h}_d}^{D'} \boldsymbol{\phi}(\tau))] + \\ \lambda_\tau [\frac{\sqrt{\tau}(1-\tau)}{T}] \sum_{j=0}^{p-1} |\phi_j(\tau)| \end{aligned} \tag{3.9}$$

where the optimization problem is the sum of the standard quantile minimization function (as in Eq. (3.2)) and a penalty function given by a scaled l_1-norm of the daily vector of parameters $\phi_j(\tau)$. The overall penalty is given by $\lambda_\tau[\sqrt{\tau(1-\tau)}/T]$, where T is the sample size. The optimal level of λ_τ (LASSO-Q penalization) is calculated as in Belloni and Chernozhukov (2011). The LASSO-Q penalty has the distinctive feature of making the coefficients of insignificant predictors exactly equal to zero, retaining only the informative predictors for the forecast.

The Zou and Hastie's (2005) EN estimator seeks to address two potential drawbacks of the original LASSO. First, if $K > T$, LASSO can select T variables at most. Second, if there is a group of variables with high pairwise correlation coefficients, LASSO tends to select only one variable from the group and does not

care which one. Both, LASSO and EN shrink the estimates and perform model selection. However, while the LASSO penalty is convex, the EN penalty is strictly convex, which means that predictors must be grouped to have similar coefficients. The EN-Q objective function is given by:

$$\min_{\beta,\phi} E\left[\rho_\tau\left(y_t - \beta_0(\tau) - \beta_1(\tau)y_{t-1} - \boldsymbol{X}_{t-\mathrm{h}_d}^{D\prime}\boldsymbol{\phi}(\tau)\right)\right] + \lambda_{1,\tau}\sum_{j=0}^{p-1}|\phi_j(\tau)| + \lambda_{2,\tau}\sum_{j=0}^{p-1}\phi_j(\tau)^2 \tag{3.10}$$

where $\lambda_{1,\tau}$ and $\lambda_{2,\tau}$ are two tuning parameters that satisfy $\frac{\lambda_{2,\tau}}{\lambda_{1,\tau}+\lambda_{2,\tau}} > 0$. This restriction implies that the EN-Q is strictly convex, so it forces high pairwise correlated predictors to have similar coefficients. As a result, EN-Q stretches the net so as to retain all the important predictors, even if they are highly correlated.

As Zou and Hastie (2005) show, the EN objective function can be reformulated as a LASSO problem.[7] This has appealing computational properties, since we can use the Belloni and Chernozhukov (2011) algorithm to estimate the EN-Q model. To implement this, let's first define (where for the sake of simplicity, we assume that $\boldsymbol{X}_t$ contains all the covariates): $y_t^+(\tau) = (y_t\boldsymbol{O}_p)'$ and $\boldsymbol{X}_t^+(\tau) = \frac{1}{\sqrt{1+\lambda_{2,\tau}}}\left(\boldsymbol{X}_t\sqrt{\lambda_{2,\tau}}\boldsymbol{I}_p\right)'$, where $\boldsymbol{O}_p$ represents a $p\times 1$ vector of zeros and $\boldsymbol{I}_p$ is a $p\times p$ identity matrix.

Based on this new formulation, Eq. (3.10) can be re-expressed as follows,

$$\min_{\boldsymbol{\phi}^{++}} E\left[\rho_\tau\left(y_t^+ - \boldsymbol{X}_t^{+\prime}\boldsymbol{\phi}(\tau)\right)\right] + \gamma_\tau\sum_{j=0}^{p-1}|\phi_j(\tau)| \tag{3.11}$$

where $\gamma_\tau = \frac{\lambda_{1,\tau}}{\sqrt{1+\lambda_{2,\tau}}}$. Notice that now the sample size is equal to $T+p$, which enables EN to select all p high-frequency predictors in all cases. To remove the double shrinkage effect from LASSO, the EN-Q estimator is $\boldsymbol{\phi}^+(\tau) = (1+\lambda_{2.\tau})\,\boldsymbol{\phi}^{++}(\tau)$ (see Zou and Hastie, 2005). In our application, we only apply this correction if we use the EN-Q model to produce the conditional quantile nowcasts directly.

[7] Bai and Ng (2008) and Lima et al. (2020) use this approach to produce conditional mean forecasts with different loss functions. The former apply the mean square error and the latter the TL function.

3.3.6 Soft and hard thresholding methods: LASSO-PCA-Q and EN-PCA-Q

In line with Lima et al. (2020) and Bai and Ng (2008), we apply soft and hard thresholding methods when making forecasts with many predictors. To implement this approach, we estimate principal components from the non-zero coefficients selected by LASSO-Q or EN-Q and, using these selected variables, we can estimate factors by PCA and select the optimal number of factors using the eigen ratio (Ahn and Horenstein, 2013). Finally, we retain the factors associated with p-values lower than 0.01 (or the statistically most significant). To differentiate these models from those that only use the soft threshold to make their forecasts (i.e. LASSO-Q and EN-Q), we label models of this type as LASSO-PCA-Q and EN-PCA-Q, with the first step being selected by LASSO-Q or EN-Q, respectively.

3.3.7 Adaptive sparse group LASSO (ASGL-Q)

In line with Mendez-Civieta et al. (2021), we introduce a novel framework based on an adaptive sparse group LASSO-Quantile (ASGL-Q) regression framework.[8] This technique is particularly suited to high-dimensional problems where ($p >> T$) and, therefore, for dealing with multiple groups of high-frequency variables, with sparsity allowed within the high-frequency lagged vector. It also uses adaptive weights in the penalization scheme, in line with Zou (2006). For simplicity of notation, we refer to $TL_\tau(\boldsymbol{\phi}(\tau))$ as the TL function of the vector of parameter $\boldsymbol{\phi}(\tau)$ (see Eq. (3.2)).

The ASGL-Q objective function is given by:

$$\min_{\phi} E\left[TL_\tau(\boldsymbol{\phi}(\tau)) + \alpha\lambda\sum_{j=0}^{p-1}\widetilde{w}_j\left|\phi_j(\tau)\right| + (1-\alpha)\lambda\sum_{l=0}^{m-1}\sqrt{p_l}\tilde{v}_l\left\|\phi(\tau)^l\right\|_2\right] \quad (3.12)$$

where $\widetilde{w}_j$ is the weight of the $j-th$ parameter $\phi_j(\tau), \tilde{v}_l$ is the weight of the $l-th$ group of parameters (or high-frequency variable) $\phi(\tau)^l$, and p_l is the size of the $l-th$ group. Overall, these weights assign a low weight to a relatively important high-frequency variable (or to a given lag) and thus penalize less. Notice that Eq. (3.12) is a linear combination of LASSO and group LASSO, given by λ and the tradeoff between them, $\alpha \in [0,1]$. Specifically, a value close to 1 leads to the additive LASSO while a value close to 0 leads to the additive sparse group LASSO. Thus, this formulation provides solutions that are both between and within groups. Also, as pointed out by Mendez-Civieta et al. (2021), this formulation defines a convex

[8] We thank an anonymous reviewer for suggesting this model.

function which ensures that the solution of the minimization process is a global minimum.

3.3.8 Forecast combination

An extensive literature reports the superior performance of forecast combinations, reflecting the fact that they draw on information from all the underlying models as opposed to relying on just one specific model (e.g., Stock and Watson, 2004; Andreou et al., 2013; Pettenuzzo et al., 2016; Ferrara et al., 2022). Indeed, selecting just one model can be both inconvenient and misleading in the presence of a misspecification (Hansen et al., 2011). While different methods have been developed for implementing forecast combinations, here we opt for the discounted meansquared forecast error combination approach (Stock and Watson, 2004; Andreou et al., 2013), using the TL as the objective function.

Combination weights are computed recursively on a daily basis as follows:

$$\begin{aligned} w_{i,t-h_d} &= \frac{\lambda_{i,t-h_d}^{-\kappa}}{\sum_i^N \lambda_{i,t-h_d}^{-\kappa}}, \\ \lambda_{i,t-h_d} &= \sum_{s=T_o}^{T_f} \delta^{T_f-s} \left(y_s - GaR_{i,s}(10\%)\right) \times \left(\tau - 1(y_s < GaR_{i,s}(10\%))\right), \end{aligned} \tag{3.13}$$

where $w_{i,t-h_d}$ is the weight corresponding to the individual $GaR_{i,s}(10\%)$ measure based on the high-frequency indicator i, which depends on the discounted TL given by $\lambda_{i,t-h_d}$, with discount factor $\delta = 0.9$ and $\kappa = 1$. Importantly, $s = T_o$ is the point at which the first prediction is computed, and $s = T_f$ is the point at which the most recent prediction can be evaluated with the high-frequency indicator up to the latest available observation. By using this framework, we can compute a combined GaR(10%) for each model.

3.3.9 GaR evaluation

We evaluate tail risk forecasts using a battery of indicators developed in the forecast and risk management literatures. Our main tool for assessing GaR(10%) point forecasts is the average TL, which has been shown to be particularly appropriate when the object of interest is the forecast of a certain quantile of the dependent variable's conditional distribution (see Giacomini and Komunjer, 2005; Gneiting and Raftery, 2007; Gneiting and Ranjan, 2011; Manzan, 2015). Carriero et al. (2022) specifically use this loss function to evaluate the predictive capacity of their models for

quantifying tail risks.

The average TL for $\tau = 0.10$ is specified as follows,

$$TL_{\tau=10\%} = \frac{1}{T}\sum_{t=1}^{T}\left(y_t - GaR_t(10\%)\right) \times \left(\tau - 1(y_t < GaR_t(10\%))\right), \tag{3.14}$$

where y_t is the actual GDP growth, $GaR_t(10\%)$ is the 10% predictive quantile of GDP growth, and the indicator function $1(y_t < GaR_t(10\%))$ takes a value of 1 if it is below the 10% forecast quantile and 0 otherwise. Following convention (see Corradi and Swanson, 2006; Clark and McCracken, 2013), we use the Diebold and Mariano (1995) test[9] to assess the relative forecasting accuracy of our GaR models. In all instances, the models compared are non-nested. In the recent literature, Andreou et al. (2013), Pettenuzzo et al. (2016), and Carriero et al. (2022) have adopted the same approach.

In addition, we employ two coverage tests commonly used in the risk management literature to assess interval forecasts. In line with Christoffersen (1998), the problem of assessing the adequacy of a VaR model can be reduced to the problem of determining whether the indicator of excess sequence (i.e. the $1(y_t < GaR_t(10\%))$ has two properties: $i)$ an unconditional coverage property, and $ii)$ an independence property. In this setting, GaR forecasts are evaluated using the TL, a loss function generally used to assess the accuracy of VaR predictions (Giacomini and Komunjer, 2005). We evaluate these two conditions using the unconditional coverage (UC), and the dynamic quantile (DQ) tests (Engle and Manganelli, 2004), respectively. Specifically, the DQ is estimated using four lags of the excess sequence indicator (see Engle and Manganelli, 2004). Brownlees and Souza (2021) follow a similar approach for a multi-country GaR evaluation. Note that these two conditions can be achieved by more than one model; thus, ultimately, the TL is used in the final selection of the best performing model.

3.4 Empirical analysis

This section presents the statistical details for the computation of each model and the outcomes of the nowcasting exercise.

[9] We use the variance adjustment proposed by Harvey et al. (1997), which is supported by the results in Clark and McCracken (2013).

3.4.1 Parameterization and computational approach

We consider different high-frequency GaR measures covering different variables and models. Below we discuss our choice of parameters for each model:

- MIDAS-Q: Eq. (3.6) is estimated by adopting the quantile approach described in Section 3.3.3, in which we consider a third degree Almon lag polynomial $(c = 3)$ with two endpoint restrictions $(r = 2)$, so that the number of parameters of the high-frequency indicator is reduced substantially to $c + 1 - r$. This lag structure presents good economic properties as it slowly decays towards zero (see Mogliani and Simoni, 2021).

- BMIDAS-Q: Based on the aforementioned constrained Almon lag structure for the high-frequency variable, Eq. (3.7) is estimated using the Bayesian methodology considered in Section 3.3.4. Specifically, the model considers standard uninformative priors on the coefficient vector to have a mean equal to 0 and a variance where all elements in the diagonal are equal to 9, except for the autoregressive lag of GDP, whose prior mean and variance are set at 0.5 and 0.1, respectively. Also, the scale and shape parameters of the inverse gamma function are set at 0.01. The Gibbs sampler is used to estimate the model parameters with 10,000 repetitions (for computational efficiency), after a burn-in period of 1,000 iterations, using the normal approximation, which simplifies the algorithm (Yang et al., 2015).[10] The choice of these parameters closely resembles those made by Ferrara et al. (2022), which constitutes a natural benchmark model for our work.

- LASSO-Q: In line with the model presented in Section 3.3.5, we set the penalty parameter λ equal to the 0.9 quantile of the pivotal distribution (see Belloni and Chernozhukov, 2011). Figure A1 shows the selected lags for LASSO-Q using each highfrequency predictor. Interestingly, historically it not only tends to select the most recent daily lag of the given quarter (as one would expect), but others from past quarters. This is a key difference of this technique when compared to MIDAS-Q and BMIDAS-Q, as the latter models have an arbitrary decaying weighting scheme.

- EN-Q: Based on the model presented in Section 3.3.5, $\lambda_{1,\tau}$ is set as the penalty parameter of the LASSO-Q model, defined as above, and $\lambda_{2,\tau}$ is obtained by minimizing the mean cross-validated errors of the model, with the EN mixing parameter set at $\alpha = 0.5$ (Friedman et al., 2010). Figure A2 shows

[10] See Kozumi and Kobayashi (2011) for details on the estimation procedure.

the selected lags for EN-Q using each highfrequency predictor. Analogous to LASSO-Q, we observe that this model historically selects different daily lags for each high-frequency variable.

- LASSO-PCA-Q and EN-PCA-Q: Based on the non-zero high-frequency lags selected with either LASSO-Q or EN-Q, we estimate factors by PCA, select the optimal number of factors using the eigen ratio (Ahn and Horenstein, 2013), and retain the factors associated with p-values lower than 0.01 (or the statistically most significant). The final step in this procedure is estimated using the quantile approach described in Section 3.3.1.

- ASGL-Q: Based on the model presented in Section 3.3.7, we consider the following parametrization procedure. First, we carry out cross-validation checks for different values of λ and α to obtain their optimal values. By estimating this model with the full sample and all the high-frequency variables (except the CISS, which is used as a benchmark), we obtain the optimal values of $\lambda = 0.010$ and $\alpha = 0.25$, which minimize the TL function. Second, we compute recursively both LASSO weights and group LASSO weights based on the regression on a subset of principal components. As suggested by Mendez-Civieta et al. (2021), this method achieves better results in terms of prediction error and the stability of the variables selected when used in real datasets.

For each of these models,[11] we construct the individual $GaR(10\%)$ nowcasts by estimating the 10% quantile forecast $\widehat{Q}_{\tau=10\%}\left(y_T \mid y_{T-1}, \boldsymbol{X}^D_{i,T-h_d}\right)$ conditional on one lag of GDP growth and the respective high-frequency indicator, as described in Table 3.1. This measure is computed recursively on a daily basis for each specification including a high-frequency indicator $\boldsymbol{X}^D_{i,T-h_d}$. The estimation sample spans the period from 1986Q1 to 2020Q4, and the daily nowcasts start on January 1, 2007.

$$GaR^*_T(10\%) = \sum_i w_{i,T-h_d} \times \widehat{Q}_{\tau=10\%}\left(y_T \mid y_{T-1}, \boldsymbol{X}^D_{i,T-h_d}\right) \tag{3.15}$$

Eq. (3.15) allows us to capture the relative importance of individual GaR(10%) estimates and to deal with the potential problem of introducing many, potentially correlated, series into a common framework. It should again be stressed that the combined GaR(10%) does not include the CISS, as it is the benchmark financial composite indicator. Figure A3 provides a recursive plot of the combination weights assigned to the various models using the forecast combination approach. We find

[11] In the case of the AGSL-Q model, since it allows for multiple groups of variables, we compute the conditional 10% quantile using all the high-frequency indicators (except the CISS, which is the benchmark); thus, it directly produces a combined GaR forecast.

that both high-frequency real and financial indicators are important in providing accurate GaR(10%) nowcasts and that the importance of each is time varying.

3.4.2 Nowcasting GaR

We recursively estimate all the specifications identified above for each quarter spanning the period from 1986Q1 to 2006Q4 and construct daily GaR nowcasts in pseudo real-time as of 1 January 2007.

We begin by showing the combined GaR(10%) forecasts made by our LASSOQ model[12] and compare these to two alternative specifications, the individual GaR(10%) using the CISS and the combined GaR(10%) estimated by ASGL-Q. Recall that while LASSO-Q combines forecasts as explained in Section 3.4.1, ASGL-Q uses all the information directly in the estimation. Figure 3.1a shows the preliminary real-time estimates of quarterly US growth rate along with the combined GaR(10%) and the two alternative models. Overall, it is evident that the large negative growth rates recorded during periods of recession, such as the GFC in 2008-2009 and the Covid-19 pandemic (that started in 2020), are captured effectively by our combined GaR(10%), while this is not the case for the second event when using the alternative specifications. First, the difference in predictive powers between LASSO-Q and ASGL-Q is due in part to the difference in their combination schemes (see Figures 3.1b and 3.1c); thus, while the weights of the former are more volatile, those of the latter are more stable. Interestingly, in both frameworks, at the onset of the Covid-19 pandemic a larger weight is assigned to the ADS indicator, highlighting the benefits of using real indicators in a GaR framework. Second, relative to the individual GaR using the CISS and the standard GaR framework that uses only a composite financial condition index (Adrian et al., 2019), an evident strength of our framework is that it permits the use of a wider range of indicators which improves the accuracy of our predictions. Figure 3.1b provides a clearer indication of this by presenting the daily combination weights assigned to the different individual GaR nowcasts. Here, it is apparent that the relative importance of real and financial indicators is time varying. In the case of the 2008 GFC, the ADS, VXO and CSPREAD indicators receive a relatively high weight across all models; in contrast, on the onset of the Covid-19 pandemic, all the models assign higher weights to the ADS. This first result is in line with the general consensus in the macro-financial literature stressing the financial nature of the GFC, in which both financial intermediaries and financial markets amplified the shocks to the real

[12] We opt to report here the combined GaR nowcasts of the LASSO-Q model as, in general, it performs relatively well in terms of the average TL function compared to the rest of the models (see Table 3.2). The results for the other models are available upon request.

economy (Isohätälä et al., 2016; Brunnermeier and Sannikov, 2016; Gertler and Gilchrist, 2018). However, the second result indicates that the Covid-19 crisis was a product of the supply restrictions imposed to contain the pandemic, which were real and supply-side in nature (Guerrieri et al., 2022). Consequently, our optimal estimated weights suggest that it is fundamental to include both real and financial daily indicators to improve GaR nowcasts. Interestingly, the closely related studies conducted by Ferrara et al. (2022) and De Santis and Van der Veken (2020), which only include daily financial variables in the GaR framework, fail to capture the real magnitude of the risks during the Covid-19 epidemic. This indicates that financial variables alone play only a modest role in gauging the effect of this last recession.

Figure 3.1: GaR results for LASSO-Q and ASGL-Q

Note: The estimation sample spans the period from 1986Q1 to 2020Q4, and the daily nowcasts start as of 1 January 2007. In Panel a, the area shaded red represents NBER recessions at the end of the period. In Panel c, we omit the weight of the lagged GDP growth as it is close to zero.

3.4.3 Evaluation

In this section we assess the relative performance of $i)$ combined GaR nowcasts based on real and financial indicators vs. individual GaR nowcasts using a financial condition index (i.e. CISS) as a benchmark; and $ii)$ individual GaR nowcasts of financial and real indicators vs. the combined GaR nowcasts, in line with Figueres and Jarociński (2020).

Combined GaR (using financial and real variables) vs. standard GaR

Table 3.2 reports the relative average TL function of a given combined GaR model compared to that of the benchmark model (an individual GaR using the CISS), together with their DM test statistic values. A TL value lower than one implies that the combined model outperforms the benchmark, while in the case of the DM test the alternative hypothesis is that the indicated forecast is more accurate than that of the benchmark (i.e. rejection of the null is our preferred outcome). Notably, most models outperform the benchmark and so we can reject the hypothesis of equality of forecasts according to the DM test with a 10% confidence level. This provides strong evidence of the benefits of combining multiple real and financial indicators within the GaR framework. Interestingly, the LASSO-Q model tends to provide a lower average TL function and often rejects the null hypothesis of the DM test for different daily horizons, for both periods (that is, before and after the Covid-19). We provide evidence that the LASSO lag selection improves forecast accuracy while imposing fewer restrictions than those imposed by traditional MIDAS models.

Table 3.3 reports the tests commonly used in the financial risk management literature, namely the UC and the DQ tests, to assess interval forecasts for the combined GaR models. Specifically, the UC tests the probability of the null hypothesis that the proportion of exceedances is equal to the quantile (non-rejection is our preferred outcome), while the DQ tests the probability of the null hypothesis that the exceedance indicator is an i.i.d. process (non-rejection is again our preferred outcome). Overall, models using LASSO or EN perform better than MIDAS on these adequacy tests, with a higher number of non-rejections at the 10% level of probability. These results hold for both the period before Covid-19 and the period including it.

Combined GaR (using financial and real variables) vs. individual GaR

Next, we address the question as to whether combined or individual indicators provide more accurate nowcasts, also building on Figueres and Jarociński (2020). Table 3.4 reports the relative average TL function of an individual GaR vs. that of the

Table 3.2: Out-of-sample forecast accuracy based on the relative TL

	$h_d = 0$		$h_d = 10$		$h_d = 20$		$h_d = 40$		$h_d = 60$	
	TL	DM	TL	DM	TL	DM	TL	DM	TL	DM
Panel A. Before COVID-19 (2007Q1 to 2019Q4)										
GaR^{MIDAS}	0.641	**0.001**	0.655	**0.001**	0.653	**0.000**	0.686	**0.001**	0.683	**0.001**
GaR^{BMIDAS}	0.606	**0.000**	0.616	**0.000**	0.631	**0.001**	0.643	**0.001**	0.654	**0.001**
GaR^{LASSO}	0.590	**0.001**	0.559	**0.000**	0.569	**0.000**	0.769	0.145	0.843	0.232
GaR^{EN}	0.956	0.415	0.978	0.461	0.932	0.366	0.853	0.273	0.858	0.277
GaR$^{LASSO-PCA}$	0.617	**0.001**	0.638	**0.002**	0.706	**0.010**	0.830	0.225	0.857	0.266
GaR^{EN-PCA}	0.617	**0.001**	0.691	**0.010**	0.741	**0.039**	0.809	0.176	0.844	0.251
GaR^{ASGL}	1.102	0.646	1.037	0.559	0.983	0.471	0.945	0.419	1.221	0.744
Panel B. Including COVID-19 (2007Q1 to 2020Q4)										
GaR^{MIDAS}	0.855	**0.027**	0.82	**0.005**	0.804	**0.022**	0.558	**0.094**	0.943	0.201
GaR^{BMIDAS}	0.878	**0.021**	0.849	**0.000**	0.839	**0.005**	0.558	**0.087**	0.932	0.141
GaR^{LASSO}	0.864	**0.002**	0.773	**0.006**	0.458	**0.096**	0.501	0.121	0.895	**0.092**
GaR^{EN}	0.953	0.243	0.969	0.330	0.822	0.153	0.563	0.139	0.917	0.173
GaR$^{LASSO-PCA}$	0.940	0.263	0.733	**0.041**	0.488	0.116	0.593	0.133	0.927	0.120
GaR^{EN-PCA}	0.911	0.102	0.850	**0.013**	0.841	**0.064**	0.691	0.116	0.903	0.123
GaR^{ASGL}	1.106	0.790	1.002	0.506	1.027	0.614	1.056	0.687	1.085	0.766

Note: This table shows the TL for each combined GaR relative to the individual GaR considering the CISS, for different daily horizons. We also report the p-values of the DM test for the null hypothesis of equality of forecasts, conducted on a one-sided basis, such that the alternative hypothesis is that the indicated forecast is more accurate than the benchmark (a rejection of the null is preferred). If the p-value is below 0.10 (bold values), we conclude that the forecast from a combined GaR model is more accurate than that of the benchmark.

combined GaR (benchmark) using LASSO-Q, together with their DM test statistic values. Again, a TL value lower than one implies that the individual GaR outperforms the benchmark (the combined GaR), while in the case of the DM test the alternative hypothesis is that the indicated forecast is more accurate than the benchmark. In this setting, we would prefer to obtain a TL with a value greater than 1 and, thus, not reject the null hypothesis, in order to have evidence of the greater accuracy of our combined GaR framework. Overall, our results suggest that we cannot reject the null hypothesis of the DM test with a 10% confidence level, indicating that our combined GaR is indeed more accurate. However, the individual GaR specification using the ADS indicator is the only model to present a relative TL value lower than one for daily horizons greater or equal to 10 days and for the period including the Covid-19 pandemic. This suggests, in line with Pettenuzzo et al. (2016) and Lima et al. (2020), that individual GaR models that include the ADS index perform relatively better than their counterparts that do not include it. Moreover, this result recognizes that the Covid-19 crisis was a product of the supply restrictions imposed

Table 3.3: Out-of-sample forecast accuracy based on coverage tests

	$h_d = 0$		$h_d = 10$		$h_d = 20$		$h_d = 40$		$h_d = 60$	
	UC	DQ	UC	DQ	UC	DQ	UC	DQ	UC	DQ
Panel A. Before COVID-19 (2007Q1 to 2019Q4)										
GaR^{MIDAS}	0.001	**0.619**	0.019	**0.164**	0.019	**0.144**	0.019	**0.141**	0.001	**0.619**
GaR^{BMIDAS}	0.001	**0.619**	0.001	**0.619**	0.001	**0.619**	0.001	**0.619**	0.001	**0.619**
GaR^{LASSO}	0.019	**0.849**	**0.273**	0.014	**0.273**	0.018	0.095	**0.590**	0.019	**0.272**
GaR^{EN}	**0.273**	**0.180**	**0.273**	**0.218**	**0.926**	**0.126**	**0.273**	0.045	**0.273**	**0.107**
GaR$^{LASSO-PCA}$	0.095	**0.316**	0.095	**0.344**	**0.273**	**0.378**	0.095	**0.630**	0.095	0.011
GaR^{EN-PCA}	0.019	**0.842**	**0.565**	0.021	**0.273**	**0.386**	0.095	**0.603**	0.095	**0.631**
GaR^{ASGL}	**0.427**	0.013	**0.226**	0.071	**0.226**	0.044	**0.926**	**0.200**	**0.226**	**0.493**
Panel B. Including COVID-19 (2007Q1 to 2020Q4)										
GaR^{MIDAS}	**0.208**	0.001	**0.455**	0.045	**0.455**	0.085	**0.455**	0.024	**0.208**	0.003
GaR^{BMIDAS}	0.068	0.040	0.068	0.063	0.068	0.080	0.068	0.080	0.068	0.080
GaR^{LASSO}	0.068	**0.917**	**0.786**	0.000	**0.786**	0.021	**0.786**	0.042	**0.208**	**0.266**
GaR^{EN}	**0.786**	0.007	**0.786**	0.009	**0.547**	0.029	**0.786**	0.042	**0.786**	0.076
GaR$^{LASSO-PCA}$	**0.455**	**0.235**	**0.455**	0.009	**0.786**	0.036	**0.455**	**0.118**	**0.455**	0.008
GaR^{EN-PCA}	**0.208**	**0.468**	**0.547**	0.000	**0.860**	**0.202**	**0.455**	**0.130**	**0.455**	**0.677**
GaR^{ASGL}	**0.160**	0.015	0.031	0.000	0.031	0.000	**0.312**	**0.237**	**0.031**	**0.371**

Note: This table shows the following two interval tests for different combined GaR models: Kupiec's (1995) unconditional coverage test (UC), where the null hypothesis is that the proportion of exceedances is equal to the quantile (non-rejection of the null is preferred); and the dynamic quantile test (DQ) of Engle and Manganelli (2004), where the null hypothesis is that the exceedance indicator is an i.i.d. process (non-rejection of the null is preferred). Bold values indicate that model passes the test with a 10% level of probability.

to contain the pandemic, which were real and supply-side in nature (Guerrieri et al., 2022). Results for alternative models are presented in Appendix 3.B.

Table 3.5 reports the UC and the DQ test results when assessing interval forecasts for the different individual GaR specifications estimated by LASSO-Q. Again, the UC tests the probability that the proportion of exceedances is equal to the quantile (where non-rejection of the null is our preferred outcome) and the DQ tests the probability that the exceedance indicator is an i.i.d. process (where non-rejection of the null is again our preferred outcome). For individual GaR specifications the evidence is mixed, depending on the daily horizon. Results for alternative models are presented in Appendix 3.C.

Overall, the evidence we present here supports the time-varying importance of both daily financial and real indicators for estimating GaR. Our results are consistent with those for the eurozone reported by Ferrara et al. (2022) and for the US reported by De Santis and Van der Veken (2020), insofar as daily financial variables provide policymakers with timely warnings about the downside risks of GDP.

Table 3.4: LASSO-Q out-of-sample forecast accuracy based on the relative TL

	$h_d = 0$		$h_d = 10$		$h_d = 20$		$h_d = 40$		$h_d = 60$	
	TL	DM	TL	DM	TL	DM	TL	DM	TL	DM
Panel A. Before COVID-19 (2007Q1 to 2019Q4)										
$GaR^{ISPREAD}$	2.232	**0.978**	2.072	**0.990**	1.768	**0.988**	1.772	**0.997**	1.692	**0.996**
GaR^{EEFR}	2.000	**0.965**	2.392	**0.935**	1.819	**0.972**	1.711	**0.971**	1.649	**0.968**
GaR^{RET}	2.107	**0.973**	2.049	**0.962**	1.792	**0.946**	2.200	**0.994**	1.594	**0.971**
GaR^{SMB}	2.079	**0.991**	2.202	**0.991**	1.833	**0.994**	1.930	**0.986**	2.069	**0.990**
GaR^{HML}	2.200	**0.957**	1.447	**0.916**	1.570	**0.973**	1.514	**0.968**	1.655	**0.916**
GaR^{MOM}	1.448	**0.987**	2.076	**0.959**	1.578	**0.987**	2.072	**0.960**	1.756	**0.973**
GaR^{VXO}	1.813	**0.991**	1.550	**0.995**	1.521	**0.997**	1.258	**0.921**	1.268	**0.886**
$GaR^{CSPREAD}$	2.242	**0.979**	1.789	**0.993**	1.367	**1.000**	1.275	**0.963**	1.259	**0.951**
GaR^{TERM}	2.198	**0.984**	1.946	**0.991**	1.728	**0.989**	1.754	**0.990**	1.684	**0.989**
GaR^{TED}	1.643	**0.918**	1.603	**0.968**	1.485	**0.964**	1.440	**0.960**	1.397	**0.931**
GaR^{ADS}	1.678	**0.950**	1.496	**0.910**	1.175	**0.717**	0.939	**0.375**	1.263	**0.915**
Panel B. Including COVID-19 (2007Q1 to 2020Q4)										
$GaR^{ISPREAD}$	1.445	**0.968**	1.555	**0.995**	1.530	**0.990**	1.837	**0.973**	1.346	**0.983**
GaR^{EEFR}	1.449	**0.982**	1.707	**0.992**	1.550	**0.987**	1.855	**0.963**	1.367	**0.979**
GaR^{RET}	1.408	**0.992**	1.556	**0.989**	1.503	**0.976**	1.776	**0.964**	1.208	**0.957**
GaR^{SMB}	1.271	**0.948**	1.510	**0.989**	1.301	**0.991**	1.667	**0.960**	1.302	**0.996**
GaR^{HML}	1.453	**0.995**	1.504	**0.983**	1.281	**0.913**	1.834	**0.942**	1.300	**0.975**
GaR^{MOM}	1.274	**0.981**	1.712	**0.971**	1.510	**0.969**	1.722	**0.934**	1.307	**0.988**
GaR^{VXO}	1.196	**0.908**	1.335	**0.995**	1.317	**0.994**	1.426	**0.893**	1.129	**0.950**
$GaR^{CSPREAD}$	1.336	**0.991**	1.351	**0.993**	1.280	**0.939**	1.501	**0.888**	1.133	**0.956**
GaR^{TERM}	1.42	**0.974**	1.502	**0.995**	1.432	**0.993**	1.789	**0.971**	1.334	**0.989**
GaR^{TED}	1.315	**0.960**	1.433	**0.994**	1.420	**0.985**	1.731	**0.950**	1.279	**0.980**
GaR^{ADS}	1.375	**0.923**	0.595	**0.174**	0.655	**0.159**	0.504	**0.152**	0.743	**0.260**

Note: This table shows the TL for each individual GaR forecast relative to the combined GaR forecast, for different daily horizons. We also report the p-values of the DM test for the null hypothesis of equality of forecasts, conducted on a one-sided basis, such that the alternative hypothesis is that the indicated forecast is more accurate than the combined GaR (non-rejection of the null is preferred). If the p-value is above 0.10 (bold values), we conclude that the forecast from the combined GaR is more accurate than that of the individual GaR.

Nevertheless, we are able to provide further and clearer evidence, in line with the suggestions made by Pettenuzzo et al. (2016), that stress the benefits of incorporating a high-frequency real indicator, such as the ADS index, in the forecasting regressions. Furthermore, when comparing our combined GaR framework with that of the standard GaR using a financial condition index (specifically the CISS), we show that our framework performs significantly better. This is also true when comparing our combined GaR framework with different individual GaR specifications, although the performance of those that only include the ADS index is similar when considering the Covid-19 period. This evidence suggests that financial vari-

Table 3.5: LASSO-Q out-of-sample forecast accuracy based on coverage tests

	$h_d = 0$		$h_d = 10$		$h_d = 20$		$h_d = 40$		$h_d = 60$	
	UC	DQ	UC	DQ	UC	DQ	UC	DQ	UC	DQ
Panel A. Before COVID-19 (2007Q1 to 2019Q4)										
$GaR^{ISPREAD}$	**0.926**	**0.161**	**0.926**	0.072	**0.926**	**0.121**	**0.565**	0.070	**0.565**	**0.052**
GaR^{EEFR}	**0.717**	**0.131**	**0.226**	0.012	**0.427**	0.070	**0.226**	0.089	**0.107**	0.014
GaR^{RET}	**0.226**	0.001	0.001	0.000	0.046	0.000	0.046	0.000	0.001	0.000
GaR^{SMB}	0.046	0.001	**0.427**	0.015	**0.226**	**0.103**	0.006	0.001	**0.107**	0.002
GaR^{HML}	0.046	0.050	**0.107**	0.000	**0.226**	0.001	0.018	0.006	0.018	0.003
GaR^{MOM}	**0.427**	**0.781**	**0.717**	**0.146**	0.046	0.099	0.046	0.000	**0.226**	0.003
GaR^{VXO}	**0.107**	0.066	0.046	**0.812**	0.018	0.063	0.046	0.067	0.046	**0.707**
$GaR^{CSPREAD}$	**0.226**	0.036	**0.226**	0.038	**0.717**	**0.741**	**0.717**	**0.799**	**0.565**	**0.921**
GaR^{TERM}	**0.565**	0.087	**0.565**	0.088	**0.565**	0.080	**0.926**	**0.280**	**0.273**	**0.701**
GaR^{TED}	**0.226**	0.011	**0.107**	0.003	**0.107**	0.003	0.046	0.003	0.046	0.023
GaR^{ADS}	**0.107**	0.067	0.018	0.050	**0.107**	0.043	**0.226**	**0.186**	**0.226**	**0.230**
Panel B. Including COVID-19 (2007Q1 to 2020Q4)										
$GaR^{ISPREAD}$	**0.312**	0.003	**0.312**	0.002	**0.312**	0.002	**0.547**	0.001	**0.547**	0.001
GaR^{EEFR}	**0.160**	0.007	0.031	0.000	0.074	0.001	0.031	0.002	0.012	0.000
GaR^{RET}	0.074	0.000	0.000	0.000	0.004	0.000	0.004	0.000	0.000	0.000
GaR^{SMB}	0.012	0.001	**0.160**	0.004	0.074	0.083	0.001	0.000	0.031	0.001
GaR^{HML}	0.004	0.000	0.012	0.000	0.031	0.001	0.001	0.000	0.004	0.002
GaR^{MOM}	**0.160**	**0.425**	**0.160**	0.018	0.004	0.001	0.004	0.000	0.074	0.000
GaR^{VXO}	0.031	**0.338**	0.004	**0.267**	0.001	0.011	0.004	0.042	0.004	**0.215**
$GaR^{CSPREAD}$	0.031	0.005	0.031	0.011	**0.160**	**0.204**	**0.160**	**0.427**	**0.547**	**0.921**
GaR^{TERM}	**0.547**	0.002	**0.547**	0.001	**0.547**	0.002	**0.312**	0.008	**0.860**	0.021
GaR^{TED}	0.031	0.003	0.012	0.000	0.012	0.000	0.004	0.000	0.004	0.001
GaR^{ADS}	0.074	**0.137**	0.004	0.003	0.031	0.001	0.074	**0.230**	0.031	0.018

Note: This table shows the following two interval tests for different combined GaR models: Kupiec's (1995) unconditional coverage test (UC), where the null hypothesis is that the proportion of exceedances is equal to the quantile (non-rejection of the null is preferred); and the dynamic quantile test (DQ) of Engle and Manganelli (2004), where the null hypothesis is that the exceedance indicator is an i.i.d. process (non-rejection of the null is preferred). Bold values indicate that model passes the test with a 10% level of probability.

ables alone played a limited role in gauging the downside risk for GDP during the Covid-19 pandemic and highlights the complex ways in which real and financial variables interconnect to determine economic growth in what is a causal fashion.

3.5 Conclusions

We show that both real and financial variables reported with a daily frequency provide valuable information for monitoring periods of economic vulnerability. Here, our main contribution has been to demonstrate that by incorporating both types of

variable simultaneously in the GaR framework, it is possible to provide an early warning of a downturn in GDP in pseudo real-time and that this framework works well for both the GFC and the Covid-19 episode.

The flexible approach reported allows us to emphasize the importance of both economic theory and economic intuition when interpreting the results of forecast combinations and for improving the point forecast itself. By acknowledging the complexity of the nowcasting task in macroeconomics, especially when using high-frequency data, we contribute to a better understanding of the economic signals that can be extracted from this daily information when seeking to anticipate downturns in the economy. More specifically, here, we show that during the GFC and the Covid-19 pandemic, the optimal forecasting weights of real and financial variables underwent a marked change. In the earlier of these two periods, financial indicators such as credit spreads and the VXO were fundamental; however, they failed to capture the magnitude of the decline in GDP observed with the onset of the Covid-19 pandemic. This difference in behaviour is attributable to the specific nature of each of the two crises, something we can only grasp because we understand (to some extent) the economic mechanisms underpinning these two events.

Interestingly, among the set of financial variables, VXO and CSPREAD are especially relevant for all models during the GFC, highlighting the prominent role played by uncertainty in determining economic outcomes. However, as discussed, the financial indicators alone were unable to forecast low quantiles of GDP growth during the Covid-19 pandemic. Indeed, only by including the ADS index were we able to gauge both the sign and magnitude of the downside GDP risk in this period.

We show that our combined GaR model outperforms the standard GaR model, which only takes financial indicators into consideration (Adrian et al., 2019; Ferrara et al., 2022). We have been able to evaluate this outcome by comparing the performance of combined GaR nowcasts with that of i) individual GaR nowcasts using the CISS as a benchmark; and ii) individual GaR nowcasts using different financial and real indicators relative to the combined GaR nowcasts. Our specific implementation uses different dimension reduction techniques including MIDAS and shrinkage.

In this study, we have compared seven different models and 12 high-frequency predictors using a forecast combination approach with time-varying optimal weights. In addition, we have used a novel approach based on adaptive sparse group LASSO for quantile regressions, which allows for multiple groups and sparsity within the high-frequency lagged vector (Mendez-Civieta et al., 2021). While this model presents some good properties for addressing high-dimensional problems, we found that LASSO-Q tends to outperform the rest of the models in terms of forecast accuracy at different daily horizons. This is probably a consequence of traditional

MIDAS restrictions on the lag structure of the high-frequency indicator, which do not necessarily improve forecast accuracy. As such, our results lend further support to past evidence, inasmuch as shrinkage models should ideally be used to select the number of lags of the highfrequency predictors. Additionally, the ASGL-Q model displays more stable weights than those displayed by the LASSO-Q model, which is arguably a potential cause of the difference in accuracy. Nonetheless, these two weighting schemes emphasize the importance of the ADS indicator for forecasting during the Covid-19 period. Here, we used a single indicator to capture the role of real economic activity - that is, the ADS index - essentially because it is the only that is available at a daily frequency. We also introduced weekly vintages of this indicator to perform the nowcasting exercise in pseudo real-time. Nevertheless, we believe that more indicators gauging the informational content of different facets of economic activity and the credit markets will prove to be fundamental in the future, not only for achieving greater forecasting accuracy in real time, but also for understanding the causes of ongoing crises, before, that is, the actual causal mechanisms become clear to the professionals. In short, our models can be considered as making a contribution to anticipating and understanding economic dangers while the latter are actually unfolding.

3.A Appendix A

Figure 3.A1: Selected high-frequency LASSO-Q lags from individual GaR specifications

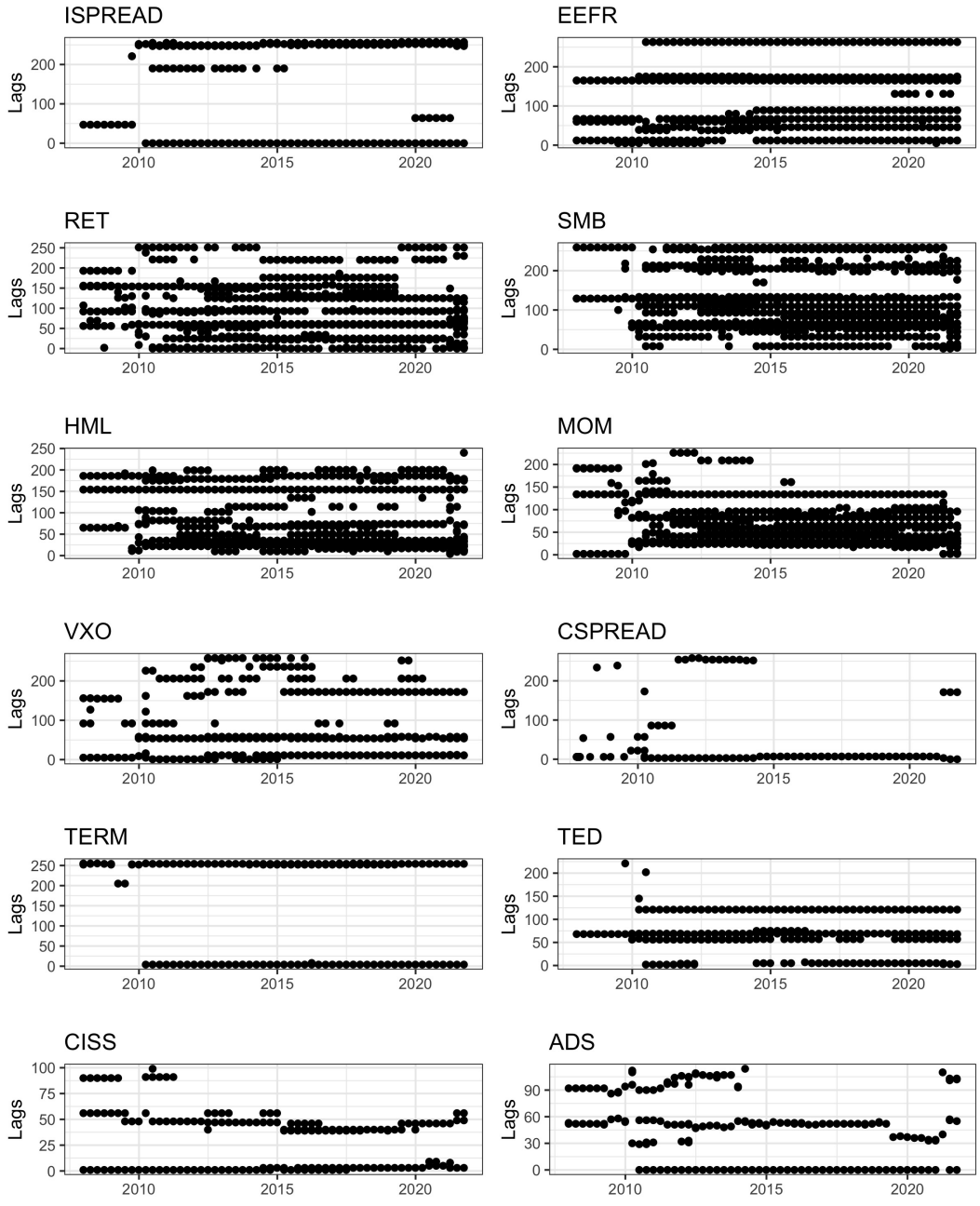

Note: The figure shows selected daily lags from the individual LASSO-Q models corresponding to the last day of each quarter.

Figure 3.A2: Selected high-frequency EN-Q lags from individual GaR specifications

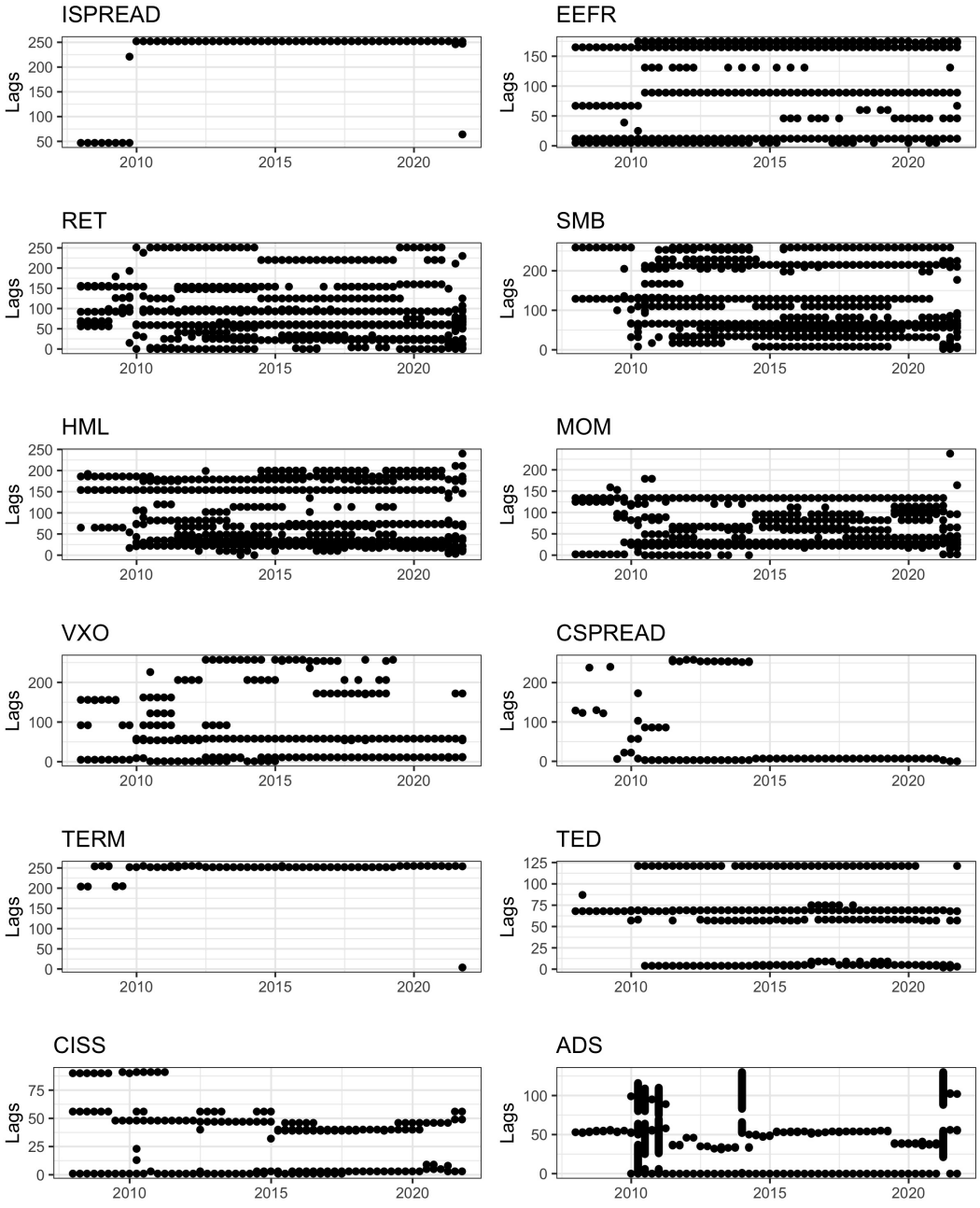

Note: The figure shows selected daily lags from the individual EN-Q models corresponding to the last day of each quarter.

Figure 3.A3: Daily forecast combination weights

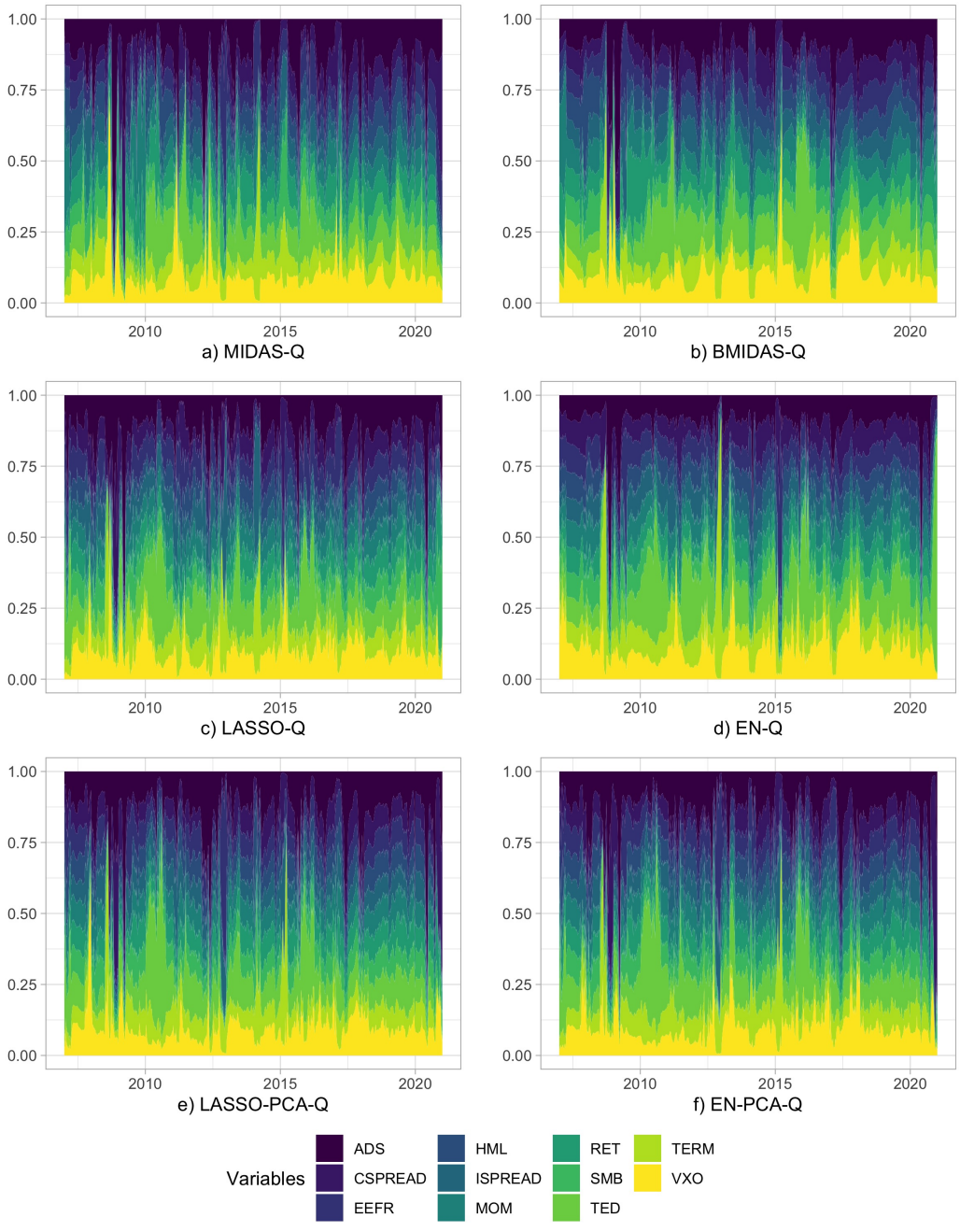

Note: The estimation sample spans the period from 1986Q1 to 2020Q4, and the daily nowcasts commence as of 1 January 2007.

3.B Appendix B

Table 3.B1: MIDAS-Q out-of-sample forecast accuracy based on the relative TL

	$h_d = 0$		$h_d = 10$		$h_d = 20$		$h_d = 40$		$h_d = 60$	
	TL	DM	TL	DM	TL	DM	TL	DM	TL	DM
Panel A. Before COVID-19 (2007Q1 to 2019Q4)										
$GaR^{ISPREAD}$	2.338	**0.990**	2.285	**0.990**	2.313	**0.99**	2.212	**0.991**	2.234	**0.987**
GaR^{EEFR}	2.317	**0.971**	2.185	**0.962**	2.221	**0.967**	2.12	**0.968**	1.999	**0.955**
GaR^{RET}	1.446	**0.989**	1.506	**0.994**	1.595	**0.997**	1.808	**0.996**	1.637	**0.996**
GaR^{SMB}	2.11	**0.988**	2.124	**0.991**	2.07	**0.993**	2.008	**0.992**	2.058	**0.989**
GaR^{HML}	2.141	**0.987**	2.204	**0.986**	2.29	**0.978**	2.452	**0.980**	2.169	**0.981**
GaR^{MOM}	2.097	**0.978**	1.987	**0.978**	1.945	**0.979**	1.752	**0.978**	1.780	**0.974**
GaR^{VXO}	1.617	**0.951**	1.589	**0.959**	1.537	**0.975**	1.493	**0.986**	1.467	**0.994**
$GaR^{CSPREAD}$	2.052	**0.996**	1.834	**0.997**	1.579	**1.000**	1.363	**0.997**	1.414	**1.000**
GaR^{TERM}	2.313	**0.989**	2.253	**0.989**	2.252	**0.988**	2.173	**0.991**	2.198	**0.987**
GaR^{TED}	1.957	**0.982**	1.929	**0.978**	1.889	**0.977**	1.758	**0.980**	1.784	**0.981**
GaR^{ADS}	1.474	**0.936**	1.527	**0.953**	1.377	**0.928**	1.100	**0.698**	1.433	**0.908**
Panel B. Including COVID-19 (2007Q1 to 2020Q4)										
$GaR^{ISPREAD}$	1.437	**0.996**	1.470	**0.998**	1.489	**0.992**	2.201	**0.952**	1.334	**0.991**
GaR^{EEFR}	1.327	**0.988**	1.375	**0.984**	1.418	**0.969**	2.087	**0.923**	1.231	**0.969**
GaR^{RET}	1.370	**0.977**	1.460	**0.984**	1.494	**0.981**	2.235	**0.951**	1.327	**0.954**
GaR^{SMB}	1.491	**0.990**	1.539	**0.993**	1.537	**0.985**	2.267	**0.951**	1.355	**0.985**
GaR^{HML}	1.585	**0.989**	1.650	**0.996**	1.633	**0.997**	2.433	**0.966**	1.433	**0.996**
GaR^{MOM}	1.664	**0.970**	1.698	**0.975**	1.729	**0.972**	2.453	**0.959**	1.511	**0.948**
GaR^{VXO}	1.202	**0.935**	1.251	**0.961**	1.300	**0.960**	1.918	**0.927**	1.107	**0.892**
$GaR^{CSPREAD}$	1.300	**0.995**	1.307	**0.991**	1.270	**0.946**	1.819	**0.871**	1.115	**0.984**
GaR^{TERM}	1.438	**0.995**	1.471	**0.997**	1.486	**0.990**	2.18	**0.948**	1.318	**0.990**
GaR^{TED}	1.407	**0.994**	1.454	**0.993**	1.465	**0.984**	2.113	**0.935**	1.276	**0.987**
GaR^{ADS}	1.089	**0.796**	0.788	**0.247**	0.762	**0.248**	0.764	**0.231**	0.978	**0.446**

Note: This table shows the TL for each combined GaR relative to the individual GaR considering the CISS, for different daily horizons. We also report the p-values of the DM test for the null hypothesis of equality of forecasts, conducted on a one-sided basis, such that the alternative hypothesis is that the indicated forecast is more accurate than the benchmark (a rejection of the null is preferred). If the p-value is below 0.10 (bold values), we conclude that the forecast from a combined GaR model is more accurate than that of the benchmark.

Table 3.B2: BMIDAS-Q out-of-sample forecast accuracy based on the relative TL

	$h_d = 0$		$h_d = 10$		$h_d = 20$		$h_d = 40$		$h_d = 60$	
	TL	DM	TL	DM	TL	DM	TL	DM	TL	DM
Panel A. Before COVID-19 (2007Q1 to 2019Q4)										
$GaR^{ISPREAD}$	2.133	**0.972**	2.109	**0.971**	2.075	**0.970**	2.054	**0.970**	2.026	**0.967**
GaR^{EEFR}	1.892	**0.969**	1.842	**0.965**	1.802	**0.964**	1.799	**0.965**	1.685	**0.956**
GaR^{RET}	1.259	**0.966**	1.348	**0.989**	1.331	**0.975**	1.333	**0.969**	1.346	**0.973**
GaR^{SMB}	2.217	**0.978**	2.215	**0.979**	2.160	**0.981**	2.181	**0.977**	2.152	**0.977**
GaR^{HML}	2.15	**0.965**	2.227	**0.965**	2.265	**0.954**	2.432	**0.948**	2.058	**0.942**
GaR^{MOM}	2.706	**0.979**	2.546	**0.983**	2.325	**0.984**	2.101	**0.972**	2.100	**0.980**
GaR^{VXO}	1.378	**0.959**	1.360	**0.965**	1.335	**0.970**	1.311	**0.971**	1.245	**0.957**
$GaR^{CSPREAD}$	1.561	**1.000**	1.544	**1.000**	1.528	**1.000**	1.519	**1.000**	1.493	**1.000**
GaR^{TERM}	2.163	**0.973**	2.128	**0.971**	2.089	**0.970**	2.068	**0.970**	2.056	**0.969**
GaR^{TED}	1.488	**0.917**	1.458	**0.916**	1.421	**0.914**	1.395	**0.930**	1.374	**0.935**
GaR^{ADS}	1.177	**0.908**	1.197	**0.935**	1.125	**0.884**	0.961	**0.330**	1.119	**0.784**
Panel B. Including COVID-19 (2007Q1 to 2020Q4)										
$GaR^{ISPREAD}$	1.342	**0.989**	1.368	**0.991**	1.367	**0.977**	2.054	**0.923**	1.245	**0.972**
GaR^{EEFR}	1.232	**0.982**	1.248	**0.983**	1.26	**0.960**	1.909	**0.910**	1.135	**0.934**
GaR^{RET}	1.183	**0.951**	1.26	**0.969**	1.248	**0.947**	1.834	**0.877**	1.117	**0.980**
GaR^{SMB}	1.392	**0.993**	1.414	**0.991**	1.403	**0.975**	2.150	**0.928**	1.295	**0.983**
GaR^{HML}	1.435	**0.983**	1.491	**0.990**	1.496	**0.985**	2.268	**0.945**	1.304	**0.975**
GaR^{MOM}	1.51	**0.991**	1.488	**0.995**	1.445	**0.994**	2.094	**0.933**	1.285	**0.990**
GaR^{VXO}	1.039	**0.720**	1.067	**0.894**	1.112	**0.927**	1.704	**0.892**	1.009	**0.545**
$GaR^{CSPREAD}$	1.194	**0.991**	1.227	**0.998**	1.229	**0.985**	1.850	**0.902**	1.127	**1.000**
GaR^{TERM}	1.354	**0.990**	1.377	**0.991**	1.376	**0.977**	2.073	**0.925**	1.26	**0.977**
GaR^{TED}	1.242	**0.969**	1.263	**0.969**	1.257	**0.935**	1.885	**0.882**	1.142	**0.964**
GaR^{ADS}	1.000	**0.501**	0.754	**0.204**	0.742	**0.215**	0.689	**0.196**	0.907	**0.305**

Note: This table shows the TL for each combined GaR relative to the individual GaR considering the CISS, for different daily horizons. We also report the p-values of the DM test for the null hypothesis of equality of forecasts, conducted on a one-sided basis, such that the alternative hypothesis is that the indicated forecast is more accurate than the benchmark (a rejection of the null is preferred). If the p-value is below 0.10 (bold values), we conclude that the forecast from a combined GaR model is more accurate than that of the benchmark.

Table 3.B3: EN-Q out-of-sample forecast accuracy based on the relative TL

	$h_d = 0$		$h_d = 10$		$h_d = 20$		$h_d = 40$		$h_d = 60$	
	TL	DM	TL	DM	TL	DM	TL	DM	TL	DM
Panel A. Before COVID-19 (2007Q1 to 2019Q4)										
$GaR^{ISPREAD}$	1.339	**0.988**	1.327	**0.992**	1.305	**0.991**	1.462	**0.981**	1.456	**0.976**
GaR^{EEFR}	1.373	**0.959**	1.569	**0.919**	1.41	**0.956**	1.564	**0.969**	1.549	**0.959**
GaR^{RET}	1.589	**0.992**	1.536	**0.971**	1.919	**0.992**	1.732	**0.98**	2.263	**0.986**
GaR^{SMB}	1.308	**1.000**	1.362	**1.000**	1.611	**0.992**	1.756	**0.997**	1.681	**0.996**
GaR^{HML}	1.631	**0.991**	1.182	**0.925**	1.289	**0.993**	1.854	**0.997**	1.809	**0.993**
GaR^{MOM}	1.050	**0.808**	1.355	**0.950**	1.312	**0.989**	1.870	**0.984**	1.450	**0.951**
GaR^{VXO}	1.315	**0.974**	1.328	**0.979**	1.293	**0.970**	1.257	**0.890**	1.284	**0.924**
$GaR^{CSPREAD}$	1.170	**0.907**	1.177	**0.934**	1.144	**0.911**	1.303	**0.961**	1.250	**0.955**
GaR^{TERM}	1.273	**0.987**	1.255	**0.993**	1.253	**0.994**	1.427	**0.974**	1.398	**0.971**
GaR^{TED}	1.200	**0.830**	1.195	**0.853**	1.181	**0.855**	1.364	**0.915**	1.261	**0.845**
GaR^{ADS}	1.038	**0.589**	1.038	**0.588**	0.96	**0.405**	0.865	**0.230**	1.048	**0.672**
Panel B. Including COVID-19 (2007Q1 to 2020Q4)										
$GaR^{ISPREAD}$	1.165	**0.967**	1.151	**0.988**	1.33	**0.955**	1.926	**0.906**	1.202	**0.993**
GaR^{EEFR}	1.216	**0.981**	1.261	**0.977**	1.382	**0.953**	1.983	**0.910**	1.159	**0.976**
GaR^{RET}	1.414	**0.988**	1.381	**0.988**	1.649	**0.972**	1.992	**0.911**	1.414	**0.991**
GaR^{SMB}	1.203	**0.980**	1.429	**0.989**	1.409	**0.986**	2.108	**0.921**	1.268	**0.992**
GaR^{HML}	1.367	**0.994**	1.436	**0.980**	1.179	**0.975**	2.634	**0.951**	1.266	**0.996**
GaR^{MOM}	1.222	**0.952**	1.374	**0.982**	1.439	**0.949**	2.247	**0.931**	1.196	**0.973**
GaR^{VXO}	1.078	**0.926**	1.127	**0.992**	1.264	**0.931**	1.839	**0.877**	1.135	**0.959**
$GaR^{CSPREAD}$	1.152	**0.952**	1.132	**0.972**	1.293	**0.877**	1.845	**0.872**	1.114	**0.928**
GaR^{TERM}	1.145	**0.945**	1.157	**0.985**	1.35	**0.958**	1.988	**0.918**	1.187	**0.989**
GaR^{TED}	1.140	**0.911**	1.155	**0.960**	1.316	**0.903**	1.927	**0.885**	1.132	**0.923**
GaR^{ADS}	0.961	**0.380**	0.809	**0.169**	0.672	**0.146**	0.733	**0.190**	0.845	**0.316**

Note: This table shows the TL for each combined GaR relative to the individual GaR considering the CISS, for different daily horizons. We also report the p-values of the DM test for the null hypothesis of equality of forecasts, conducted on a one-sided basis, such that the alternative hypothesis is that the indicated forecast is more accurate than the benchmark (a rejection of the null is preferred). If the p-value is below 0.10 (bold values), we conclude that the forecast from a combined GaR model is more accurate than that of the benchmark.

Table 3.B4: LASSO-PCA-Q out-of-sample forecast accuracy based on the relative TL

	$h_d = 0$		$h_d = 10$		$h_d = 20$		$h_d = 40$		$h_d = 60$	
	TL	DM	TL	DM	TL	DM	TL	DM	TL	DM
Panel A. Before COVID-19 (2007Q1 to 2019Q4)										
$GaR^{ISPREAD}$	2.200	**0.978**	2.260	**0.988**	1.868	**0.988**	1.723	**0.997**	1.678	**0.996**
GaR^{EEFR}	2.254	**0.961**	2.295	**0.957**	2.074	**0.973**	1.795	**0.974**	1.822	**0.976**
GaR^{RET}	2.222	**0.980**	2.270	**0.968**	1.777	**0.927**	2.197	**0.984**	1.544	**0.978**
GaR^{SMB}	2.288	**0.992**	1.851	**0.971**	1.826	**0.988**	1.649	**0.981**	1.588	**0.989**
GaR^{HML}	2.163	**0.940**	2.425	**0.957**	1.938	**0.960**	2.188	**0.988**	1.726	**0.942**
GaR^{MOM}	1.475	**0.995**	1.958	**0.95**	1.622	**0.988**	1.976	**0.971**	1.700	**0.989**
GaR^{VXO}	1.785	**0.990**	1.714	**0.994**	1.591	**0.999**	1.328	**0.940**	1.220	**0.867**
$GaR^{CSPREAD}$	2.271	**0.982**	1.939	**0.996**	1.406	**1.000**	1.241	**0.915**	1.227	**0.931**
GaR^{TERM}	2.204	**0.986**	2.105	**0.987**	1.816	**0.987**	1.730	**0.992**	1.656	**0.990**
GaR^{TED}	1.644	**0.923**	1.736	**0.965**	1.562	**0.965**	1.407	**0.951**	1.379	**0.933**
GaR^{ADS}	1.187	**0.847**	1.186	**0.834**	0.928	**0.307**	0.943	**0.374**	1.228	**0.884**
Panel B. Including COVID-19 (2007Q1 to 2020Q4)										
$GaR^{ISPREAD}$	1.418	**0.964**	1.807	**0.994**	2.591	**0.952**	2.139	**0.957**	1.319	**0.977**
GaR^{EEFR}	1.502	**0.969**	1.938	**0.988**	2.834	**0.958**	2.284	**0.955**	1.445	**0.975**
GaR^{RET}	1.392	**0.992**	1.743	**0.974**	2.423	**0.909**	2.070	**0.947**	1.171	**0.981**
GaR^{SMB}	1.239	**0.908**	1.602	**0.952**	2.201	**0.926**	1.857	**0.893**	1.227	**0.995**
GaR^{HML}	1.314	**0.971**	2.051	**0.99**	2.658	**0.964**	3.143	**0.963**	1.209	**0.968**
GaR^{MOM}	1.14	**0.882**	1.990	**0.983**	2.444	**0.912**	2.059	**0.926**	1.208	**0.992**
GaR^{VXO}	1.087	**0.700**	1.480	**0.983**	2.122	**0.921**	1.688	**0.881**	1.090	**0.963**
$GaR^{CSPREAD}$	1.271	**0.963**	1.532	**0.983**	2.139	**0.888**	1.725	**0.874**	1.079	**0.981**
GaR^{TERM}	1.377	**0.956**	1.742	**0.995**	2.385	**0.940**	2.091	**0.952**	1.300	**0.984**
GaR^{TED}	1.274	**0.932**	1.662	**0.988**	2.450	**0.934**	2.018	**0.930**	1.247	**0.978**
GaR^{ADS}	1.499	**0.851**	0.606	**0.139**	0.610	**0.113**	0.605	**0.122**	0.902	**0.301**

Note: This table shows the TL for each combined GaR relative to the individual GaR considering the CISS, for different daily horizons. We also report the p-values of the DM test for the null hypothesis of equality of forecasts, conducted on a one-sided basis, such that the alternative hypothesis is that the indicated forecast is more accurate than the benchmark (a rejection of the null is preferred). If the p-value is below 0.10 (bold values), we conclude that the forecast from a combined GaR model is more accurate than that of the benchmark.

Table 3.B5: EN-PCA-Q out-of-sample forecast accuracy based on the relative TL

	$h_d = 0$		$h_d = 10$		$h_d = 20$		$h_d = 40$		$h_d = 60$	
	TL	DM	TL	DM	TL	DM	TL	DM	TL	DM
Panel A. Before COVID-19 (2007Q1 to 2019Q4)										
$GaR^{ISPREAD}$	2.232	**0.978**	2.072	**0.990**	1.768	**0.988**	1.772	**0.997**	1.692	**0.996**
GaR^{EEFR}	2.000	**0.965**	2.392	**0.935**	1.819	**0.972**	1.711	**0.971**	1.649	**0.968**
GaR^{RET}	2.107	**0.973**	2.049	**0.962**	1.792	**0.946**	2.200	**0.994**	1.594	**0.971**
GaR^{SMB}	2.079	**0.991**	2.202	**0.991**	1.833	**0.994**	1.930	**0.986**	2.069	**0.990**
GaR^{HML}	2.200	**0.957**	1.447	**0.916**	1.57	**0.973**	1.514	**0.968**	1.655	**0.916**
GaR^{MOM}	1.448	**0.987**	2.076	**0.959**	1.578	**0.987**	2.072	**0.960**	1.756	**0.973**
GaR^{VXO}	1.813	**0.991**	1.550	**0.995**	1.521	**0.997**	1.258	**0.921**	1.268	**0.886**
$GaR^{CSPREAD}$	2.242	**0.979**	1.789	**0.993**	1.367	**1.000**	1.275	**0.963**	1.259	**0.951**
GaR^{TERM}	2.198	**0.984**	1.946	**0.991**	1.728	**0.989**	1.754	**0.990**	1.684	**0.989**
GaR^{TED}	1.643	**0.918**	1.603	**0.968**	1.485	**0.964**	1.440	**0.960**	1.397	**0.931**
GaR^{ADS}	1.678	**0.950**	1.496	**0.910**	1.175	**0.717**	0.939	**0.375**	1.263	**0.915**
Panel B. Including COVID-19 (2007Q1 to 2020Q4)										
$GaR^{ISPREAD}$	1.445	**0.968**	1.555	**0.995**	1.530	**0.99**	1.837	**0.973**	1.346	**0.983**
GaR^{EEFR}	1.449	**0.982**	1.707	**0.992**	1.550	**0.987**	1.855	**0.963**	1.367	**0.979**
GaR^{RET}	1.408	**0.992**	1.556	**0.989**	1.503	**0.976**	1.776	**0.964**	1.208	**0.957**
GaR^{SMB}	1.271	**0.948**	1.510	**0.989**	1.301	**0.991**	1.667	**0.960**	1.302	**0.996**
GaR^{HML}	1.453	**0.995**	1.504	**0.983**	1.281	**0.913**	1.834	**0.942**	1.300	**0.975**
GaR^{MOM}	1.274	**0.981**	1.712	**0.971**	1.510	**0.969**	1.722	**0.934**	1.307	**0.988**
GaR^{VXO}	1.196	**0.908**	1.335	**0.995**	1.317	**0.994**	1.426	**0.893**	1.129	**0.950**
$GaR^{CSPREAD}$	1.336	**0.991**	1.351	**0.993**	1.280	**0.939**	1.501	**0.888**	1.133	**0.956**
GaR^{TERM}	1.420	**0.974**	1.502	**0.995**	1.432	**0.993**	1.789	**0.971**	1.334	**0.989**
GaR^{TED}	1.315	**0.960**	1.433	**0.994**	1.420	**0.985**	1.731	**0.950**	1.279	**0.980**
GaR^{ADS}	1.375	**0.923**	0.595	**0.174**	0.655	**0.159**	0.504	**0.152**	0.743	**0.260**

Note: This table shows the TL for each combined GaR relative to the individual GaR considering the CISS, for different daily horizons. We also report the p-values of the DM test for the null hypothesis of equality of forecasts, conducted on a one-sided basis, such that the alternative hypothesis is that the indicated forecast is more accurate than the benchmark (a rejection of the null is preferred). If the p-value is below 0.10 (bold values), we conclude that the forecast from a combined GaR model is more accurate than that of the benchmark.

3.C Appendix C

Table 3.C1: MIDAS-Q out-of-sample forecast accuracy based on coverage tests

	$h_d = 0$		$h_d = 10$		$h_d = 20$		$h_d = 40$		$h_d = 60$	
	UC	DQ	UC	DQ	UC	DQ	UC	DQ	UC	DQ
Panel A. Before COVID-19 (2007Q1 to 2019Q4)										
$GaR^{ISPREAD}$	**0.565**	0.039	**0.565**	0.042	**0.565**	0.032	**0.565**	0.034	**0.565**	0.032
GaR^{EEFR}	**0.273**	0.003	0.095	**0.142**	**0.273**	0.002	**0.273**	0.003	**0.273**	0.004
GaR^{RET}	**0.427**	**0.452**	**0.226**	**0.713**	0.046	**0.281**	0.046	0.027	0.046	0.015
GaR^{SMB}	**0.926**	**0.200**	**0.717**	**0.509**	**0.717**	**0.553**	**0.926**	**0.191**	**0.926**	0.153
GaR^{HML}	**0.565**	**0.560**	**0.565**	**0.561**	**0.717**	**0.506**	**0.717**	0.077	**0.926**	**0.273**
GaR^{MOM}	**0.926**	**0.142**	**0.926**	0.054	**0.565**	**0.147**	**0.273**	**0.368**	0.095	**0.141**
GaR^{VXO}	**0.926**	**0.903**	**0.717**	**0.878**	**0.717**	**0.867**	**0.717**	**0.863**	**0.226**	**0.887**
$GaR^{CSPREAD}$	**0.717**	0.088	**0.926**	0.090	**0.926**	**0.102**	**0.273**	**0.925**	0.095	**0.826**
GaR^{TERM}	**0.565**	0.056	**0.565**	0.060	**0.273**	0.002	**0.273**	0.002	**0.273**	0.002
GaR^{TED}	**0.226**	**0.273**	**0.107**	**0.265**	**0.226**	**0.309**	**0.226**	**0.310**	**0.226**	**0.323**
GaR^{ADS}	**0.226**	**0.229**	**0.226**	**0.201**	**0.226**	**0.230**	0.006	0.000	**0.107**	0.072
Panel B. Including COVID-19 (2007Q1 to 2020Q4)										
$GaR^{ISPREAD}$	**0.547**	0.001	**0.547**	0.001	**0.547**	0.000	**0.547**	0.000	**0.547**	0.000
GaR^{EEFR}	**0.860**	0.001	**0.786**	0.004	**0.860**	0.000	**0.860**	0.000	**0.860**	0.000
GaR^{RET}	0.074	0.059	0.031	0.015	0.004	0.005	0.004	0.001	0.004	0.001
GaR^{SMB}	**0.312**	0.004	**0.160**	0.014	**0.160**	0.015	**0.312**	0.003	**0.312**	0.003
GaR^{HML}	**0.547**	0.008	**0.547**	0.007	**0.160**	0.007	**0.160**	0.001	**0.312**	0.005
GaR^{MOM}	**0.312**	0.005	**0.312**	0.000	**0.547**	0.004	**0.860**	0.008	**0.786**	0.000
GaR^{VXO}	**0.547**	**0.675**	**0.160**	**0.763**	**0.160**	**0.685**	**0.160**	**0.656**	0.031	**0.584**
$GaR^{CSPREAD}$	**0.160**	0.100	**0.312**	0.035	**0.312**	0.056	**0.860**	**0.626**	**0.786**	**0.405**
GaR^{TERM}	**0.547**	0.001	**0.547**	0.001	**0.860**	0.000	**0.860**	0.000	**0.860**	0.000
GaR^{TED}	0.031	**0.242**	0.012	0.028	0.031	0.033	0.031	0.041	0.031	0.032
GaR^{ADS}	**0.160**	**0.146**	**0.160**	0.088	0.074	0.015	0.004	0.002	0.031	0.008

Note: This table shows the following two interval tests for different combined GaR models: Kupiec's (1995) unconditional coverage test (UC), where the null hypothesis is that the proportion of exceedances is equal to the quantile (non-rejection of the null is preferred); and the dynamic quantile test (DQ) of Engle and Manganelli (2004), where the null hypothesis is that the exceedance indicator is an i.i.d. process (non-rejection of the null is preferred). Bold values indicate that model passes the test with a 10% level of probability.

Table 3.C2: BMIDAS-Q out-of-sample forecast accuracy based on coverage tests

	$h_d = 0$		$h_d = 10$		$h_d = 20$		$h_d = 40$		$h_d = 60$	
	UC	DQ	UC	DQ	UC	DQ	UC	DQ	UC	DQ
Panel A. Before COVID-19 (2007Q1 to 2019Q4)										
$GaR^{ISPREAD}$	0.095	**0.139**	0.095	**0.141**	0.095	**0.142**	0.095	**0.141**	**0.273**	0.012
GaR^{EEFR}	**0.273**	0.006	**0.273**	0.006	0.095	0.082	0.095	**0.109**	0.095	0.074
GaR^{RET}	**0.427**	0.058	**0.926**	**0.682**	**0.565**	**0.877**	**0.427**	**0.638**	**0.717**	**0.383**
GaR^{SMB}	**0.565**	0.000	**0.565**	0.000	**0.565**	0.000	**0.565**	0.000	**0.565**	0.000
GaR^{HML}	**0.565**	0.029	**0.565**	0.022	**0.273**	**0.228**	**0.273**	0.005	**0.273**	**0.139**
GaR^{MOM}	**0.273**	0.012	**0.273**	0.013	**0.273**	0.013	**0.273**	0.012	0.095	**0.125**
GaR^{VXO}	**0.565**	**0.907**	**0.565**	**0.908**	**0.565**	**0.909**	**0.926**	**0.907**	**0.717**	**0.710**
$GaR^{CSPREAD}$	0.095	**0.885**	0.095	**0.881**	0.095	**0.880**	0.095	**0.874**	0.019	0.811
GaR^{TERM}	0.095	**0.139**	0.095	**0.142**	0.095	**0.142**	0.095	**0.14**	**0.273**	0.012
GaR^{TED}	**0.717**	**0.731**	**0.717**	**0.713**	**0.717**	**0.695**	**0.717**	**0.686**	**0.717**	**0.696**
GaR^{ADS}	**0.565**	**0.892**	**0.926**	**0.901**	**0.565**	**0.758**	**0.095**	**0.432**	0.095	**0.375**
Panel B. Including COVID-19 (2007Q1 to 2020Q4)										
$GaR^{ISPREAD}$	**0.455**	0.015	**0.455**	0.015	**0.455**	0.015	**0.455**	0.014	**0.786**	0.004
GaR^{EEFR}	**0.786**	0.000	**0.786**	0.000	**0.455**	0.001	**0.455**	0.004	**0.455**	0.002
GaR^{RET}	**0.160**	**0.140**	**0.547**	**0.163**	**0.860**	**0.362**	**0.16**	**0.168**	**0.312**	0.052
GaR^{SMB}	**0.860**	0.000	**0.860**	0.000	**0.860**	0.000	**0.86**	0.000	**0.860**	0.000
GaR^{HML}	**0.860**	0.001	**0.860**	0.000	**0.786**	0.007	**0.786**	0.001	**0.786**	0.050
GaR^{MOM}	**0.786**	0.003	**0.786**	0.003	**0.786**	0.004	**0.786**	0.004	**0.455**	0.009
GaR^{VXO}	**0.786**	**0.864**	**0.860**	**0.462**	**0.860**	**0.68**	**0.547**	**0.709**	**0.312**	**0.119**
$GaR^{CSPREAD}$	**0.455**	**0.875**	**0.455**	**0.860**	**0.455**	**0.856**	**0.455**	**0.856**	**0.208**	**0.616**
GaR^{TERM}	**0.455**	0.015	**0.455**	0.015	**0.455**	0.015	**0.455**	0.015	**0.786**	0.004
GaR^{TED}	**0.312**	**0.328**	**0.312**	**0.327**	**0.312**	**0.320**	**0.312**	**0.315**	**0.312**	**0.324**
GaR^{ADS}	**0.860**	**0.716**	**0.547**	**0.529**	**0.547**	**0.835**	**0.208**	**0.569**	**0.455**	**0.372**

Note: This table shows the following two interval tests for different combined GaR models: Kupiec's (1995) unconditional coverage test (UC), where the null hypothesis is that the proportion of exceedances is equal to the quantile (non-rejection of the null is preferred); and the dynamic quantile test (DQ) of Engle and Manganelli (2004), where the null hypothesis is that the exceedance indicator is an i.i.d. process (non-rejection of the null is preferred). Bold values indicate that model passes the test with a 10% level of probability.

Table 3.C3: EN-Q out-of-sample forecast accuracy based on coverage tests

	$h_d = 0$		$h_d = 10$		$h_d = 20$		$h_d = 40$		$h_d = 60$	
	UC	DQ	UC	DQ	UC	DQ	UC	DQ	UC	DQ
Panel A. Before COVID-19 (2007Q1 to 2019Q4)										
$GaR^{ISPREAD}$	**0.717**	**0.488**	**0.717**	**0.464**	**0.717**	**0.488**	**0.926**	**0.216**	**0.717**	**0.481**
GaR^{EEFR}	**0.926**	0.099	**0.565**	**0.147**	**0.926**	0.002	**0.926**	**0.124**	**0.926**	0.073
GaR^{RET}	**0.717**	0.007	**0.107**	0.000	**0.427**	0.000	**0.717**	0.002	**0.226**	0.010
GaR^{SMB}	**0.565**	0.071	**0.565**	0.064	**0.926**	**0.131**	**0.717**	0.012	**0.926**	0.021
GaR^{HML}	**0.107**	0.000	**0.717**	0.032	**0.926**	0.032	**0.427**	0.003	**0.427**	0.017
GaR^{MOM}	**0.565**	0.001	**0.273**	**0.648**	**0.107**	0.000	**0.427**	0.007	**0.427**	**0.134**
GaR^{VXO}	**0.427**	**0.656**	**0.427**	**0.645**	**0.226**	**0.358**	**0.427**	**0.583**	**0.926**	**0.922**
$GaR^{CSPREAD}$	**0.717**	**0.856**	**0.717**	**0.879**	**0.717**	**0.855**	**0.717**	**0.856**	**0.565**	**0.900**
GaR^{TERM}	**0.926**	**0.244**	**0.565**	**0.779**	**0.565**	**0.783**	**0.565**	**0.783**	**0.565**	**0.780**
GaR^{TED}	**0.107**	**0.330**	0.046	**0.235**	**0.107**	**0.329**	0.018	0.068	**0.107**	**0.521**
GaR^{ADS}	**0.565**	**0.741**	**0.926**	**0.678**	**0.565**	**0.573**	0.019	**0.286**	**0.565**	**0.889**
Panel B. Including COVID-19 (2007Q1 to 2020Q4)										
$GaR^{ISPREAD}$	**0.312**	**0.145**	**0.312**	**0.144**	**0.160**	0.028	**0.312**	0.007	**0.160**	0.015
GaR^{EEFR}	**0.547**	0.085	**0.86**	**0.313**	**0.547**	0.001	**0.547**	0.079	**0.547**	0.094
GaR^{RET}	**0.312**	0.000	0.031	0.000	**0.160**	0.000	**0.312**	0.003	0.074	0.001
GaR^{SMB}	**0.86**	0.011	**0.547**	0.000	**0.547**	0.038	**0.312**	0.002	**0.547**	0.016
GaR^{HML}	0.031	0.000	**0.160**	0.000	**0.547**	0.069	0.074	0.000	**0.160**	0.011
GaR^{MOM}	**0.86**	0.000	**0.860**	0.002	0.012	0.000	**0.160**	0.001	**0.160**	0.080
GaR^{VXO}	**0.312**	**0.498**	**0.160**	**0.111**	0.074	0.056	**0.160**	**0.113**	**0.547**	**0.458**
$GaR^{CSPREAD}$	**0.312**	**0.402**	**0.312**	**0.389**	**0.312**	**0.420**	**0.312**	**0.384**	**0.860**	**0.426**
GaR^{TERM}	**0.312**	0.014	**0.547**	**0.129**	**0.547**	0.088	**0.547**	0.074	**0.547**	0.072
GaR^{TED}	0.031	0.039	0.012	0.020	0.031	0.040	0.004	0.003	0.031	0.082
GaR^{ADS}	**0.786**	**0.921**	**0.547**	**0.551**	**0.547**	0.022	**0.208**	**0.432**	**0.547**	**0.776**

Note: This table shows the following two interval tests for different combined GaR models: Kupiec's (1995) unconditional coverage test (UC), where the null hypothesis is that the proportion of exceedances is equal to the quantile (non-rejection of the null is preferred); and the dynamic quantile test (DQ) of Engle and Manganelli (2004), where the null hypothesis is that the exceedance indicator is an i.i.d. process (non-rejection of the null is preferred). Bold values indicate that model passes the test with a 10% level of probability.

Table 3.C4: LASSO-PCA-Q out-of-sample forecast accuracy based on coverage tests

	$h_d = 0$		$h_d = 10$		$h_d = 20$		$h_d = 40$		$h_d = 60$	
	UC	DQ	UC	DQ	UC	DQ	UC	DQ	UC	DQ
Panel A. Before COVID-19 (2007Q1 to 2019Q4)										
$GaR^{ISPREAD}$	**0.926**	**0.226**	**0.717**	**0.227**	**0.926**	**0.16**	**0.926**	0.069	**0.565**	0.050
GaR^{EEFR}	**0.565**	**0.394**	**0.926**	**0.110**	**0.926**	0.025	**0.926**	0.022	**0.717**	0.029
GaR^{RET}	**0.107**	0.050	**0.717**	**0.364**	**0.926**	**0.905**	0.006	0.000	0.018	0.007
GaR^{SMB}	**0.427**	**0.154**	**0.717**	**0.239**	**0.926**	**0.279**	**0.717**	**0.435**	**0.565**	**0.089**
GaR^{HML}	**0.107**	**0.123**	**0.427**	0.009	**0.427**	**0.133**	**0.226**	0.008	**0.427**	**0.336**
GaR^{MOM}	**0.226**	0.084	**0.926**	**0.884**	**0.427**	**0.626**	**0.926**	0.096	0.046	0.006
GaR^{VXO}	**0.107**	**0.481**	**0.226**	**0.570**	**0.226**	**0.382**	**0.107**	**0.189**	**0.717**	**0.711**
$GaR^{CSPREAD}$	**0.717**	**0.146**	**0.717**	**0.148**	**0.926**	**0.923**	**0.926**	**0.925**	**0.565**	**0.929**
GaR^{TERM}	**0.273**	0.003	**0.273**	0.003	**0.926**	**0.200**	**0.565**	0.079	**0.273**	**0.678**
GaR^{TED}	**0.427**	**0.469**	**0.226**	**0.180**	**0.226**	**0.180**	**0.107**	**0.185**	**0.107**	**0.450**
GaR^{ADS}	**0.226**	0.043	**0.427**	0.100	**0.226**	**0.085**	**0.226**	0.014	**0.226**	**0.229**
Panel B. Including COVID-19 (2007Q1 to 2020Q4)										
$GaR^{ISPREAD}$	**0.312**	0.004	**0.160**	0.004	**0.312**	0.001	**0.312**	0.001	**0.547**	0.001
GaR^{EEFR}	**0.547**	0.009	**0.312**	0.002	**0.312**	0.001	**0.312**	0.000	**0.160**	0.002
GaR^{RET}	0.031	0.001	**0.312**	0.046	**0.312**	0.035	0.000	0.000	0.004	0.007
GaR^{SMB}	**0.160**	0.009	**0.160**	0.007	**0.312**	0.028	**0.160**	0.028	**0.547**	0.000
GaR^{HML}	0.031	0.082	0.074	0.000	0.074	0.005	0.031	0.003	0.074	0.041
GaR^{MOM}	0.031	0.038	**0.312**	0.031	0.074	**0.136**	**0.547**	0.037	0.004	0.000
GaR^{VXO}	0.031	0.066	0.074	0.163	0.074	0.074	0.031	0.023	**0.312**	**0.372**
$GaR^{CSPREAD}$	**0.312**	**0.436**	**0.312**	**0.566**	**0.547**	**0.925**	**0.547**	**0.928**	**0.860**	**0.954**
GaR^{TERM}	**0.860**	0.000	**0.860**	0.000	**0.312**	0.006	**0.547**	0.001	**0.860**	0.014
GaR^{TED}	0.074	0.018	0.031	0.002	0.031	0.001	0.012	0.001	0.012	0.015
GaR^{ADS}	0.074	0.001	**0.312**	0.095	0.074	0.023	**0.160**	0.021	0.031	0.004

Note: This table shows the following two interval tests for different combined GaR models: Kupiec's (1995) unconditional coverage test (UC), where the null hypothesis is that the proportion of exceedances is equal to the quantile (non-rejection of the null is preferred); and the dynamic quantile test (DQ) of Engle and Manganelli (2004), where the null hypothesis is that the exceedance indicator is an i.i.d. process (non-rejection of the null is preferred). Bold values indicate that model passes the test with a 10% level of probability.

Table 3.C5: EN-PCA-Q out-of-sample forecast accuracy based on coverage tests

	$h_d = 0$		$h_d = 10$		$h_d = 20$		$h_d = 40$		$h_d = 60$	
	UC	DQ	UC	DQ	UC	DQ	UC	DQ	UC	DQ
Panel A. Before COVID-19 (2007Q1 to 2019Q4)										
$GaR^{ISPREAD}$	**0.717**	**0.422**	**0.717**	**0.256**	**0.926**	**0.159**	**0.926**	0.061	**0.565**	0.054
GaR^{EEFR}	**0.565**	**0.769**	**0.427**	0.060	**0.926**	**0.114**	**0.427**	**0.455**	**0.427**	**0.589**
GaR^{RET}	**0.427**	0.042	**0.427**	**0.507**	**0.226**	0.061	0.006	0.000	0.006	0.002
GaR^{SMB}	**0.427**	**0.607**	0.046	0.001	**0.226**	0.035	**0.226**	**0.219**	**0.926**	0.009
GaR^{HML}	**0.107**	**0.115**	**0.717**	**0.333**	**0.926**	**0.253**	**0.427**	**0.120**	**0.717**	**0.155**
GaR^{MOM}	**0.226**	0.083	**0.717**	0.092	**0.226**	**0.716**	**0.427**	0.003	**0.226**	0.021
GaR^{VXO}	**0.226**	**0.614**	**0.107**	**0.188**	**0.226**	**0.383**	**0.107**	**0.337**	**0.427**	**0.725**
$GaR^{CSPREAD}$	**0.717**	**0.147**	**0.717**	**0.148**	**0.926**	**0.919**	**0.926**	**0.925**	**0.565**	**0.930**
GaR^{TERM}	**0.565**	0.062	**0.273**	0.003	**0.926**	**0.198**	**0.565**	0.074	**0.273**	**0.680**
GaR^{TED}	**0.427**	**0.469**	**0.226**	**0.180**	**0.226**	**0.180**	**0.107**	**0.185**	**0.107**	**0.451**
GaR^{ADS}	**0.107**	0.031	**0.226**	0.096	**0.226**	0.006	**0.226**	0.008	**0.226**	**0.390**
Panel B. Including COVID-19 (2007Q1 to 2020Q4)										
$GaR^{ISPREAD}$	**0.160**	0.010	**0.160**	0.005	**0.312**	0.001	**0.312**	0.001	**0.547**	0.001
GaR^{EEFR}	**0.547**	0.026	0.074	0.002	**0.312**	0.003	0.074	0.011	0.074	0.018
GaR^{RET}	**0.160**	0.005	0.074	0.002	0.031	0.000	0.000	0.000	0.001	0.000
GaR^{SMB}	**0.160**	**0.260**	0.004	0.000	0.031	0.000	0.031	0.009	**0.312**	0.000
GaR^{HML}	0.012	0.001	**0.160**	0.003	**0.312**	0.049	0.074	0.014	**0.160**	0.012
GaR^{MOM}	0.031	**0.254**	**0.160**	0.003	0.031	0.032	**0.160**	0.009	0.031	0.000
GaR^{VXO}	0.031	0.074	0.012	0.004	0.031	0.020	0.031	0.053	**0.160**	**0.388**
$GaR^{CSPREAD}$	**0.160**	0.053	**0.160**	**0.107**	**0.312**	**0.407**	**0.547**	**0.923**	**0.860**	**0.953**
GaR^{TERM}	**0.547**	0.001	**0.860**	0.000	**0.312**	0.003	**0.547**	0.001	**0.860**	0.014
GaR^{TED}	0.074	0.018	0.031	0.002	0.031	0.001	0.012	0.001	0.012	0.016
GaR^{ADS}	0.074	0.029	0.074	0.006	0.074	0.001	0.074	0.003	0.031	**0.109**

Note: This table shows the following two interval tests for different combined GaR models: Kupiec's (1995) unconditional coverage test (UC), where the null hypothesis is that the proportion of exceedances is equal to the quantile (non-rejection of the null is preferred); and the dynamic quantile test (DQ) of Engle and Manganelli (2004), where the null hypothesis is that the exceedance indicator is an i.i.d. process (non-rejection of the null is preferred). Bold values indicate that model passes the test with a 10% level of probability.

4 Daily Unemployment at Risk

4.1 Introduction

A primary task of macroeconomic policymaking is to provide accurate forecasts of the unemployment rate so governments can decide on the most appropriate monetary policy stance to adopt at any given time. This is particularly challenging during episodes of market distress. For instance, at the onset of the Covid-19 pandemic, the Federal Open Market Committee (FOMC) reported that job gains were solid and the U.S. unemployment rate could be expected to remain low (Federal Open Market Committee, 2020). However, during the next quarter, the average unemployment rate spiked at 13%, the highest increase recorded since 1948. This paper seeks to provide real-time daily unemployment nowcasts to inform policymakers at the highest possible frequency about the tail-risks surrounding current or near-future unemployment and, in so doing, contribute to the literature of 'unemployment at risk' (URisk) pioneered by Kiley (2021) and Adams et al. (2021).

We extend the framework developed by Adams et al. (2021). These authors use quantile regressions to construct quarterly predictive distributions of unemployment around the median forecasts of the Survey of Professional Forecasters (SPF), conditional on a quarterly National Financial Conditions Index. This approach has two limitations: $i)$ it fails to incorporate daily flows of information, which have proven to be valuable for monitoring macroeconomic risks in real time (Ferrara et al., 2022); and $ii)$ it ignores the stable relationship between unemployment and economic activity - Okun's Law - widely documented in the literature (Okun, 1962; Ball et al., 2017).

We address these two issues by means of a mixed data sampling quantile (Q-MIDAS) model, which conditions unemployment density on the ADS index, a daily indicator of real economic activity developed by Aruoba et al. (2009) and regularly updated by the Federal Reserve Bank of Philadelphia (FRBP). We center our analysis on the Global Financial Crisis (GFC) and the Covid-19 pandemic.

Our primary motivation here is captured by Figure 4.1, which shows the relationship between quarterly SPF's forecast errors and the real-time daily ADS index. As can be observed, there is a negative relationship between the two variables, which

Figure 4.1: Quarterly SPF's forecast errors and real-time daily ADS index

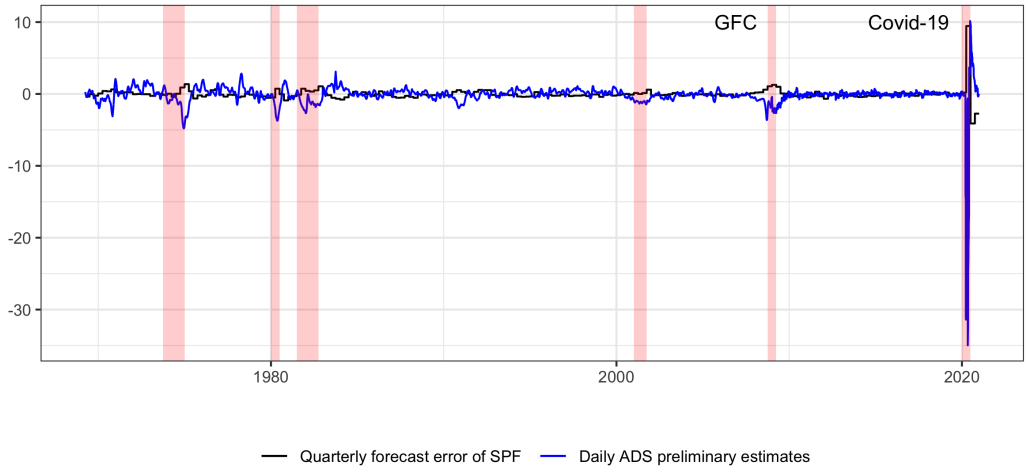

Sources: FRBP and authors' computation.
Note: Time span 1969-04-01 to 2020-12-31. The daily ADS index is calculated using preliminary estimates as they were released at each point in time, so that nowcast can be made in real-time. Shaded areas represent NBER recessions.

is more evident in crisis episodes and we show that this relationship can be used to significantly improve the accuracy of nowcasting exercises to inform policy making.

The rest of the document is organized as follows. Sections 4.2 and 4.3 present our data and methodology, respectively. Section 4.4 presents our main results, while section 4.5 concludes.

4.2 Data

We draw on data from real-time survey forecasts of unemployment provided by the quarterly SPF, as conducted by the FRBP. This survey, carried out since 1990Q3, publishes its forecasts in the middle month of each quarter. For each survey, participants provide quarterly point forecasts for a particular variable for the next five quarters, including the current quarter. Specifically, we use the one-quarter-ahead forecasts for the median unemployment rate from the survey corresponding to the current quarter. For the unemployment rate, which is the target variable, we use the average unemployment rate obtained from the Federal Reserve Bank of St. Louis database (FRED). As for the ADS index, we use weakly vintages starting from November 30, 2008 from the FRBP to conduct the nowcasting exercise. Table 4.1 shows the description of the daily variables used as additional conditioning vari-

ables to construct unemployment nowcasts. Our data sample spans the period from 1969-01-01 to 2020-12-31. In the case of the VXO and CSPREAD, pre-1986 information is unavailable in the corresponding websites. Thus, in the first case, following Bloom (2009), the daily VXO is calculated as the 20-day standard deviation of the S&P500 index normalized to the same mean and variance as the VXO index when they overlap from 1986 onward. In the second case, we use the information provided in the online appendix of Lima et al. (2020).

Table 4.1: Detailed description of variables

Variable	Description	Source
ISPREAD	Interest rate spread between the 10-year government bond rate and the federal fund rate	FRED
VXO	Option-based implied volatility measure of S&P100	FRED
CSPREAD	BAA-AAA corporate bond yield credit spread	FRED
ADS	ADS index vintages collected in real-time from November 30, 2008	FRBP

Source: Authors' elaboration.

4.3 Methodology

We extend the methodology developed by Adams et al. (2021) to accommodate daily predictors in a Q-MIDAS framework.

4.3.1 Parameter proliferation problem

Let $e^{SPF}_{t+1|t}$ denote the one-step-ahead median forecast error from the SPF, such that $e^{SPF}_{t+1|t} = y_{t+1} - y^{SPF}_{t+1|t}$, where y_{t+1} is the unemployment rate at quarter $t+1$ and $y^{SPF}_{t+1|t}$ is the one-step-ahead median SPF forecast of y_{t+1}, given the survey conducted at quarter t. $\boldsymbol{X}^{D}_{t+1} = (x^{0}_{t+1}, x^{1}_{t+1}, \ldots, x^{p-1}_{t+1})'$ is a $p \times 1$ vector of the high-frequency variable available on a daily basis, with $x^{j}_{t+1}, j = (0, 1, 2, \ldots, p-1)$, which is observed d times between quarter $t+1$ and t. In this setup, we consider that conditional quantile of $e^{SPF}_{t+1|t}$ is affected by up to one year ($q = 4$ quarters) of past daily shocks of $\boldsymbol{X}^{D}_{t+1-h_d}$, giving a total number of parameters (including the constant) approximately equal to $K = q \times d + 1 = 4 \times 60 + 1 = 241$, assuming a five-day working week ($d = 60$ days); that is, $\boldsymbol{X}^{D}_{t+1-h_d} = \left(x^{0}_{t+1}, x^{2}_{t+1-\frac{1}{60}}, \ldots, x^{239}_{t+1-\frac{239}{60}}\right)'$. Note that the number of parameters K is relatively larger than the total number of observations T, so we are faced with a parameter proliferation problem, which invalidates the standard estimation procedure of the quantile regression.

4.3.2 MIDAS quantile

In this context, the mixed data sampling quantile (Q-MIDAS) model offers an effective solution to incorporate high-frequency indicators, which relies on a restriction of the form in which the distributed lags of the high frequency variable are included in the quantile regression. Specifically, we consider the Almon lag polynomial as in other recent works (Lima et al., 2020; Mogliani and Simoni, 2021; Ferrara et al., 2022).[1]

Let $\boldsymbol{X}^{D}_{t+1-h_d}$ follows the Almon lag polynomial given by:

$$B\left(L^{\frac{i}{d}};\boldsymbol{\theta_j}(\tau)\right) = \sum_{i=0}^{p-1} b\left(i;\boldsymbol{\theta_j}(\tau)\right) L^{\frac{i}{d}} x^{j}_{t+1}$$

where $L^{\frac{i}{d}} x^{j}_{t+1}$ works as a daily lag operator and $b(i;\boldsymbol{\theta}_j(\tau)) = \sum_{k=0}^{c} \theta_{k,j} i^k$ is the weighting function that depends on the vector of parameters $\boldsymbol{\theta}_j(\tau)$, the lag order $i = (0,1,2,\ldots,p-1)$, and the order of the Almon lag polynomial given by c.

Thus, the $p \times 1$ vector of the high-frequency variable $\boldsymbol{X}^{D}_{t+1-h_d}$, can be transformed based on the following polynomial weighting matrix:

$$Q = \begin{pmatrix} 1 & 1 & 1 & \ldots & 1 \\ 1 & 2 & 3 & \ldots & p^1 \\ \vdots & \vdots & \vdots & \ddots & \vdots \\ 1^c & 2^c & 3^c & \ldots & p^c \end{pmatrix}$$

By multiplying $Q \times \boldsymbol{X}^{D}_{t+1-h_d}$ we get the vector of transformed daily predictors $\widetilde{\boldsymbol{X}}^{D}_{t+1-h_d}$, which enters into our quantile framework. In our specification, we set $c = 3$ (third degree Almon lag), and impose two zero restrictions on the slope and value of the lag polynomial (see Mogliani and Simoni, 2021). This last causes the weighting structure to slowly reduce to zero.

4.3.3 Density forecasts

In the first step, we estimate a Q-MIDAS model using quantile regressions (Koenker and Bassett, 1978):

$$e^{SPF}_{t+1|t} = \alpha_0(\tau) + \widetilde{\boldsymbol{X}'}_{t+1-h_d}\boldsymbol{\phi} + \epsilon_t \tag{4.1}$$

where $\beta(\tau) = (\alpha_0(\tau), \boldsymbol{\phi})'$ denotes the vector of parameters corresponding to the τ-th quantile, and ϵ_t is a random noise. Notice that the forecast error only depends

[1] Since at least Pettenuzzo et al. (2016) many works in the literature have chosen to use the Almon lag polynomial for MIDAS, since it is parsimonious and linear in the parameters.

on the vector of daily information $\widetilde{\boldsymbol{X}}^{D}_{t+1-h_d}$ which is updated until the last day of the next quarter minus h_d days. In this formulation, the forecast horizon is expressed in high-frequency terms, that is, a given day between quarters t and $t+1$.

The predictive value of Equation (4.1),

$$\widehat{Q_\tau}\left(e^{SPF}_{t+1|t} \mid \widetilde{\boldsymbol{X}}^{D}_{t+1-h_d}\right) = \alpha_0(\tau) + \widetilde{\boldsymbol{X}'}_{t+1-h_d}\boldsymbol{\phi} \tag{4.2}$$

produces an estimate of the conditional quantile of $e^{SPF}_{t+1|t}$ conditional on the information contained in the high-frequency variable $\widetilde{\boldsymbol{X}}^{D}_{t+1-h_d}$ for different $\tau = \{0.05, 0.25, 0.75, 0.95\}$. Then, to construct the predicted quantiles for the target variable y_{t+1}, we add the forecast point $y^{SPF}_{t+1|t}$ available at time t:

$$\widehat{Q_\tau}\left(y_{t+1} \mid \widetilde{\boldsymbol{X}}^{D}_{t+1-h_d}\right) = \widehat{Q_\tau}\left(e^{SPF}_{t+1|t} \mid \widetilde{\boldsymbol{X}}^{D}_{t+1-h_d}\right) + y^{SPF}_{t+1|t} \tag{4.3}$$

In the second step, to construct the full conditional probability distribution from our quantile regression estimates, we follow the methodology proposed by Adrian et al. (2019). We consider Azzalini and Capitanio's (2003) four-parameter skew-t distribution with the probability density function given by:

$$f(y;\mu,\sigma,\alpha,v) = \frac{2}{\sigma}t\left(\frac{y-\mu}{\sigma};v\right) * T\left(\alpha\left(\frac{y-\mu}{\sigma};v\right)\sqrt{\frac{v+1}{v+\frac{y-\mu}{\sigma}}};v+1\right) \tag{4.4}$$

where $t(\cdot)$ and $T(\cdot)$ denote the probability density function and cumulative distribution function of the Student's t-distribution, respectively. This distribution is specified by its location μ, scale σ, shape α, and fatness v. In essence, this distribution allows us to capture fat tails and skewness (see Azzalini and Capitanio, 2003).

Finally, for each quarter, we fit a skew-t distribution by choosing the parameters $(\mu_{t+1}, \sigma_{t+1}, \alpha_{t+1}, v_{t+1})$ that minimize the squared differences between our quantile regression estimates and the skew-t implied quantiles for $\tau = \{0.05, 0.25, 0.75, 0.95\}$:

$$(\widehat{\mu_{t+1}}, \widehat{\sigma_{t+1}}, \widehat{\alpha_{t+1}}, \widehat{v_{t+1}}) = \underset{\mu,\sigma,\alpha,v}{\operatorname{argmin}} \sum \left(\widehat{Q_\tau}\left(y_{t+1}\right) - F^{-1}(y;\mu,\sigma,\alpha,v)\right)^2. \tag{4.5}$$

In addition, as a natural benchmark for our estimates, we construct the unconditional predictive distributions based only on the current $y^{SPF}_{t+1|t}$ and the distribution of historical forecast errors (see Reifschneider and Tulip, 2019).[2]

[2]Following Adams et al. (2021), we estimate quantile regressions in Equation 4.1 with only a

4.4 Nowcasting unemployment at risk

Using the ADS index collected in real-time our nowcasting exercise starts on January 1, 1992. Figure 4.2 displays the nowcasts results for the historical quantile estimates, the density nowcasts during the GFC, approximately from 2008Q3 to 2009Q1, and the Covid-19 pandemic, from 20201 to 20203. The historical nowcasts show that our daily quantile estimates capture the dynamic of the unemployment rate (Figure 4.2a). Particularly, during the first of these events, we observe that the model conditioning on the ADS index precisely captures the upside risks in the unemployment rate as the distribution of our model (blue line) moves to the right (Figure 4.2b). Likewise, during the second of these events, the density distribution moves significantly to the right after the onset of the pandemic, coinciding with the Federal Reserve Press Release (Federal Open Market Committee, 2020). Importantly, in the second quarter, the average unemployment rate spiked at 13%, the highest increase recorded since 1948 (Figure 4.2c). Also, the asymmetry of shifts in the density forecasts highlights the differences in unemployment risk over the time span of each event. In the Appendix 4.A, we show the results for the alternative indicators ISPREAD, VXO and CSPREAD.

constant term included in the set of conditioning variables. We then center these estimates around the current $y^{SPF}_{t+1|t}$, and fit the skew-t distribution as in Equation (4.5).

Figure 4.2: Daily nowcasts of ADS index in real time

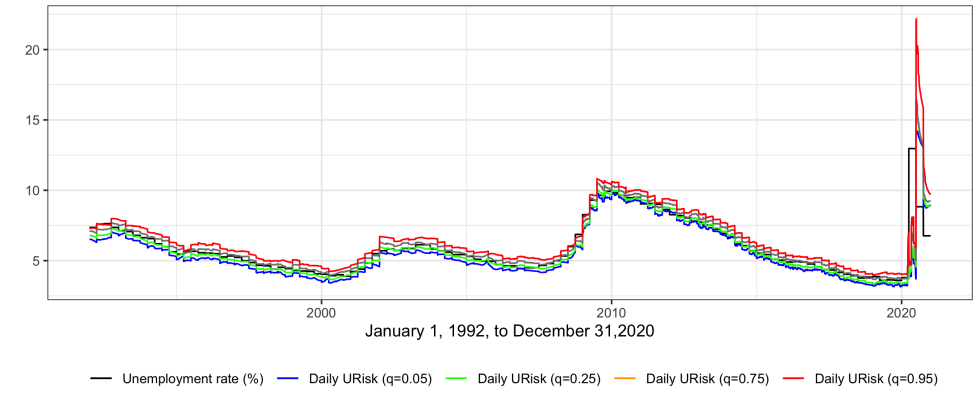

(a) Historical quantile estimates

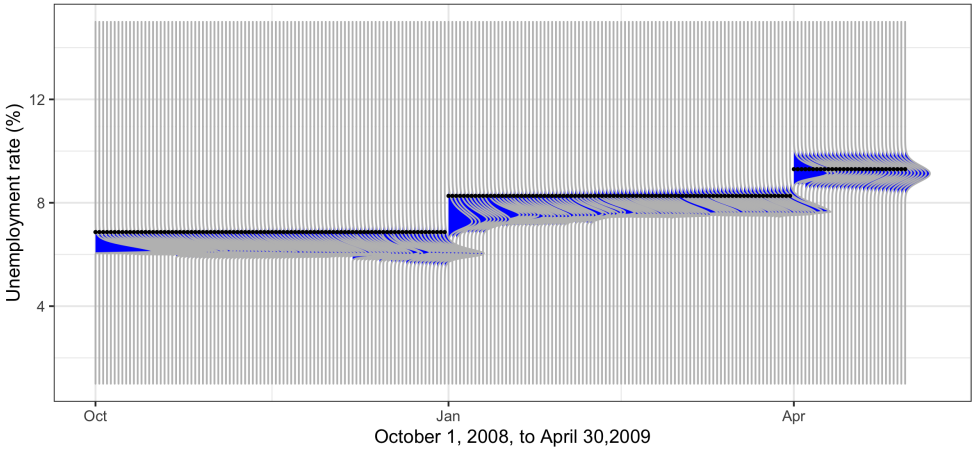

(b) GFC

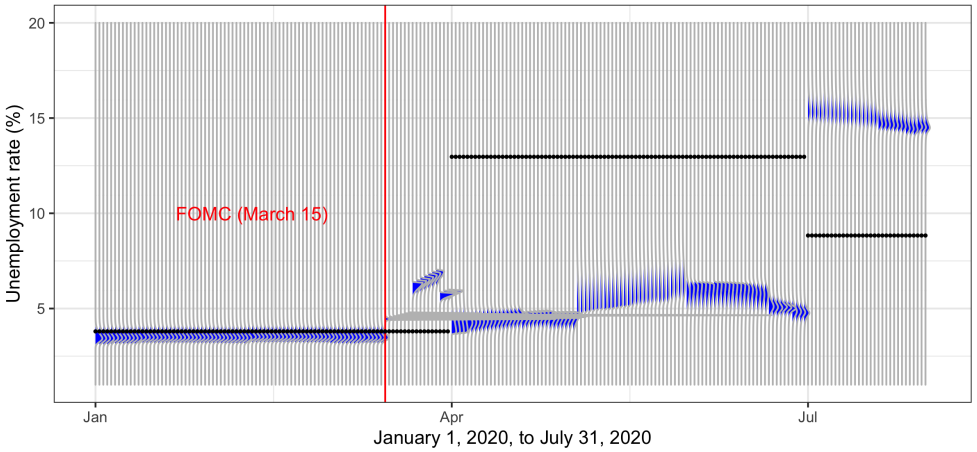

(c) Covid-19

Sources: FRED and authors' computation.
Note: The blue daily density nowcasts correspond to the model that incorporates the ADS as the high-frequency indicator. The black dots indicate the realized value of the unemployment rate in the given quarter.

To assess the accuracy of our daily unemployment nowcasts, we calculate predictive scores by evaluating the model's density at the realized value of the unemployment rate. Table 4.2 reports differences in average log predictive scores between the predictive densities that considers daily predictors and the benchmark distribution of historical forecast errors, for different daily horizons. Positive values indicate a superior average forecasting performance of the densities that incorporate the corresponding daily predictor.

Overall, we find strong support for the superior predictive ability of the ADS index to nowcast the conditional probability distribution of unemployment rate when compared to other daily predictors, for both periods the pre-Covid 19 period and the period including the Covid-19 pandemic (both periods include the GFC). More specifically, it is the only indicator that manages to gauge the increase in unemployment with 40 days' lagged information when the sample period includes the Covid-19 pandemic.

Table 4.2: Evaluation of out-of-sample nowcasts for different daily horizons

	$h_d = 0$	$h_d = 10$	$h_d = 20$	$h_d = 40$	$h_d = 60$
Before COVID-19 (1992Q1 to 2019Q4)					
ISPREAD	**0.008**	**0.015**	**0.015**	-0.033	-0.024
VXO	-0.096	-0.113	-0.128	-0.624	-0.118
CSPREAD	-0.013	-0.006	-0.014	-0.052	-0.079
ADS	**0.12**	**0.059**	**0.172**	**0.194**	**0.195**
Including COVID-19 (1992Q1 to 2020Q4)					
ISPREAD	-0.526	-0.547	-0.212	-0.037	-0.019
VXO	-0.454	-0.938	-0.419	-1.16	-0.499
CSPREAD	-0.026	-0.3	-0.233	-0.07	-0.082
ADS	-1.829	-1.11	-0.426	-0.774	**0.218**

Note: This table reports differences in average log predictive scores. Column names h_d represent the lag of the high frequency daily information (i.e., minus h_d days before the quarter ends).

4.5 Conclusions

We construct daily unemployment at risk around consensus forecasts conditional on the ADS business conditions index, using a Q-MIDAS model. Our results suggest that this indicator $i)$ has better nowcasting properties than those provided by daily

financial conditioning variables, and $ii)$ provides early signal of unemployment rate increases, especially during episodes of distress. Our results are relevant for risk monitoring and nowcasting purposes of central banks and other institutions.

4.A Appendix A

Figure 4.A1: Daily nowcasts of ISPREAD in real time

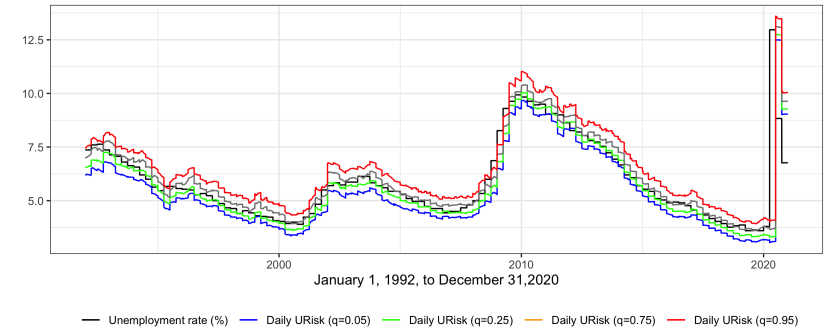

(a) Historical quantile estimates

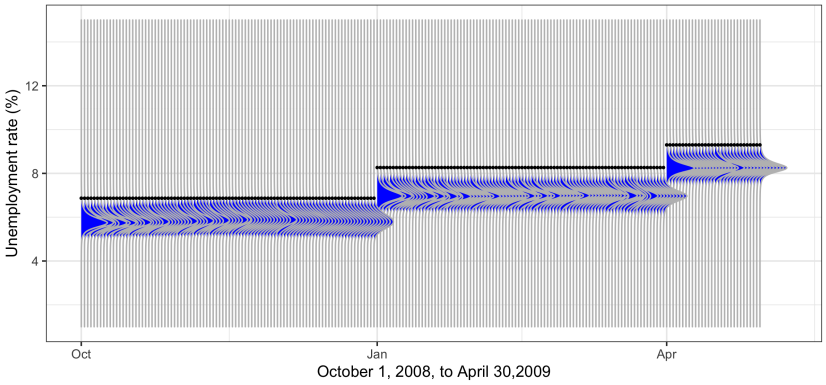

(b) GFC

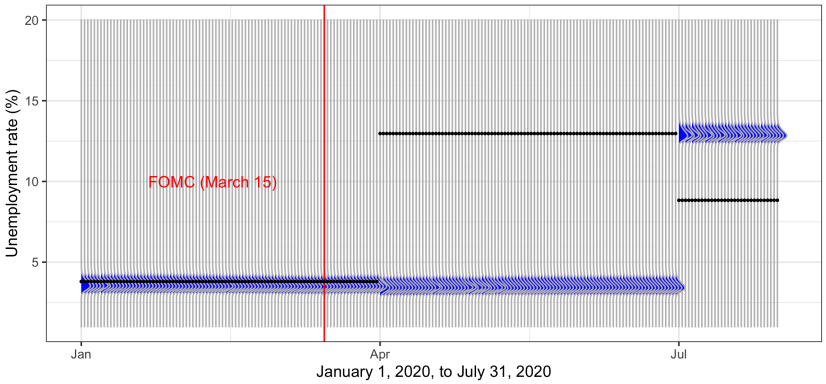

(c) Covid-19

Sources: FRED and authors' computation.
Note: The blue daily density nowcasts correspond to the model that incorporates the ISPREAD as the high-frequency indicator. The black dots indicate the realized value of the unemployment rate in the given quarter.

Figure 4.A2: Daily nowcasts of VXO in real time

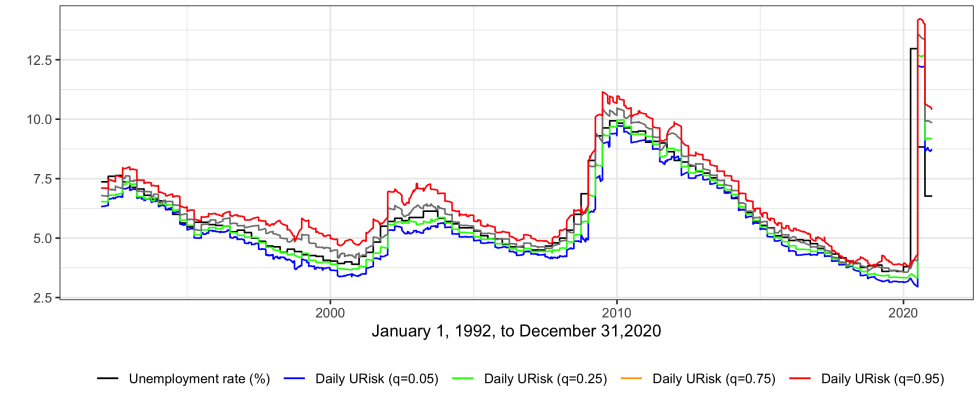

(a) Historical quantile estimates

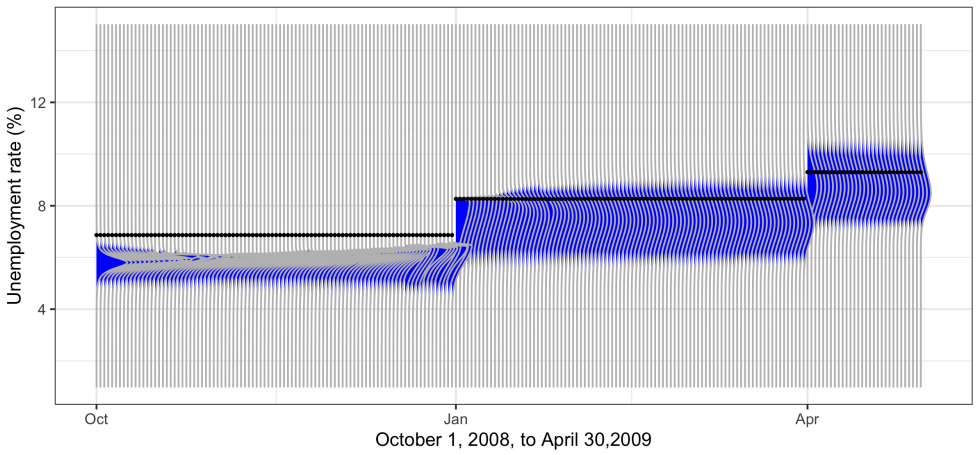

(b) GFC

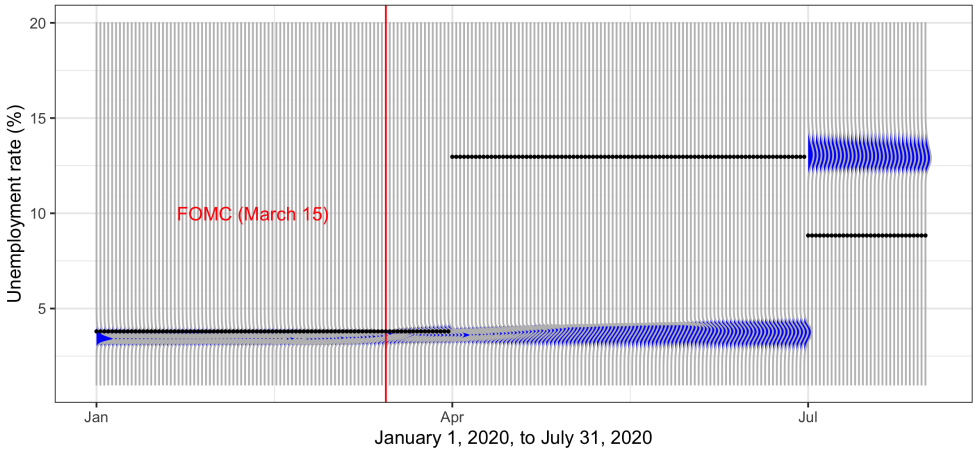

(c) Covid-19

Sources: FRED and authors' computation.
Note: The blue daily density nowcasts correspond to the model that incorporates the VXO as the high-frequency indicator. The black dots indicate the realized value of the unemployment rate in the given quarter.

Figure 4.A3: Daily nowcasts of CSPREAD in real time

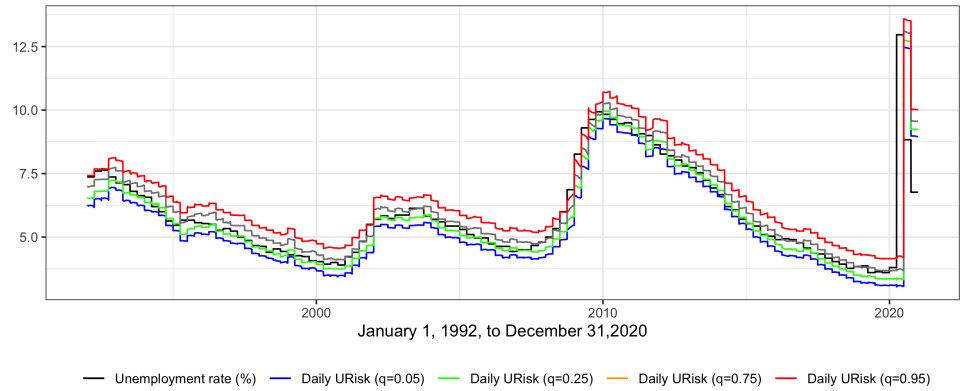

(a) Historical quantile estimates

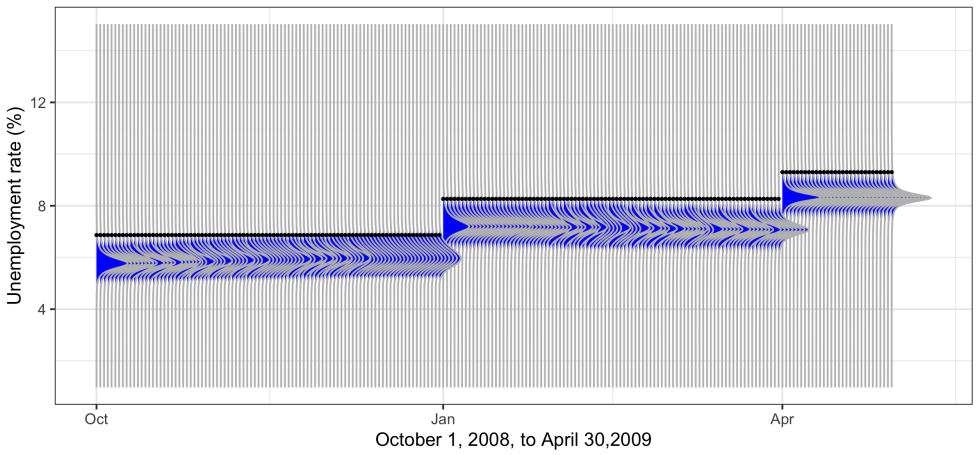

(b) GFC

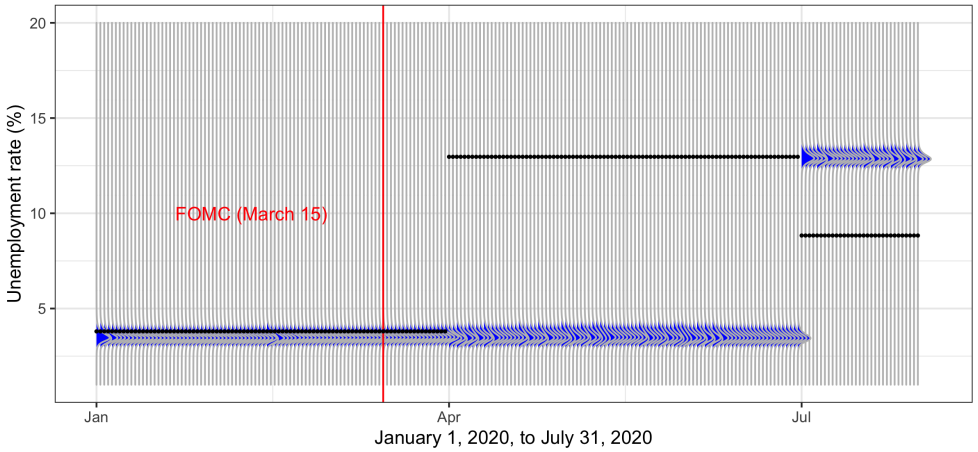

(c) Covid-19

Sources: FRED and authors' computation.
Note: The blue daily density nowcasts correspond to the model that incorporates the CSPREAD as the high-frequency indicator. The black dots indicate the realized value of the unemployment rate in the given quarter.

5 Forecasting Inflation Risk Around the Globe

5.1 Introduction

Traditional inflation predictions can help central banks make their monetary policy decisions; yet, few insights can be provided into the probability of either high or low inflation. As Alan Greenspan (2004), former Governor of the Federal Reserve, has pointed out, a central bank needs to consider "not only the most likely future path for the economy but also the distribution of possible outcomes about that path". To facilitate them in this task, a growing number of studies propose inflation risk indicators based on tail risk measures (Kilian and Manganelli, 2007; Adams et al., 2021; Lopez-Salido and Loria, 2022; Clark et al., 2022; Pfarrhofer, 2022), market-based measures (Kitsul and Wright, 2013; Fleckenstein et al., 2017), and survey-based measures (Adams et al., 2021; Ryngaert, 2022). Of these, indicators based on the distribution of realized inflation have received special attention, as they can be applied to a wider range of countries (see, e.g., Banerjee et al., 2020; Lopez-Salido and Loria, 2022; Pfarrhofer, 2022; Queyranne et al., 2022).[1] Moreover, most of these works rely on quantile regressions that can be fitted on a skew-t distribution (see Adrian et al., 2019; Azzalini and Capitanio, 2003). Yet, while they offer insights on inflation risk measures, they do not study extensively the out-of-sample predictive performance of their measures nor do they consider specific world regions.

Here, by drawing on a broader set of countries and employing state-of-the-art machine learning techniques, I am able to make three contributions to the field. First, I compute inflation density forecasts for a large panel of countries – European (20), North American (15), South American (7), Asian and Oceanian (16), and African (18) (75 in total; see Table 5.A1) – using a set of global factors as predictors. In so doing, I provide evidence that, in general, global inflation factors improve the accuracy of density forecasts. This contrasts with the previous literature which has tended to focus specifically on point estimates (e.g. Ciccarelli

[1] For instance, Banerjee et al. (2020) estimate inflation-at-risk statistics for 41 advanced and emerging market economies, and Queyranne et al. (2022) for seven Middle East and Central Asian countries.

and Mojon, 2010; Kamber and Wong, 2020; Medeiros et al., 2022; Arango-Castillo et al., 2023). I show that a global real economic factor based on commodity prices and a crude oil index is important for the one-year-ahead forecast horizon, thus highlighting the importance of including commodity price indicators as potential predictors, as in Kamber and Wong (2020). Overall, this eclectic approach is supported by evidence that inflation is largely a global phenomenon (e.g. Ciccarelli and Mojon, 2010; Ha et al., 2021; Kamber and Wong, 2020; Arango-Castillo et al., 2023). For instance, Ciccarelli and Mojon (2010) report that the inflation rates of 22 OECD countries have a common component that accounts for approximately 70% of the total variance, while Kamber and Wong (2020) show that global inflation factors and commodity prices play an important role in determining inflation, particularly its cyclical component, among a group of advanced and emerging market economies. Finally, Arango-Castillo et al. (2023) provide further evidence that global factors strongly influence both headline and core inflation in these countries. More recently, Medeiros et al. (2022), in a cross-country setting, corroborate the earlier findings of Ciccarelli and Mojon (2010) and show that global and regional factors are relevant predictors of future inflation. As such, this paper contributes to the literature on forecasting global inflation from a risk perspective.

Second, while most studies in the literature only follow the quantile framework developed by Adrian et al. (2019) to produce density forecasts, I use both quantile regressions and a random forest estimator. Specifically, I show that the latter method provides superior predictive performance, as documented in the literature (see Medeiros et al., 2021, 2022; Goulet Coulombe et al., 2022; Clark et al., 2022). I develop an inflation risk framework using a rolling window following Medeiros et al. (2021, 2022), and extend it to quantile regression methods (Adrian et al., 2019). To compute the density forecasts, I consider the standard quantile regressions (QRs) (Koenker and Bassett, 1978) and the quantile random forest (QRF) estimator developed by Athey et al. (2019), which is an extension of Breiman's (2001) random forest that provides a flexible method for estimating any quantity identified by local moment conditions. The latter method is inspired by the findings of Medeiros et al. (2021, 2022) and Goulet Coulombe et al. (2022), who show that random forest outperforms a wide range of other machine learning methods for forecasting inflation. To assess forecast accuracy, I rely on the quantile-weighted continuous ranked scores (Gneiting and Ranjan, 2011).

Third, using the estimated inflation density forecasts, I am able to derive inflation risk measures – namely, the probability of high and low inflation – across regions (see Lopez-Salido and Loria, 2022; Garratt and Petrella, 2022). Thus, I provide novel evidence of these inflation risk measures across regions for the out-of-sample period. Previous studies have tended to focus on a group of advanced and emerging

market economies (Banerjee et al., 2020; Lopez-Salido and Loria, 2022; Queyranne et al., 2022); however, I find interesting heterogeneous patterns across regions. For example, in Africa, the probability of having high inflation is more persistent and higher than in other regions. This ultimately indicates a systematic issue, as the results suggest that the probability of high inflation in other regions has fallen since 2000. In America and Asia, the probability of high inflation is similar to that in Africa before the Global Financial Crisis (GFC), but after that event the probability displays a downward-sloping trend. In contrast, the probability of deflation or inflation below 0% is, in general, lower than 10% in all regions, except in Europe, where the probability around 2015 was, according to Ha et al. (2021), "unusually persuasive".

The rest of this document is organized as follows. Section 5.2 describes the data and presents details about the construction of the indicators. Section 5.3 explains the framework for forecasting inflation risk. Section 5.4 outlines the models and forecast evaluation scheme. Section 5.5 reports the main findings and Section 5.6 concludes.

5.2 Data

In this section, I present the data sources, calculations and results for the indicators used in this study: namely $i)$ inflation rates, $ii)$ global and regional inflation factors, $iii)$ a real global economic activity factor, $iv)$ a crude oil index; and $v)$ a financial indicator.

Inflation rates. I draw primarily on the large global inflation database in Ha et al. (2021). This dataset contains various inflation measures for multiple countries at different frequencies (monthly, quarterly and annual). Additionally, it provides aggregate measures of inflation, as well as measures of global commodity prices. Specifically, I use the monthly headline Consumer Price Index (CPI) series to construct inflation measures because it has a broader country coverage (83) compared to that of the core CPI series (17) since 1970 (see, Ha et al., 2021).[2] The sample size is restricted to 75 countries from five regions (Europe, Asia and Oceania, Africa, North America, and South America) based on data availability for the period January 1980 to December 2021. Table 5.A1 lists the countries considered in each region.

Global and regional inflation factors. I construct a global common factor

[2]The data have been collected from country-specific sources as well as from multiple organizations. The headline CPI includes all goods and services, while the core CPI does not include the more volatile components of the former, including food and energy.

and five regional factors based on the 75 country-specific inflation rates mentioned above. As in previous studies, I use the monthly year-on-year inflation rates, which, by construction, have no seasonal pattern (see Ciccarelli and Mojon, 2010; Arango-Castillo et al., 2023). One important concern in calculating these factors for the period 1980 to 2021 is that many countries, especially those that have experienced inflationary episodes, share a common trend and high-volatility episodes. To account for the mix of stationary and non-stationary inflation rates, I use the approach developed by Hamilton and Xi (2023). This approach requires filtering each series using Hamilton's filter (Hamilton, 2018), and performing principal component analysis (PCA) on the regression residuals.[3] The authors show that this technique provides similar benefits to those of traditional PCA, albeit with some advantages, such as dealing with some non-stationary series.[4] I apply this procedure to all the dataset and each region, and retain the first principal component. The details of the resulting factors are presented in Appendix 5.A.1. Figure 5.A1a shows the global inflation factor using the simple cross-country average and Hamilton's approach. Relative to the former approach, the latter closely tracks the general movement of inflation while subtracting the trend component. In addition, Figure 5.A1b shows the regional inflation factors using Hamilton's approach.

Real global economic factor. To control for supply-side fluctuations, I consider a real global economic factor based on commodity prices (see Alquist et al., 2020). As pointed out by Kamber and Wong (2020), the influence of global inflation factors may reflect commodity price shocks. This factor closely resembles the factor used in Baumeister and Guérin (2021), inasmuch as I use the same 23 basic industrial and agricultural commodities related directly to the production of final goods and which, as such, are related to real output from World Bank commodity price data.[5] Before conducting the PCA, I normalize each CPI series by the US CPI and take logs. This index has the advantage of arguably being calculated in real-time (the US CPI has a one-month lag) relative to other indicators that are based on industrial production indexes (e.g. Baumeister and Hamilton, 2019) or cost of shipping data (e.g. Kilian, 2009).[6]

Oil prices and global financial conditions. Additionally, to control for other oil

[3] Following Hamilton's suggestion, I run an ordinary least squares (OLS) regression for the two-year-ahead inflation rate and include 12 lags.

[4] Another strategy involves searching for the order of integration of all the countries and transforming them to achieve stationarity (e.g., as in McCracken and Ng, 2016, 2021). One problem with this strategy is that it ends up mixing many $I(0)$ with $I(1)$ series, with different properties (i.e. the acceleration of inflation rather than inflation).

[5] See https://www.worldbank.org/en/research/commodity-markets.

[6] See Baumeister and Guérin (2021) for a full discussion of the forecasting power of different monthly global indicators for forecasting output growth.

and financial shocks, I include two indicators. The first is the World Bank crude oil price index, measured as the average of WTI, Brent, and Dubai crude oil prices. In this case, the log difference of this variable is used. The second is the VIX index, used as a proxy of the global financial cycle (see Rey, 2015), and which is a measure of uncertainty and risk aversion in the financial markets.

5.3 Forecasting inflation risk framework

This section presents the general forecasting framework, which is similar to that used by Medeiros et al. (2021, 2022). More specifically, however, I extend it to QRs, as in Adrian et al. (2019). Finally, I derive two measures of inflation risk (see Garratt and Petrella, 2022; Lopez-Salido and Loria, 2022).

In the spirit of Stock and Watson (2002), let $\pi^h_{i,t+h}$ be the annualized monthly average inflation rate,

$$\pi^h_{i,t+h} = (1200/h)/ln(P_{i,t+h}/P_{i,t}), \tag{5.1}$$

where $h = 1, ..., H$ denotes the forecast horizon, $t = 1, ..., T$ the time period, $i = 1, ..., N$ the country-specific index, and $P_{i,t}$ the headline CPI for country i at time t.

To characterize the τ-quantile of the distribution of future inflation $\pi^h_{i,t+h}$ on a d-dimension vector X_{it} of predictors, I consider the following general model:

$$\pi^h_{i,t+h} = Q_{h,\tau}(X_{i,t}) + u_{i,t}, \tag{5.2}$$

where $Q_{h,\tau}(.)$ is the target quantile function that relates covariates and the distribution of future inflation; and $u_{i,t}$ is an zero-mean $i.i.d$ error term. For each country, the target quantile function could be linear or nonlinear and have a different set of covariates, but it is the same for each forecasting horizon.

The forecast equation is given by

$$\widehat{Q}_{t+h|t,\tau}(\pi^h_{i,t+h}|X_{i,t}) = \widehat{Q}_{t-R_h+1:t,\tau}(X_{i,t}), \tag{5.3}$$

where $\widehat{Q}_{t+h|t,\tau}(\pi^h_{i,t+h}|X_{i,t})$ is an estimate of the future quantile function of $\pi^h_{i,t+h}$ for $\tau = \{0.05, 0.25, 0.50, 0.75, 0.95\}$ conditional on the data observed from $t - R_h + 1$ to t, where R_h is the window size. Importantly, the forecasts are based on a rolling-window framework in line with Medeiros et al. (2021, 2022). In this case, the number of observations for the in-sample estimation window is $R_h = 240 - p + 1$, where p is the is number of lags considered in the model.[7] This

[7] In all cases, due to the training procedure of Hamilton's filter explained ebove (Hamilton, 2018), the sample size decreases by 36, because we use the two-year-ahead inflation (24 months)

rolling-window scheme is especially relevant for forecasting inflation around multiple countries as it attenuates the effects of potentially structural breaks and it avoids problems of running superior predictive performance tests (for a complete discussion, see, Corradi and Swanson (2006) and Clark and McCracken (2013)).

Using the quantile forecasts from Eq. (5.3), the full conditional probability distribution can be constructed. I follow the methodology proposed by Adrian et al. (2019) and consider the Azzalini and Capitanio (2003) four-parameter skew-t distribution with the probability density function given by:

$$f(\pi;\mu,\sigma,\alpha,v) = \frac{2}{\sigma} t\left(\frac{\pi-\mu}{\sigma};v\right) * T\left(\alpha\left(\frac{\pi-\mu}{\sigma};v\right)\sqrt{\frac{v+1}{v+\frac{\pi-\mu}{\sigma}}};v+1\right), \quad (5.4)$$

where $t(\cdot)$ and $T(\cdot)$ denote the probability density function and cumulative distribution function of the Student's t-distribution, respectively. This distribution is specified by its location μ, scale σ, shape α, and fatness v. This distribution, moreover, has the distinctive characteristic of capturing fat tails and skewness (see Azzalini and Capitanio, 2003), which are relevant from a risk-management perspective.

Subsequently, for each forecasting horizon and country, the skew-t distribution is fitted by choosing the parameters (μ,σ,α,v) that minimize the squared differences between the quantile regression estimates and the skew-t implied quantiles for $\tau = \{0.05, 0.25, 0.50, 0.75, 0.95\}$:

$$(\widehat{\mu},\widehat{\sigma},\widehat{\alpha},\widehat{v}) = \underset{\mu,\sigma,\alpha,v}{\operatorname{argmin}} \sum \left(\widehat{Q}_{t-R_h+1:t,\tau}(X_{i,t}) - F^{-1}(\pi^h_{i,t+h};\mu,\sigma,\alpha,v)\right)^2. \quad (5.5)$$

Finally, I consider two measures of probability events for gauging inflation risk events: i) inflation-at-risk (IaR_h) defined as the probability where π^h_{t+h} falls above certain threshold π^*; and ii) deflation-at-risk (DaR_h) defined as the probability where π^h_{t+h} falls below certain threshold π^*. Galbraith and Norden (2012), Lopez-Salido and Loria (2022) and Garratt and Petrella (2022) consider similar probabilities measures. While other risk measures are considered in the literature (e.g. Kilian and Manganelli, 2007; Garratt and Petrella, 2022), these probability measures are widely used by market participants, policy makers and organizations (see Gneiting (2008) for a discussion). Some examples of this type of publicly available information can be found in the Survey of Professional Forecasters, which provides survey-based estimates for the probabilities of inflation rates, and the Federal Reserve Bank of Minneapolis's market-based probabilities, which provide implicit

and the 12 lags in the auxiliary OLS regression.

probabilities based on market indicators. However, in both cases, the information is restricted to a number of developed countries. Here, by contrast, I measure these probabilities for a wide range of countries around the world.

Formally, the conditional probability that the h-step-ahead inflation conditional on $X_{i,t}$ is greater than certain threshold π^* is,

$$IaR_h = P(\pi^h_{i,t+h} > \pi^* | X_{i,t}), \tag{5.6}$$

with the probability density,

$$\int_{\pi^*}^{\infty} f(\pi^h_{i,t+h} | X_{i,t}, \widehat{\mu}, \widehat{\sigma}, \widehat{\alpha}, \widehat{v}) d\pi_{i,t+h}. \tag{5.7}$$

Eq. (5.7) defines the risk measures as the integral of the skew-t density function over a specified threshold conditional on a vector $X_{i,t}$ and the skew-t parameters. Conversely, DaR_h is defined by changing the sign of the inequality inside Eq. (5.6), and setting the lower limit of the integral to $-\infty$ and its upper limit to π^* in Eq. (5.7).

5.4 Models and evaluation

5.4.1 Quantile Regression

As in the standard growth-at-risk framework developed by Adrian et al. (2019), I rely on quantile regressions (QRs) (Koenker and Bassett, 1978). In this setting, the vector of parameters $\beta_{i,\tau}$ is chosen to minimize the following loss function:

$$\beta_{i,\tau} = \frac{1}{T} \sum_{t}^{T} \left[\rho_\tau \left(\pi^h_{i,t+h} - X'_{i,t} \beta_{i,\tau} \right) \right] \tag{5.8}$$

where $\rho_\tau(\epsilon_t) = u_{i,t}(\tau - 1(u_{i,t} < 0)$, with $1(\epsilon_t < 0)$ taking a value of 1 when the subscript is true and 0 otherwise (for details regarding the estimation, see Koenker (2005)).

The forecast equation is given by:

$$\widehat{Q}_{t+h,\tau}(\pi^h_{i,t+h} | X_{i,t}) = X'_{i,t} \widehat{\beta}_{i,\tau}. \tag{5.9}$$

Koenker and Bassett (1978) further prove that $\widehat{Q}_{t+h,\tau}(\pi_{i,t+h} | X_{i,t})$ is a consistent linear estimator of the quantile function of $\pi_{i,t+h}$ conditional on $X_{i,t}$.[8]

[8] Since quantile forecasts are not necessarily monotone, I rearrange them so that they are always monotone (Chernozhukov et al., 2009).

5.4.2 Quantile Random Forest

I use QRF regressions based on the method proposed by Athey et al. (2019) and as used by Coulombe et al. (2022). This method extends Breiman's (2001) random forests into a flexible method for estimating any quantity identified by local moment conditions. Specifically, Athey et al. (2019) propose building a forest using a splitting scheme that is sensitive to changes in any of the quantiles of interest. Their strategy of simultaneously estimating different quantiles has been shown to be computationally efficient and to eliminate the risk of crossing quantiles, which is a critical issue when forecasting multiple quantiles.

For each country and forecasting horizon, let $\{\pi_s, X_s\}$ be an independent sample of the inflation rate and its covariates, indexed by $s = 1, ..., S$. The forest-based estimates are obtained by solving the following minimization problem:

$$(\widehat{\theta}_\tau(x), \widehat{v}(x)) = argmin_{\theta_\tau, v} \| \sum_{s=1}^{S} \alpha_s(x) \psi_\theta(\pi_s) \|_2, \tag{5.10}$$

with weights,

$$\alpha_{bs} = \frac{1(\{X_s \in L_B(x) | X_s = x\})}{|L_B(x)|}, \alpha_s(x) = \frac{1}{B} \sum_{b=1}^{B} \alpha_{bs}(x), \tag{5.11}$$

where $\psi_\theta(\pi_s) = \tau 1(\pi_s > \theta_\tau) - (1-\tau)1(\pi_s <= \theta_\tau)$ is the quantile loss function, with θ_τ being the conditional quantiles of π_s; $v(x)$ refers to an optional nuisance parameter; and $\alpha_s(x)$ is the weighting function. Eq. (5.11) further defines the random forest weighting function as a forest-based neighborhood of x. The algorithm grows b trees indexed by $b = 1, ..., B$ and, for each such tree, it defines $L_b(x)$ as the set of training samples that falls into the same leaf as x (e.g. see Figure 5.1). Intuitively, the gradient-based QR trees separate observations that fall above the τ-th quantile of the parent node from those below it, and label each observation by the interval into which they fall. Then, it finds the best split for a particular node given x (see Athey et al. (2019), for details on the splitting scheme and the algorithm).

In this setting, the forecast equation (5.3) is computed as the quantiles of the weighted leaves that share a leaf with the test sample:

$$\widehat{F}(\pi^h_{i,t+h} | X_{i,t}) = \frac{1}{B} \sum_{b=1}^{B} \alpha_{bs}(x) 1(\pi^h_{i,t+h} <= \widehat{\theta}_\tau(x)) \tag{5.12}$$

where,

$$\widehat{Q}(\pi^h_{i,t+h} | X_{i,t}) = inf\{\pi^h_{i,t+h} : \widehat{F}(\pi^h_{i,t+h} | X_{i,t}) >= \tau\}. \tag{5.13}$$

For the computation of this model, I use the standard parameters suggest by Athey et al. (2019).[9] I set the number of bootstrapping samples B (trees) to 2000. This is four times larger than the bootstrap sample used in Meinshausen (2006) to build QRF regressions. The fraction of the data used to grow each tree is set to 0.5, and following "honesty" splitting, it is further cut by a factor of 0.5. The algorithm tries $min\{\lceil(\sqrt{p}+20)\rceil, p\}$ variables for each splitting, where p is the number of covariates.

Figure 5.1: Example of a random tree

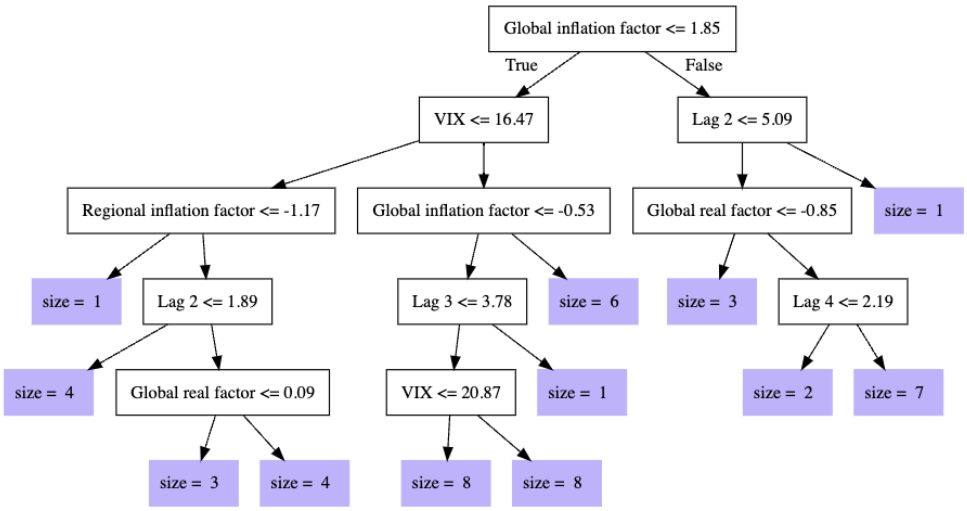

Note: Random computed tree using all covariates (see Section 5.4.3).

5.4.3 Summary of models and information sets

Table 5.1 shows the different specifications of $X_{i,t}$ considered for each country and forecasting horizon. For the two models, i.e., QRs and QRFs, I consider four variable sets. The baseline model is an autoregressive (AR) quantile model that includes four lags of the dependent variable. This model ultimately serves as a benchmark for the empirical analysis. The second model is the Cicarelli and Mojon model (CM1) (2010), which includes a global inflation factor π^g and a regional inflation factor π^r_t corresponding to the country's region. Medeiros et al. (2022) consider a similar version of the CM1 model. The third model (CM2) includes the global real indicator based on commodity prices g_t, and the crude oil price index

[9] I use the "grf" R package available at https://grf-labs.github.io/grf/index.html.

oil_t. Finally, the last model (CM3) incorporates the VIX indicator to capture the global financial cycle.

5.4.4 Forecast evaluation

To assess the accuracy of the quantile density forecasts based on the skew-t distribution (see Eq. (5.5)), I rely on the quantile weighted continuous ranked probability score (CRPS) (see Gneiting and Ranjan, 2011). This measured is used widely in the literature to asses quantile density forecasts (e.g. see Pfarrhofer, 2022; Ferrara et al., 2022; Carriero et al., 2022).

First, I define the quantile score (QS), which is a common metric used for evaluating a specific quantile forecast (see Gneiting and Raftery, 2007; Giacomini and Komunjer, 2005), as follows,

$$QS_{t+h,\tau} = (\widehat{Q}_{t+h,\tau} - \pi^h_{t+h})(1(\widehat{Q}_{t+h,\tau} < \pi^h_{t+h}) - \tau), \tag{5.14}$$

where π^h_{t+h} refers to the actual inflation rate observed at $t+h$, $\widehat{Q}_{t+h,\tau}$ is the estimated quantile forecast based on the skew-t density distribution (see Eq. (5.5)), and $1(\widehat{Q}_{t+h,\tau} < \pi^h_{t+h})$ is the indicator function that takes a value of 1 if the outcome is below the forecast quantile and 0 otherwise.

Then, I define the quantile weighted CRPS (Gneiting and Ranjan, 2011),

$$CRPS_{t+h} = \int 2w(\tau)QS_{t+h,\tau}d\tau \tag{5.15}$$

where $w(\tau)$ is the weighting scheme considered by Gneiting and Ranjan (2011). Following the authors, I consider five different weighting schemes to emphasize specific parts of the distribution: $i)$ equal $w(\tau) = 1$; $ii)$ tails $w(\tau) = (2\tau - 1)^2$; $iii)$ left tail $w(\tau) = (\tau - 1)^2$; $iv)$ center $w(\tau) = \tau(\tau - 1)^2$; and $v)$ right tail $w(\tau) = \tau^2$. Finally, I assess the statistically significance of the tests using the Diebold and Mariano (DM) (1995) test for equality of the average loss.[10] I conduct the tests on a one-sided basis, so that the alternative hypothesis is that the indicated forecast is more accurate than the benchmark.

5.5 Empirical analysis

In this section, I present the results of the out-of-sample exercise for the forecasting horizon of $h = \{1, 12\}$, across all 75 countries. Due to space constraints, the analysis mainly focuses on the shortest horizon ($h = 1$) and the longest horizons

[10] I use the bias correction of the DM test statistic given by Harvey et al. (1997).

Table 5.1: Summary of models and information sets

Mame	Model	Variable sets
QR-AR	Quantile regression	$X_{i,t} = [\{\pi_{i,t-j}\}_{j=o}^{4-1}]'$
QR-CM1	Quantile regression	$X_{i,t} = [\{\pi_{i,t-j}\}_{j=o}^{4-1}, \pi_t^g, \pi_t^r]'$
QR-CM2	Quantile regression	$X_{i,t} = [\{\pi_{i,t-j}\}_{j=o}^{4-1}, \pi_t^g, \pi_t^r, g_t, oil_t]'$
QR-CM3	Quantile regression	$X_{i,t} = [\{\pi_{i,t-j}\}_{j=o}^{4-1}, \pi_t^g, \pi_t^r, g_t, oil_t, VIX_t]'$
QRF-AR	Quantile random forest	$X_{i,t} = [\{\pi_{i,t-j}\}_{j=o}^{4-1}]'$
QRF-CM1	Quantile random forest	$X_{i,t} = [\{\pi_{i,t-j}\}_{j=o}^{4-1}, \pi_t^g, \pi_t^r]'$
QRF-CM2	Quantile random forest	$X_{i,t} = [\{\pi_{i,t-j}\}_{j=o}^{4-1}, \pi_t^g, \pi_t^r, g_t, oil_t]'$
QRF-CM3	Quantile random forest	$X_{i,t} = [\{\pi_{i,t-j}\}_{j=o}^{4-1}, \pi_t^g, \pi_t^r, g_t, oil_t, VIX_t]'$

($h = 12$).[11] The out-of-sample evaluation window runs from January 2000 to December 2021. Regardless of the model, all factors are estimated recursively using a rolling window. I begin by providing an overview of the accuracy of all models compared to a QR-AR benchmark model. Then, I seek to explain the results for the best model by disaggregating the role of the temporal, cross-sectional, and variable importance spectra. Finally, I present the inflation risk indicators, namely, the probability of low and high inflation around the globe.

5.5.1 Aggregate forecast evaluation

Table 5.2 reports the global forecasting results as summary statistics across all models and horizons under consideration. Each row denotes the variable set and the two models considered, namely, QRs and QRFs. Columns (1) to (5) report the average CRPS ratios for different weighting schemes: equal, center, tails, right, and left. For these columns, the rows containing QR-AR models show only the average CRPS value across all countries, while the other rows display the average CRPS ratios across all countries, where the ratios are computed between the model of interest and the QR-AR model as a benchmark. Columns (7), (8), and (9) report the percentage of countries that have a DM test p-value below 10%. For each country, the DM test is conducted on a one-sided basis, so that the alternative hypothesis is that the indicated model is more accurate than the benchmark (a rejection of the null is preferred). The best results for each horizon are highlighted in bold.

Four conclusions can be drawn from Table 5.2. First, in general, QRF offers a more accurate performance than that offered by QR models. These results are in

[11] For example, Lopez-Salido and Loria (2022) focus their analysis on the one-year-ahead inflation rate.

line with those of Medeiros et al. (2021, 2022) and Goulet Coulombe et al. (2022), in which non-linearities derived from random forest models are important for forecasting macroeconomic series, such as the inflation rate. This is the case for all the weighting schemes considered. Second, the gains associated with incorporating the additional set of variables are most frequently found when QRF is used. In this sense, the percentage of countries that outperform the benchmark increases when QRF is applied, relative to QR. This effect is notably higher for the one year-ahead forecasting horizon. Third, global inflation factors, global real factors, and oil price shocks are relevant, depending on the forecasting horizon. In the case of the short forecasting horizon ($h = 1$), the QRF-CM1 model generally has the lowest average CRPS ratio and the highest percentage of countries for which it is statistically better than the benchmark. In the case of the longest horizon ($h = 12$), the QRF-CM2 model, which considers the global real factor and the oil price index, has the highest percentage of countries that outperform the benchmark, independent of the weighting scheme. The gains are substantial, with an increase of more than 10 percentage points across weighting schemes. Also, this model has the lowest average CRPS ratio across all weighting schemes. Finally, I find no supporting evidence of the role of a global financial indicator, such as the VIX, in forecasting the country-specific inflation rates. Indeed, once the global real factor and the oil price index are included in the equation, its effect tends to weaken the forecasting accuracy.

In summary, the results further support the evidence that inflation is a global phenomenon and that, on average, there are important forecasting gains to be made by including global inflation factors (Ciccarelli and Mojon, 2010; Arango-Castillo et al., 2023; Medeiros et al., 2022). Additionally, in general, I find that the global real factors and the oil price index are relevant for forecasting longer horizons, such as the one-year-ahead inflation rate. As Kamber and Wong (2020) point out, commodity price shocks are important for explaining future inflation. The results also suggest that global real factors are not only important for forecasting a nation's GDP growth (Baumeister and Guérin, 2021; Alquist et al., 2020), but also for predicting national inflation rates.

5.5.2 Where do the cross-sectional gains come from?

To disentangle the cross-sectional gains, I present the distribution of the CRPS ratios across the regions' forecasting horizons. As in Section 5.5.1, these ratios are computed between the model of interest and the QR-AR benchmark model. Figures 5.2 and 5.3 show the CRPS ratios with the three weighting schemes obtained, when using the best model of each forecasting horizon $h = \{1, 12\}$, respectively. The best model for $h = 1$ is QRF-CM1; for $h = 12$, it is QRF-CM2 (see Section 5.5.1). The

Table 5.2: Aggregate forecasting results

Models	Weighting schemes					DM test		
	(2)	(3)	(4)	(5)	(6)	(7)	(8)	(9)
	Equal	Center	Tails	Right	Left	Equal	Right	left
				$h = 1$				
QR-AR	4.033	0.715	1.172	1.377	1.225	-	-	-
QR-CM1	0.990	0.989	0.991	0.990	0.990	30.7	24.0	26.7
QR-CM2	0.996	0.994	1.001	1.000	0.994	21.3	17.3	17.3
QR-CM3	1.004	1.001	1.011	1.009	1.001	17.3	9.3	18.7
QRF-AR	0.984	0.986	**0.977**	0.988	0.976	38.7	33.3	38.7
QRF-CM1	**0.983**	**0.985**	0.978	0.988	**0.974**	**46.7**	**44.0**	**44.0**
QRF-CM2	0.988	0.990	0.984	**0.997**	0.975	44.0	33.3	42.7
QRF-CM3	0.991	0.993	0.986	1.002	0.976	41.3	33.3	42.7
				$h = 12$				
QR-AR	1.830	0.325	0.529	0.654	0.525	-	-	-
QR-CM1	1.085	1.075	1.111	1.059	1.129	8.0	12.0	9.3
QR-CM2	1.066	1.055	1.093	1.039	1.110	9.3	18.7	9.3
QR-CM3	1.094	1.083	1.122	1.063	1.145	9.3	16.0	5.3
QRF-AR	1.020	1.017	1.029	1.003	1.050	33.3	37.3	20.0
QRF-CM1	0.991	0.992	0.989	0.984	1.000	36.0	40.0	32.0
QRF-CM2	**0.972**	**0.975**	**0.967**	**0.970**	**0.974**	**49.3**	**50.7**	**45.3**
QRF-CM3	0.981	0.985	0.971	0.982	0.977	44.0	44.0	44.0

Note: The table reports summary statistics for out-of-sample forecast accuracy for each model, computed across 75 countries. The out-of-sample evaluation window runs from December 2000 to December 2021. Columns (1) to (5) report the average CRPS for different weighting schemes: equal, center, tails, right, and left. For these columns, the rows containing QR-AR models show the average CRPS value across all countries, while the other rows display the ratios of the average CRPS across all countries, where the ratios are computed between the model of interest and the QR-AR benchmark model. Columns (7), (8), and (9) report the percentage of countries that have a DM test p-value below 10%. For each country, the DM test is conducted on a one-sided basis, so that the alternative hypothesis is that the indicated model is more accurate than the benchmark (a rejection of the null is preferred). The best results for each horizon are highlighted in bold.

benchmark model for both is the QR-AR. For each region, green indicates that the model has a lower CRPS ratio than that of the benchmark (QR-AR), while red indicates a higher CRPS ratio. Interestingly, in the case of Europe, Africa, and Asia and Oceania, more than half the countries are better explained by global factors, regardless of the horizon. In the case of North and South America, results are more balanced. This landscape is generally the same across weighting schemes.

5.5.3 Where do the temporal gains come from?

In this section, I examine the temporal distribution of CRPS ratios using an equal weighting scheme for all forecasting horizons.[12] Figure 5.4 plots the median and interquartile range of the CRPS ratio distribution at each time for the best model corresponding to each forecast horizon. Panel 5.4a shows the results for $h = 1$ computed by QRF-CM1, and Panel 5.4b the results for $h = 12$ computed by the QRF-CM2. While this approach does not allow conclusions to be drawn about the CRPS ratio for any particular country, it provides a more general overview of the predictive capability of the best model compared to the QR-AR benchmark over time. In the case of forecasting horizon $h = 1$, results show that the relative advantage of QRF-CM1 is more stable across time and the different quantiles. In contrast, in the case of forecasting horizon $h = 12$, there is a clear pattern for some periods of time where QRF-CM2 offers a greater advantage over QR-AR.

Figure 5.2: Forecast accuracy across countries for $h = 1$

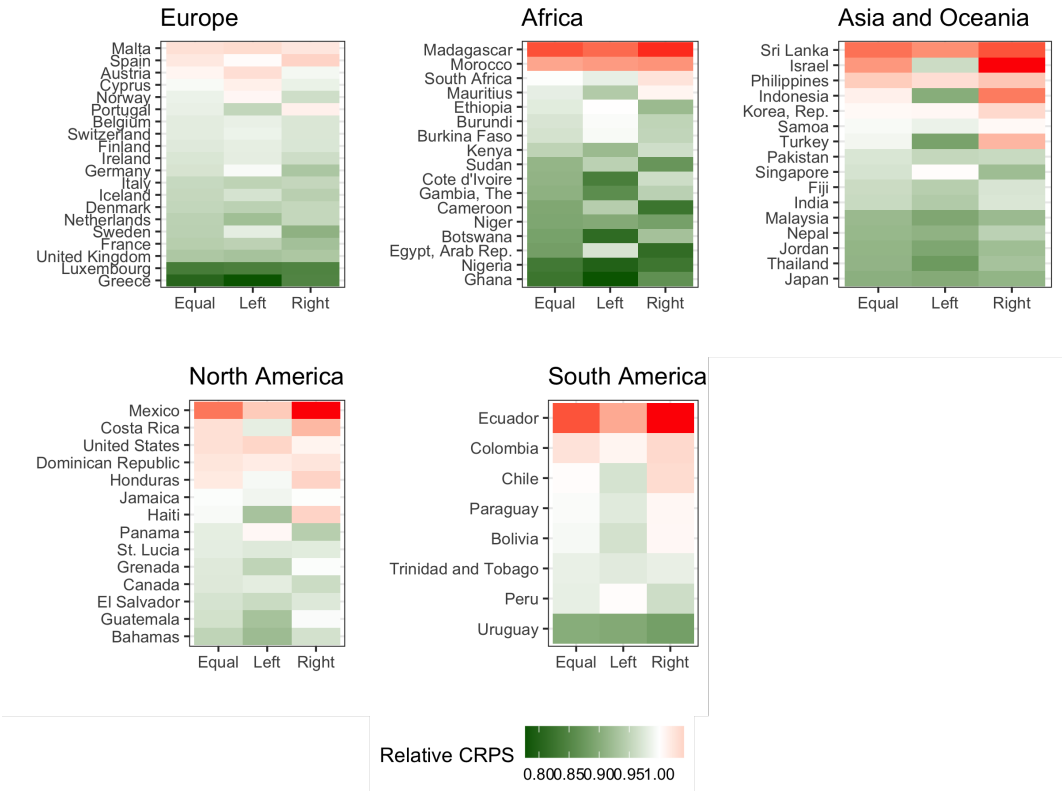

This figure shows for the QRF-CM1 model and $h = 1$, the CRPS ratios across all countries, computed between the QRF-CM1 model and the QR-AR model as a benchmark. Green (red) blocks show that the given model has a lower (higher) CRPS than that of the benchmark (QR-AR).

[12] Results are largely unaltered when using other weighting schemes.

Figure 5.3: Forecast accuracy across countries for $h = 12$

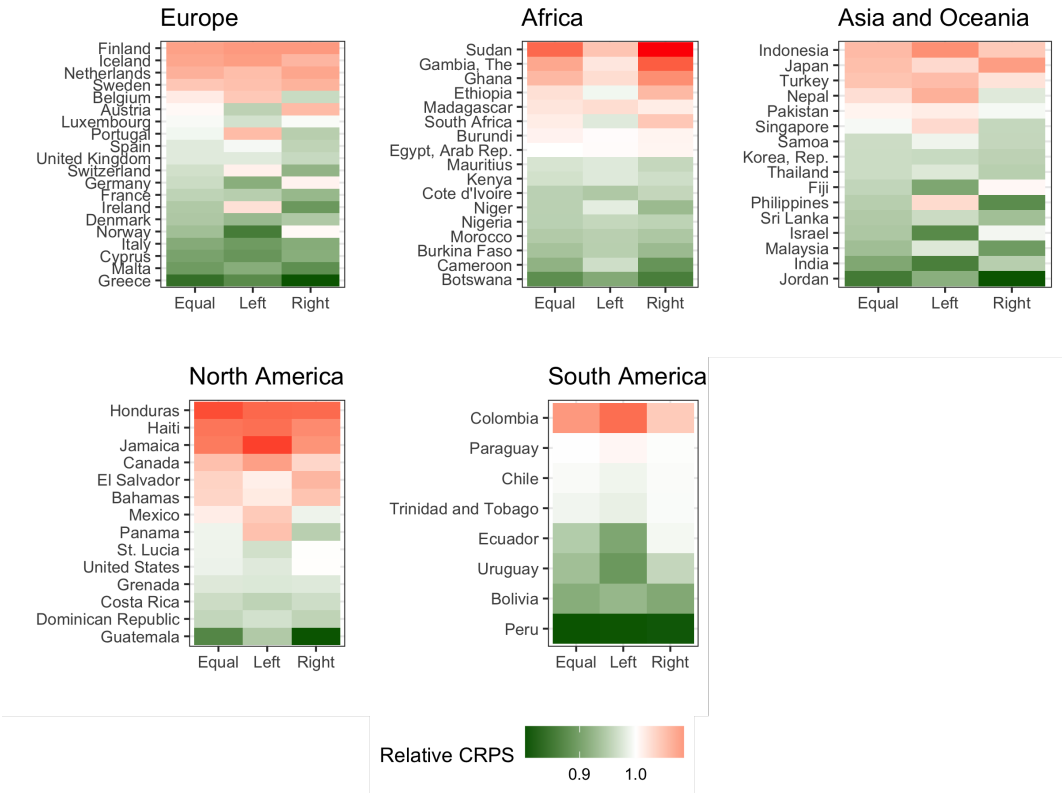

Note: This figure shows for the QRF-CM2 model and h = 12, the CRPS ratio across all countries, computed between the QRF-CM2 model and the QR-AR model as a benchmark. Green (red) blocks show that the given model has a lower (higher) CRPS than that of the benchmark (QR-AR).

Figure 5.4: Forecast accuracy across time

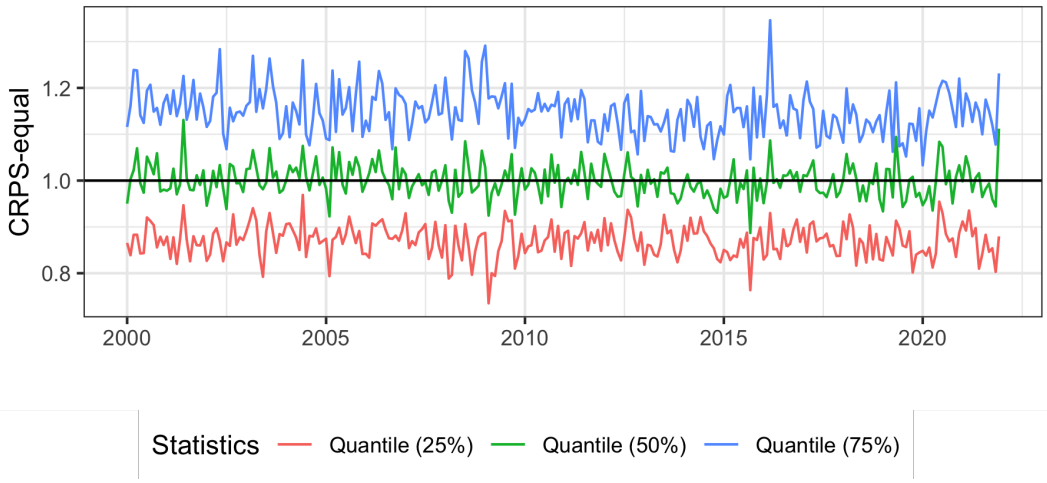

(a) QRF-CM1 for $h = 1$

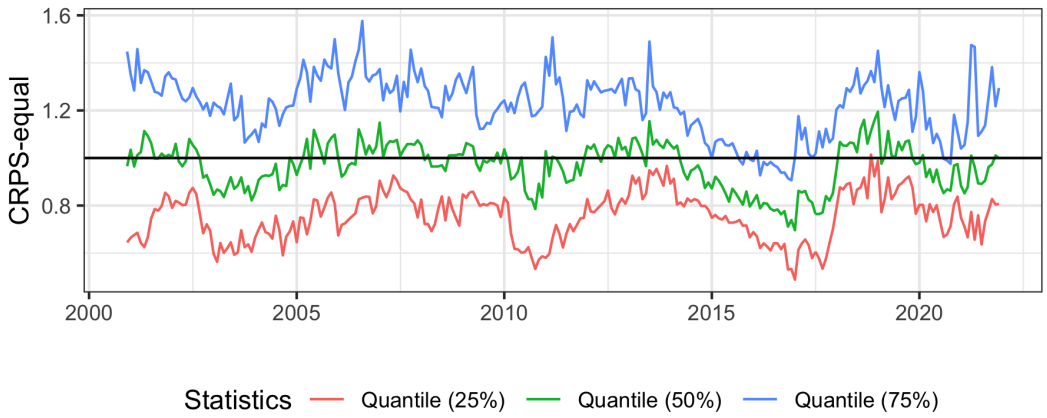

(b) QRF-CM2 for $h = 12$

Note: Panel (a) reports the median and interquartile range of the CRPS ratios for equal weights computed by the QRF-CM1 model for $h = 1$, and Panel (b) reports the same statistics computed by the QRF-CM2 model for $h = 12$. The ratios are computed between the model of interest and the QR-AR benchmark model. Green (red) indicates that the given model has a lower (higher) CRPS than that of the benchmark (QR-AR).

5.5.4 What is the relative importance of variables across time and regions?

In this section, I identify the importance of each variable for the best model corresponding to each forecasting horizon. Figure 5.5 shows the importance of each variable for the QRF-CM1 model and $h = 1$, and Figure 5.6 shows the importance of each variable for the QRF-CM2 model and $h = 12$. Variable importance is defined as a simple weighted sum of the number of times a given variable was selected to split on. It is then averaged in the time dimension, so that the sum at each time is equal to one. In the case of forecasting horizon $h = 1$, roughly 25% of the variable importance can be attributed to global and regional factors and these results, in general, are stable across time. In contrast, when forecasting horizon $h = 12$, a larger proportion of the variable importance – in this instance, approximately 50% – can be explained by global inflation factors, the global real factor and the oil price index. The results, in general, provide additional support for using global and regional inflation factors for forecasting country-specific inflation series (Ciccarelli and Mojon, 2010; Arango-Castillo et al., 2023; Medeiros et al., 2022). Moreover, the results suggest that the global real factor and the oil price index improve forecasts for longer horizons. This finding is in line with Kamber and Wong (2020), who show that commodity price shocks are important for explaining future rates of inflation.

Figure 5.5: Variable importance for the QRF-CM1 model and $h = 1$

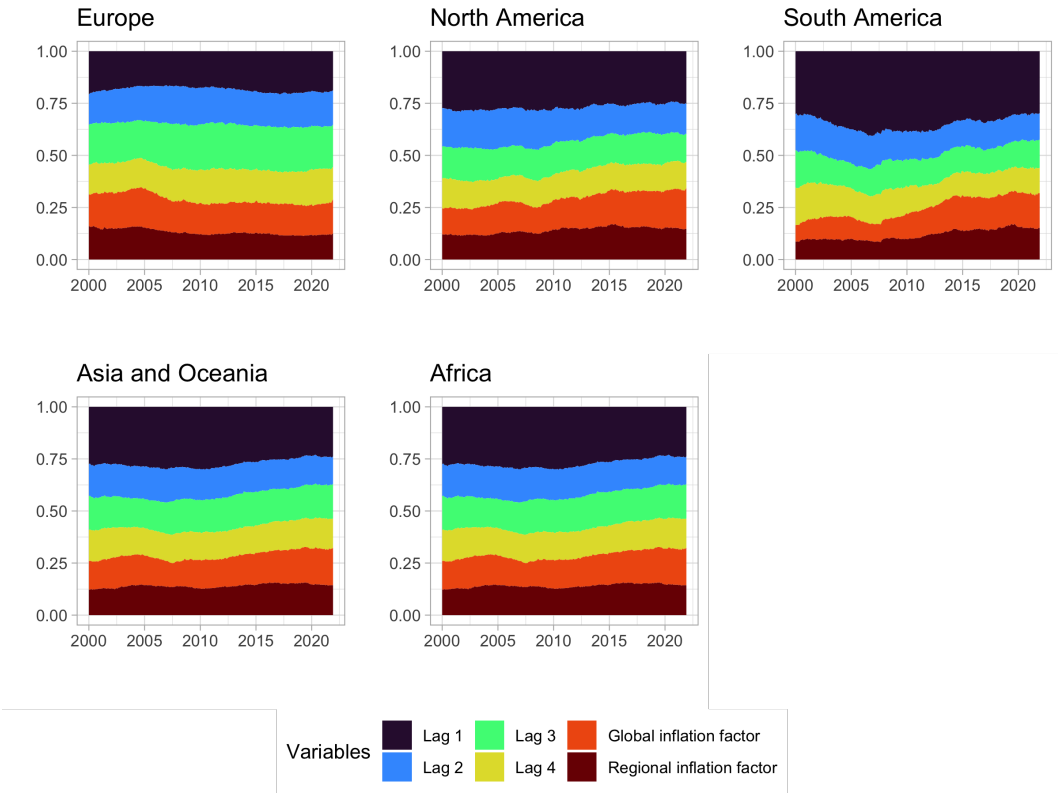

Note: This figure plots the variable importance in the QRF-CM1 model, computed as how often a given variable was split on.

Figure 5.6: Variable importance for the QRF-CM2 model and $h = 12$

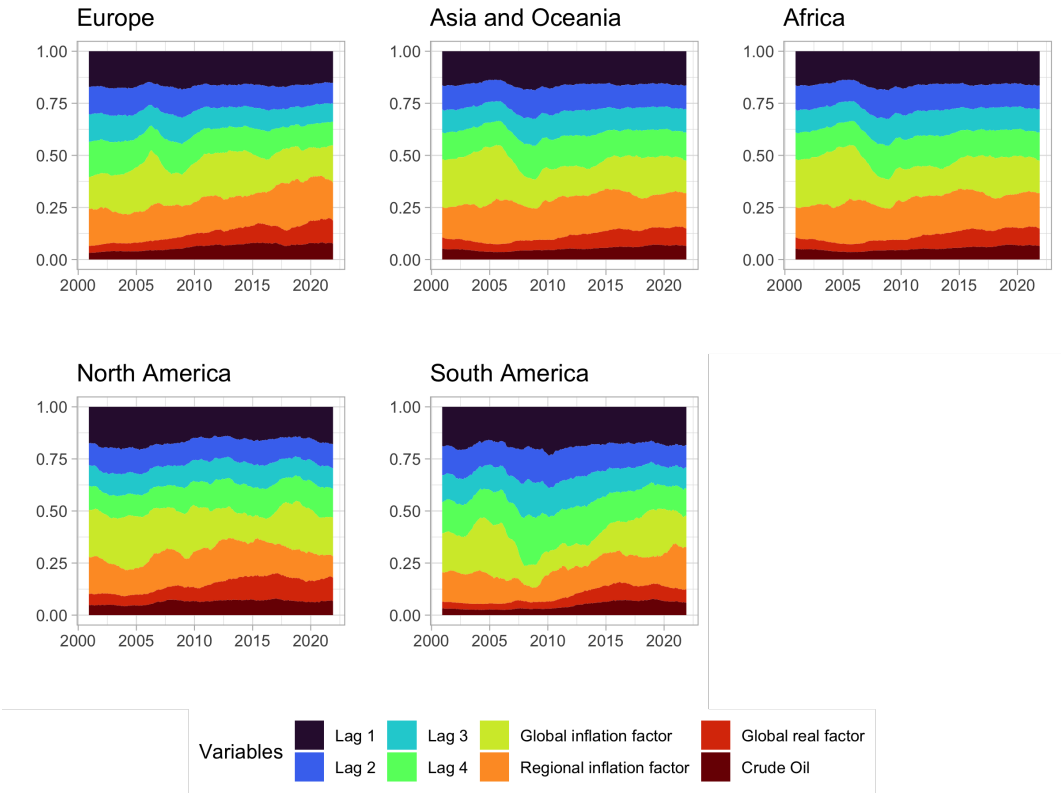

Note: This figure plots the variable importance in the QRF-CM2 model, computed as how often a given variable was split on.

5.5.5 Evolution of inflation risk across regions

In this section, I present novel evidence on inflation risk across regions, while previous works have tended to focus on groups of advanced and emerging market economies (Banerjee et al., 2020; Lopez-Salido and Loria, 2022; Queyranne et al., 2022). For each country, I calculate two measures of inflation risk: namely, the probability of both high and low inflation for the out-of-sample period. These estimates are based on the skew-t distribution calculated as in Eq. (5.5) with the QRF-CM2 model for forecasting horizon $h = 12$. I then proceed to calculate the median value for each region over time.

Figure 5.7 shows the one-year-ahead median probabilities of having inflation rates higher than 3% and lower than 0%, computed at time t, across regions. Interestingly, we find heterogeneity in the patterns across regions. First, the probability of high inflation is more persistent and higher in Africa than in the rest of the regions. This highlights a systematic problem, given that in the rest of the regions there is a downward-sloping trend in the probability of high inflation. For instance, in the case of America and Asia prior to the GFC around 2009, this probability was similar to that in Africa; however, thereafter it declined rapidly. In contrast, the probability of deflation or inflation below 0% is somewhat lower than 10% across regions, except Europe, where this probability was higher around 2015. According to Ha et al. (2021), after the GFC, deflation or low inflation was common in advanced economies. In 2015, more than half the advanced economies had negative inflation and, in 2016, three-quarters of the advanced economies had inflation in the low single digits, giving rise to concerns that low inflation, or even deflation, would become a permanent feature of inflation expectations. While the central banks of European countries implemented very accommodating monetary policies after the GFC, including the introduction of unconventional measures, the risk of deflation persisted up to 2020. As shown by Ha et al. (2021), during the onset of the Covid-19 pandemic, monthly global inflation fell between January and May 2020, picking up thereafter to return to pre-pandemic levels. All in all, this historic perspective is in agreement with the probability results presented here.

Figure 5.7: Probability of high and low inflation across world regions (2000-2020)

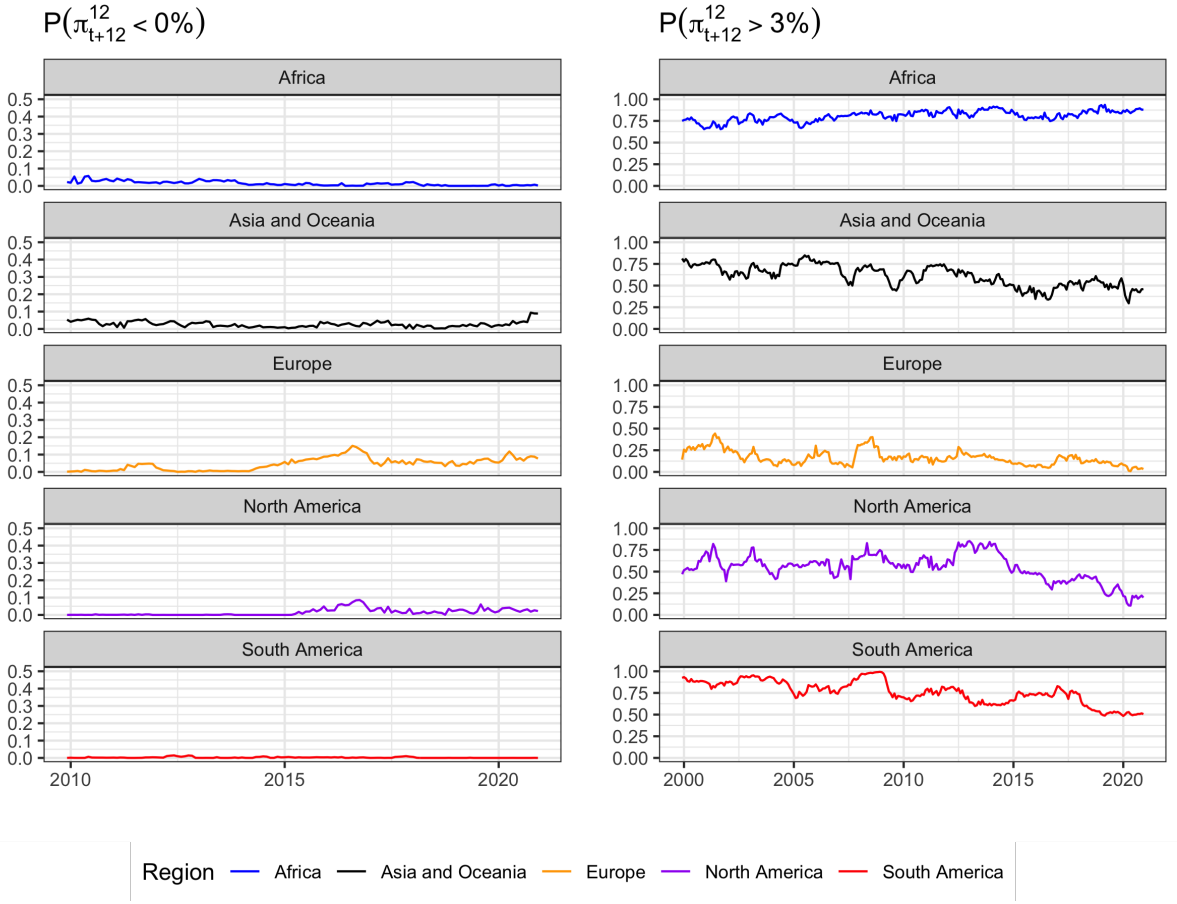

Note: This figure plots the one-year-ahead median probabilities of having an inflation rates higher than 3% and lower than 0%, computed at time t, across regions.

5.6 Conclusions

This paper has set itself the goal of investigating potential future inflation risks in a large group of countries. To this end, I first compute inflation density forecasts for a large panel of countries using a set of global factors as predictors. I provide evidence that, in general, global inflation factors improve the accuracy of density forecasts. This contrast with the previous literature which has tended to focus on point estimates (e.g. Ciccarelli and Mojon, 2010; Kamber and Wong, 2020; Medeiros et al., 2022; Arango-Castillo et al., 2023). Second, I present further evidence that random forests improve inflation density forecasts. Specifically, I report that this method provides a superior predictive performance, as has been documented elsewhere (see Medeiros et al., 2021, 2022; Goulet Coulombe et al., 2022; Clark et al., 2022). Third, using the inflation density forecast estimates, I derive inflation risk measures, that is, the probability of high and low inflation, across regions (see Lopez-Salido and Loria, 2022; Garratt and Petrella, 2022). Here, I report interesting heterogeneous patterns across regions: for instance, while the risk of high inflation, in general, presents a downward sloping trend around the world, it continues to be a structural problem in Africa.

To conclude, the inflation risk framework presented in this paper can be applied to a wide range of countries, with minimum data requirements. This is especially relevant from the perspective of a central bank or an international organization, as they will often have to assess risk across different regions. In this regard, I find that global factors are generally robust predictors of density forecasts across countries. This also draws attention to the synchronized reaction of the largest central banks around the world as this is likely to contribute to maintaining global price stability. Importantly, this framework can be tailored to any specific country in the sample by simply modifying the lower and upper bounds of inflation, depending on the characteristics of that country. For example, an inflation rate higher than 3% may not be perceived as problematic in some Latin American countries, where average inflation is usually higher than 3%. This highlights the importance of calibrating the bounds.

5.A Appendix

5.A.1 Data details

Table 5.A1 reports the complete list of 75 countries considered in the empirical exercise. Table 5.A2 displays the variance explained by the factors estimated as described in Section 5.2. Results show that the variance explained by one factor is 24.4% for all the countries, but that this increases when it is estimated by region. European countries share the highest commonality across regions.

Table 5.A1: List of countries considered in the empirical exercise by region

Europe	North America	South America	Asia	Africa
Austria	Bahamas	Bolivia	Fiji	Algeria
Belgium	Canada	Chile	India	Botswana
Cyprus	Costa Rica	Ecuador	Indonesia	Burundi
Denmark	Dominican Republic	Paraguay	Japan	Burkina Faso
Finland	El Salvador	Peru	Jordan	Cameroon
France	Grenada	Trinidad and Tobago	Korea, Rep.	Cote d'Ivoire
Germany	Guatemala	Uruguay	Malaysia	Egypt, Arab Rep.
Greece	Haiti	Nepal	Ethiopia	
Iceland	Honduras	Pakistan	Gambia, The	
Ireland	Jamaica	Philippines	Ghana	
Italy	Mexico	Samoa	Kenya	
Luxembourg	Panama	Singapore	Madagascar	
Malta	St. Kitts and Nevis	Solomon Islands	Mauritius	
Netherlands	St. Lucia	Sri Lanka	Morocco	
Norway	United States	Thailand	Niger	
Portugal	Turkey	Nigeria		
Spain	South Africa			
Sweden	Sudan			
Switzerland				
United Kingdom				
20	15	7	16	18

Table 5.A2: Percentage of variance explained by inflation factors

	# Countries	1 factor	2 factor	3 factor	4 factor	Cumulative
Global	75	24.4	9.6	7.6	6.4	47.9
Europe	20	40.8	11.8	8.9	7.2	68.6
South America	8	35.8	18.8	11.8	10.5	76.9
North America	14	35.7	16.0	10.8	7.7	70.1
Asia	16	31.2	11.6	11.4	9.1	63.4
Africa	17	28.8	13.1	12.0	8.7	62.6

Note: See Section 5.2 for the details of the estimation procedure.

Figure 5.A1: Measures of global and regional inflation

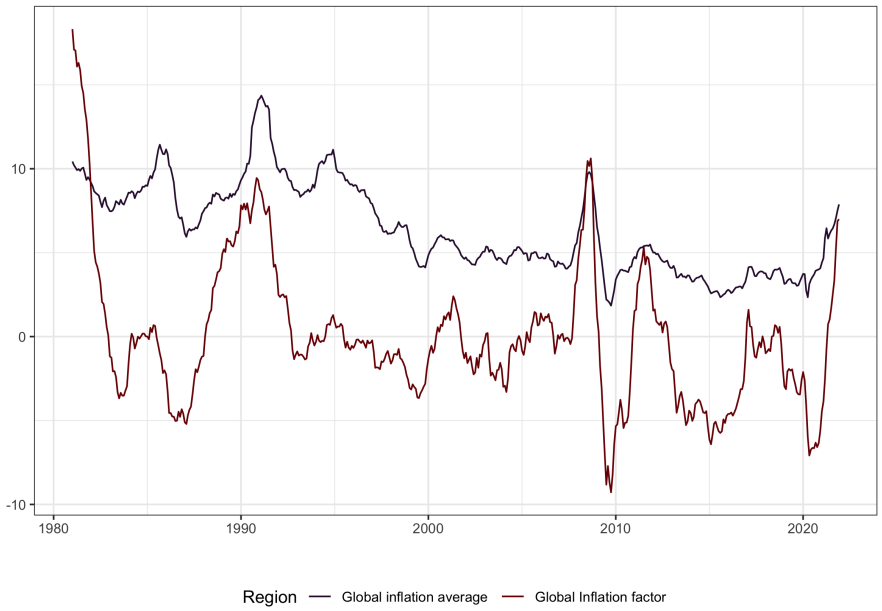

(a) Cross-country inflation average vs global inflation factor

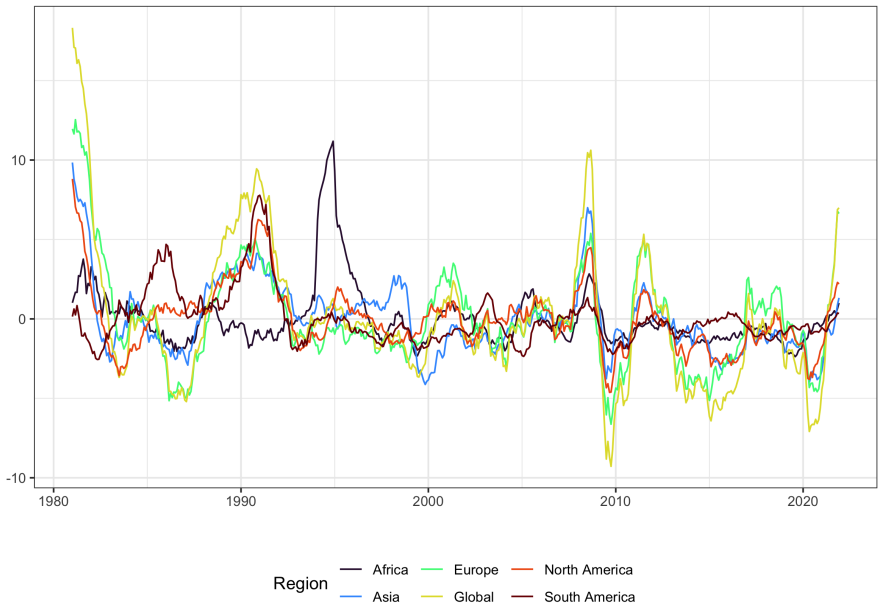

(b) Global and regional factors

Note: Panel (a) plots the cross-country inflation average and the global inflation factor using Hamilton's approach. Panel (b) displays the multiple regional factors joint with the global inflation factor using Hamilton's approach.

6 Conclusions

This thesis contributes to two problems identified in the literature: $i)$ How do US financial conditions impact funding markets (credit and stocks) in a large set of countries around the world under different scenarios of macro-financial distress?; and $ii)$ what role can be played by high-frequency data, real variables, and machine learning techniques in improving the forecasting performance of macroeconomic tail risk measures? In Chapter 2, I prove answers to the former question, while in Chapters 3, 4, and 5 I deal with the latter question. From a methodological perspective, I use time series econometrics, quantile regressions, mixed data sampling methods, machine learning models, and forecasts evaluation tests to address the various research questions. Furthermore, this dissertation has implications for risk management, monetary policy, financial stability, and forecasting.

In Chapter 2, I systematically document vulnerable funding episodes in the world economy. That is, financial conditions in the United States have significant predictive power in the lowest quantiles of credit growth and stock market prices around the global economy. I also show that vulnerable funding can be explained, mainly contemporaneously, by the relative market size in the case of credit markets and by the financial links with the US (measured by the total direct investment of the US as a percentage of the country's GDP) in the case of the stock market. The policy implication of this work is clear. I show that international funding markets are a source of persistence and amplification of financial conditions shocks across the global economy. This means that a deterioration of US financial conditions calls for policy actions in other economies around the world.

In the second part of my dissertation, I tackle the problem of producing accurate, out-of-sample tail forecasts for output growth, unemployment and inflation. In Chapter 3, I show that both real and financial variables reported with a daily frequency provide valuable information for monitoring periods of economic vulnerability. I further show that is possible to provide an early warning of a downturn in GDP in pseudo real-time and that this framework works well during episodes of distress. The flexible approach reported allows me to emphasize the importance of both economic theory and economic intuition when interpreting the results of forecast combinations and for improving the point forecast itself. All in all, I contribute to a better understanding of the economic signals that can be extracted from this

daily information when seeking to anticipate downturns in the economy.

In Chapter 4, I construct daily unemployment at risk around consensus forecasts conditional on the Aruoba-Diebold-Scotti business conditions index, using a quantile mixed sampling model. My results suggest that this indicator has better nowcasting properties than those provided by other daily financial conditioning variables, and provides early signal of unemployment rate increases, especially during episodes of distress. The results are relevant for risk monitoring and nowcasting purposes of central banks and other institutions.

In Chapter 5, I investigate potential future inflation risks in a large group of countries, using inflation density forecasts based on a set of global factors as predictors. I provides evidence that, in general, global inflation factors improve the accuracy of density forecasts. Also, I show that state-of-the-art machine learning techniques provide superior predictive performance. I document heterogeneous patterns of inflation risk measure across world regions. The results of this chapter are relevant from the perspective of a central bank or an international organization, as they often want to assess risk across different regions. In this regard, I find that global factors are generally robust predictors of density forecasts across countries. This also calls attention to a synchronized reaction of the largest central banks around the world, which is likely to contribute to sustain global price stability.

To conclude, the study of tail risks in macroeconomics is crucial for international organizations, policy makers, and central banks. The practice of reporting and discussing tail risks of the main economic and financial variables is nowadays a backbone of economic analysis, yet it has not been extensively studied in many settings. This thesis is a initial step in that direction, which I expect to explore in the following years.

Looking forward, I identify two avenues to work. The first will explore tail risks in macroeconomics using machine learning techniques and big data. The second will further study vulnerable funding episodes by analyzing the role of macroprudential policies and monetary policy, which are aimed at preventing and mitigating systemic risks.

Bibliography

Adams, P. A., Adrian, T., Boyarchenko, N., and Giannone, D. (2021). Forecasting macroeconomic risks. *International Journal of Forecasting*, 37(3):1173–1191.

Adrian, T., Boyarchenko, N., and Giannone, D. (2019). Vulnerable growth. *American Economic Review*, 109(4):1263–1289.

Adrian, T., Boyarchenko, N., and Giannone, D. (2021). MULTIMODALITY IN MACROFINANCIAL DYNAMICS. *International Economic Review*, 62(2):861–886.

Ahn, S. C. and Horenstein, A. R. (2013). Eigenvalue Ratio Test for the Number of Factors. *Econometrica*, 81(3):1203–1227.

Alessandri, P. and Bottero, M. (2020). Bank lending in uncertain times. *European Economic Review*, 128.

Alessandri, P. and Mumtaz, H. (2019). Financial regimes and uncertainty shocks. *Journal of Monetary Economics*, 101.

Alfaro, L., Chanda, A., Kalemli-Ozcan, S., and Sayek, S. (2004). FDI and economic growth: The role of local financial markets. *Journal of International Economics*, 64(1):89–112.

Alfaro, L. and Chen, M. X. (2012). Surviving the global financial crisis: Foreign ownership and establishment performance. *American Economic Journal: Economic Policy*, 4(3).

Alquist, R., Bhattarai, S., and Coibion, O. (2020). Commodity-price comovement and global economic activity. *Journal of Monetary Economics*, 112:41–56.

Amburgey, A. J. and McCracken, M. W. (2022). On the real-time predictive content of financial condition indices for growth. *Journal of Applied Econometrics*.

Ammer, J., De Pooter, M. D., Erceg, C. J., and Kamin, S. (2016). International Spillovers of Monetary Policy. *IFDP Notes*, 2016(15).

Ando, T. and Tsay, R. S. (2011). Quantile regression models with factor-augmented predictors and information criterion. *Econometrics Journal*, 14(1).

Andreou, E., Ghysels, E., and Kourtellos, A. (2013). Should Macroeconomic Forecasters Use Daily Financial Data and How? *Journal of Business & Economic Statistics*, 31(2):240–251.

Arango-Castillo, L., Orraca, M. J., and Molina, G. S. (2023). The global component of headline and core inflation in emerging market economies and its ability to improve forecasting performance. *Economic Modelling*, 120.

Arrigoni, S., Bobasu, A., and Venditti, F. (2020). The simpler the better: measuring financial conditions for monetary policy and financial stability. *ECB Working Paper Series No 2451 / August 2020*.

Aruoba, S. B., Diebold, F. X., and Scotti, C. (2009). Real-Time Measurement of Business Conditions. *Journal of Business & Economic Statistics*, 27(4):417–427.

Athey, S. (2017). Beyond prediction: Using big data for policy problems. *Science*, 355(6324):483–485.

Athey, S., Tibshirani, J., and Wager, S. (2019). Generalized random forests. *The Annals of Statistics*, 47(2):1148–1178.

Azzalini, A. and Capitanio, A. (2003). Distributions generated by perturbation of symmetry with emphasis on a multivariate skew t-distribution. *Journal of the Royal Statistical Society. Series B: Statistical Methodology*, 65(2):367–389.

Bai, J. and Ng, S. (2008). Forecasting economic time series using targeted predictors. *Journal of Econometrics*, 146(2):304–317.

Bai, J. and Ng, S. (2020). Simpler Proofs for Approximate Factor Models of Large Dimensions. *Working paper arXiv preprint arXiv:2008.00254*.

Ball, L., Leigh, D., and Loungani, P. (2017). Okun's Law: Fit at 50? *Journal of Money, Credit and Banking*, 49(7):1413–1441.

Banerjee, R. N., Contreras, J., Mehrotra, A., and Zampolli, F. (2020). Inflation at risk in advanced and emerging market economies. *BIS Working Paper Series*.

Baskaya, Y. S., di Giovanni, J., Kalemli-Özcan, , Peydro, J. L., and Ulu, M. F. (2017). Capital flows and the international credit channel. *Journal of International Economics*, 108.

Baumeister, C. and Guérin, P. (2021). A comparison of monthly global indicators for forecasting growth. *International Journal of Forecasting*, 37(3).

Baumeister, C. and Hamilton, J. D. (2019). Structural Interpretation of Vector Autoregressions with Incomplete Identification: Revisiting the Role of Oil Supply and Demand Shocks. *American Economic Review*, 109(5):1873–1910.

Belloni, A. and Chernozhukov, V. (2011). 1-penalized quantile regression in high-dimensional sparse models. *Annals of Statistics*, 39(1):82–130.

Beutel, J., Emter, L., Metiu, N., Prieto, E., and Schüler, Y. S. (2020). The Global Financial Cycle and Macroeconomic Tail Risks. *SSRN Electronic Journal*.

Bhattacharya, R., Jain, R., and Singh, A. (2019). Measuring the contribution of mark-up shock in food inflation in India. *IIMB Management Review*, 31(2):167–181.

Bloom, N. (2009). The Impact of Uncertainty Shocks. *Econometrica*, 77(3):623–685.

Bordo, M. D., Duca, J. V., and Koch, C. (2016). Economic policy uncertainty and the credit channel: Aggregate and bank level U.S. evidence over several decades. *Journal of Financial Stability*, 26:90–106.

Bräuning, F. and Ivashina, V. (2020a). Monetary Policy and Global Banking. *Journal of Finance*, 75(6).

Bräuning, F. and Ivashina, V. (2020b). U.S. monetary policy and emerging market credit cycles. *Journal of Monetary Economics*, 112:57–76.

Brave, S. A., Butters, R. A., Brave, S., and Butters, R. A. (2011). Monitoring financial stability: a financial conditions index approach. *Economic Perspectives*, 35(Q I):22–43.

Breiman, L. (2001). Random forests. *Machine Learning*, 45(1):5–32.

Brownlees, C. and Souza, A. B. (2021). Backtesting global Growth-at-Risk. *Journal of Monetary Economics*, 118:312–330.

Brunnermeier, M. K. and Sannikov, Y. (2016). Macro, Money, and Finance: A Continuous-Time Approach. *Handbook of Macroeconomics*, 2:1497–1545.

Bruno, V. and Shin, H. S. (2015). Capital flows and the risk-taking channel of monetary policy. *Journal of Monetary Economics*, 71.

Carrière-Swallow, Y. and Céspedes, L. F. (2013). The impact of uncertainty shocks in emerging economies. *Journal of International Economics*, 90(2):316–325.

Carriero, A., Clark, T. E., and Marcellino, M. (2020). Assessing international commonality in macroeconomic uncertainty and its effects. *Journal of Applied Econometrics*, 35(3).

Carriero, A., Clark, T. E., and Marcellino, M. (2022). Nowcasting tail risk to economic activity at a weekly frequency. *Journal of Applied Econometrics*, 37(5):843–866.

Cesa-Bianchi, A., Pesaran, M. H., and Rebucci, A. (2021). Uncertainty and economic activity: A multicountry perspective. *Review of Financial Studies*, 33(8).

Cetorelli, N. and Goldberg, L. S. (2012). Banking Globalization and Monetary Transmission. *The Journal of Finance*, 67(5):1811–1843.

Chernozhukov, V., Fernández-Val, I., and Galichon, A. (2009). Improving point and interval estimators of monotone functions by rearrangement. *Biometrika*, 96(3):559–575.

Choi, S. (2018). The Impact of US Financial Uncertainty Shocks on Emerging Market Economies: An International Credit Channel. *Open Economies Review*, 29(1):89–118.

Choi, S., Furceri, D., Huang, Y., and Loungani, P. (2018). Aggregate uncertainty and sectoral productivity growth: The role of credit constraints. *Journal of International Money and Finance*, 88.

Christoffersen, P. F. (1998). Evaluating Interval Forecasts. *International Economic Review*, 39(4):841.

Chudik, A. and Pesaran, M. H. (2015). Common correlated effects estimation of heterogeneous dynamic panel data models with weakly exogenous regressors. *Journal of Econometrics*, 188(2).

Ciccarelli, M., Maddaloni, A., and Peydró, J. L. (2015). Trusting the bankers: A new look at the credit channel of monetary policy. *Review of Economic Dynamics*, 18(4):979–1002.

Ciccarelli, M. and Mojon, B. (2010). Global Inflation. *The Review of Economics and Statistics*, 92(3):524–535.

Clark, T. and McCracken, M. (2013). Advances in Forecast Evaluation. *Handbook of Economic Forecasting*, 2:1107–1201.

Clark, T. E., Huber, F., Koop, G., Marcellino, M., and Pfarrhofer, M. (2022). Tail Frecasting with Multivariate Bayesian Additive Regression Trees. *International Economic Review*, 0(0).

Corradi, V. and Swanson, N. R. (2006). Chapter 5 Predictive Density Evaluation. *Handbook of Economic Forecasting*, 1:197–284.

De Santis, R. A. and Van der Veken, W. (2020). Forecasting macroeconomic risk in real time: Great and Covid-19 Recessions. *ECB Working Paper Series No 2436 / July 2020*.

Delle Monache, D., De Polis, A., and Petrella, I. (2021). Modeling and Forecasting Macroeconomic Downside Risk. *SSRN Electronic Journal*.

Di Giovanni, J., Kalemli-Özcan, S., Ulu, M. F., and Baskaya, Y. S. (2022). International Spillovers and Local Credit Cycles. *The Review of Economic Studies*, 89(2):733–773.

Diebold, F. X. and Mariano, R. S. (1995). Comparing predictive accuracy. *Journal of Business and Economic Statistics*, 13(3):253–263.

Doz, C., Giannone, D., and Reichlin, L. (2012). A Quasi–Maximum Likelihood Approach for Large, Approximate Dynamic Factor Models. *The Review of Economics and Statistics*, 94(4):1014–1024.

Engle, R. F. and Manganelli, S. (2004). CAViaR. *Journal of Business & Economic Statistics*, 22(4):367–381.

Estrella, A. and Mishkin, F. S. (1998). Predicting U.S. Recessions: Financial Variables as Leading Indicators. *The Review of Economics and Statistics*, 80(1):45–61.

Fama, E. F. and French, K. R. (1993). Common risk factors in the returns on stocks and bonds. *Journal of Financial Economics*, 33(1):3–56.

Fama, E. F. and French, K. R. (2012). Capital Structure Choices. *Critical Finance Review*, 1(1):59–101.

Faust, J., Gilchrist, S., Wright, J. H., and Zakrajšek, E. (2013). Credit Spreads as Predictors of Real-Time Economic Activity: A Bayesian Model-Averaging Approach. *The Review of Economics and Statistics*, 95(5):1501–1519.

Federal Open Market Committee (2020). Federal Reserve Press Release (2020 March 15). Technical report.

Fernández-Villaverde, J., Guerrón-Quintana, P., Rubio-Ramírez, J. F., and Uribe, M. (2011). Risk matters: The real effects of volatility shocks. *American Economic Review*, 101(6):2530–2561.

Ferrara, L., Mogliani, M., and Sahuc, J. G. (2022). High-frequency monitoring of growth at risk. *International Journal of Forecasting*, 38(2):582–595.

Figueres, J. M. and Jarociński, M. (2020). Vulnerable growth in the euro area: Measuring the financial conditions. *Economics Letters*, 191:109126.

Fink, F. and Schüler, Y. S. (2015). The transmission of US systemic financial stress: Evidence for emerging market economies. *Journal of International Money and Finance*, 55:6–26.

Fleckenstein, M., Longstaff, F. A., and Lustig, H. (2017). Deflation Risk. *The Review of Financial Studies*, 30(8):2719–2760.

Friedman, J., Hastie, T., and Tibshirani, R. (2010). Regularization Paths for Generalized Linear Models via Coordinate Descent. *Journal of Statistical Software*, 33(1):1–22.

Galbraith, J. W. and Norden, S. v. (2012). Assessing Gross Domestic Product and Inflation Probability Forecasts Derived from Bank of England Fan Charts. *Journal of the Royal Statistical Society Series A: Statistics in Society*, 175(3):713–727.

Garratt, A. and Petrella, I. (2022). Commodity prices and inflation risk. *Journal of Applied Econometrics*, 37(2):392–414.

Gertler, M. and Gilchrist, S. (2018). What Happened: Financial Factors in the Great Recession. *Journal of Economic Perspectives*, 32(3):3–30.

Gete, P. and Melkadze, G. (2018). Aggregate volatility and international dynamics. The role of credit supply. *Journal of International Economics*, 111.

Ghysels, E., Plazzi, A., and Valkanov, R. (2016). Why Invest in Emerging Markets? The Role of Conditional Return Asymmetry. *Journal of Finance*, 71(5):2145–2192.

Giacomini, R. and Komunjer, I. (2005). Evaluation and Combination of Conditional Quantile Forecasts. *Journal of Business & Economic Statistics*, 23(4):416–431.

Giglio, S., Kelly, B., and Pruitt, S. (2016). Systemic risk and the macroeconomy: An empirical evaluation. *Journal of Financial Economics*, 119(3):457–471.

Gneiting, T. (2008). Probabilistic Forecasting. *Journal of the Royal Statistical Society Series A: Statistics in Society*, 171(2):319–321.

Gneiting, T. and Raftery, A. E. (2007). Strictly Proper Scoring Rules, Prediction, and Estimation. *Journal of the American Statistical Association*, 102(477):359–378.

Gneiting, T. and Ranjan, R. (2011). Comparing Density Forecasts Using Threshold- and Quantile-Weighted Scoring Rules. *Journal of Business & Economic Statistics*, 29(3):411–422.

Goulet Coulombe, P., Leroux, M., Stevanovic, D., and Surprenant, S. (2022). How is machine learning useful for macroeconomic forecasting? *Journal of Applied Econometrics*, 37(5):920–964.

Greenspan, A. (2004). Risk and uncertainty in monetary policy. *American Economic Review*, 94(2):33–40.

Guerrieri, V., Lorenzoni, G., Straub, L., and Werning, I. (2022). Macroeconomic Implications of COVID-19: Can Negative Supply Shocks Cause Demand Shortages? *American Economic Review*, 112(5):1437–74.

Gunay, S. (2020). Seeking causality between liquidity risk and credit risk: TED-OIS spreads and CDS indexes. *Research in International Business and Finance*, 52:101189.

Ha, J., Kose, M. A., and Ohnsorge, F. (2021). One-Stop Source: A Global Database of Inflation. *Policy Research Working Paper;No. 9737. World Bank, Washington, DC. © World Bank.*

Hamilton, J. D. (2018). Why You Should Never Use the Hodrick-Prescott Filter. *The Review of Economics and Statistics*, 100(5):831–843.

Hamilton, J. D. and Xi, J. (2023). Principal Component Analysis for Nonstationary Series. *University of California at San Diego*.

Hansen, P. R., Lunde, A., and Nason, J. M. (2011). The Model Confidence Set. *Econometrica*, 79(2):453–497.

Harding, M., Lamarche, C., and Pesaran, M. H. (2020). Common correlated effects estimation of heterogeneous dynamic panel quantile regression models. *Journal of Applied Econometrics*, 35(3).

Harvey, D., Leybourne, S., and Newbold, P. (1997). Testing the equality of prediction mean squared errors. *International Journal of Forecasting*, 13(2):281–291.

Holló, D., Kremer, M., and Lo Duca, M. (2012). CISS - A Composite Indicator of Systemic Stress in the Financial System. *Working Paper Series*, 1426.

Isohätälä, J., Klimenko, N., and Milne, A. (2016). Post-Crisis Macrofinancial Modeling: Continuous Time Approaches. *The Handbook of Post Crisis Financial Modeling*, pages 235–282.

Ivashina, V., Scharfstein, D. S., and Stein, J. C. (2015). Dollar funding and the lending behavior of global banks. *Quarterly Journal of Economics*, 130(3).

Jordà, , Schularick, M., Taylor, A. M., and Ward, F. (2019). Global Financial Cycles and Risk Premiums. *IMF Economic Review*, 67(1):109–150.

Kalemli-Özcan, S. (2019). U.S. Monetary Policy and International Risk Spillovers. *NBER Working Papers Nº26297*.

Kalemli-Özcan, S., Nikolsko-Rzhevskyy, A., and Kwak, J. H. (2020). Does trade cause capital to flow? Evidence from historical rainfall. *Journal of Development Economics*, 147.

Kamber, G. and Wong, B. (2020). Global factors and trend inflation. *Journal of International Economics*, 122:103265.

Kiley, M. T. (2021). Unemployment Risk. *Journal of Money, Credit and Banking*, 54:1407–1424.

Kilian, L. (2009). Not All Oil Price Shocks Are Alike: Disentangling Demand and Supply Shocks in the Crude Oil Market. *American Economic Review*, 99(3):1053–69.

Kilian, L. and Manganelli, S. (2007). Quantifying the Risk of Deflation. *Journal of Money, Credit and Banking*, 39(2-3):561–590.

Kitsul, Y. and Wright, J. H. (2013). The economics of options-implied inflation probability density functions. *Journal of Financial Economics*, 110(3):696–711.

Koenker, R. (2005). *Quantile regression*. Cambridge University Press.

Koenker, R. and Bassett, G. (1978). Regression Quantiles. *Econometrica*, 46(1):33.

Kozumi, H. and Kobayashi, G. (2011). Gibbs sampling methods for Bayesian quantile regression. *Journal of Statistical Computation and Simulation*, 81(11):1565–1578.

Kupiec, P. H. (1995). Techniques for Verifying the Accuracy of Risk Measurement Models. *The Journal of Derivatives*, 3(2):73–84.

Lima, L. R. and Meng, F. (2017). Out-of-Sample Return Predictability: A Quantile Combination Approach. *Journal of Applied Econometrics*, 32(4):877–895.

Lima, L. R., Meng, F., and Godeiro, L. (2020). Quantile forecasting with mixed-frequency data. *International Journal of Forecasting*, 36(3):1149–1162.

Lin, S. and Ye, H. (2018). Foreign direct investment, trade credit, and transmission of global liquidity shocks: Evidence from Chinese manufacturing firms. *Review of Financial Studies*, 31(1):206–238.

Longstaff, F. A., Pan, J., Pedersen, L. H., and Singleton, K. J. (2011). How Sovereign Is Sovereign Credit Risk? *American Economic Journal: Macroeconomics*, 3(2):75–103.

Lopez-Salido, D. and Loria, F. (2022). Inflation at Risk. *Available at SSRN: https://ssrn.com/abstract=4002673*.

Loria, F., Matthes, C., and Zhang, D. (2023). Assessing Macroeconomic Tail Risk. *SSRN Electronic Journal*.

Ludvigson, S., Ma, S., and Ng, S. (2021). Uncertainty and Business Cycles: Exogenous Impulse or Endogenous Response? *American Economic Journal: Macroeconomics*.

Maldonado, J. and Ruiz, E. (2021). Accurate Confidence Regions for Principal Components Factors*. *Oxford Bulletin of Economics and Statistics*, 83(6):1432–1453.

Manzan, S. (2015). Forecasting the Distribution of Economic Variables in a Data-Rich Environment. *Journal of Business & Economic Statistics*, 33(1):144–164.

McCracken, M. W. and Ng, S. (2016). FRED-MD: A Monthly Database for Macroeconomic Research. *Journal of Business & Economic Statistics*, 34(4):574–589.

McCracken, M. W. and Ng, S. (2021). FRED-QD: A quarterly database for macroeconomic research. *Federal Reserve Bank of St. Louis Review*, 103(1).

Medeiros, C. M., Schütte, E. C. M., and Soussi, T. S. (2022). Global Inflation: Implications for forecasting and monetary policy. *SSRN Electronic Journal*.

Medeiros, M. C., Vasconcelos, G. F., Veiga, , and Zilberman, E. (2021). Forecasting Inflation in a Data-Rich Environment: The Benefits of Machine Learning Methods. *Journal of Business and Economic Statistics*, 39(1):98–119.

Meinshausen, N. (2006). Quantile Regression Forests. *Journal of Machine Learning Research*, 7(35):983–999.

Mendez-Civieta, A., Aguilera-Morillo, M. C., and Lillo, R. E. (2021). Adaptive sparse group LASSO in quantile regression. *Advances in Data Analysis and Classification*, 15(3).

Miranda-Agrippino, S. and Rey, H. (2020a). The Global Financial Cycle after Lehman. *AEA Papers and Proceedings*, 110.

Miranda-Agrippino, S. and Rey, H. (2020b). U.S. Monetary Policy and the Global Financial Cycle. *The Review of Economic Studies*, 87(6):2754–2776.

Mogliani, M. and Simoni, A. (2021). Bayesian MIDAS penalized regressions: Estimation, selection, and prediction. *Journal of Econometrics*, 222(1):833–860.

Monnet, E. and Puy, D. (2019). One Ring to Rule Them All? New Evidence on World Cycles. *IMF Working Paper No. 19/202*.

Nakamura, E. and Steinsson, J. (2018). Identification in macroeconomics. *Journal of Economic Perspectives*, 32(3):59–86.

Okun, A. M. (1962). Potential GNP: its measurement and significance. *Proceedings of the Business and Economics Statistics Section*, pages 98–104.

Parsons, C. and Titman, S. (2008). Empirical capital structure: A review. *Foundations and Trends in Finance*, 3(1):1–93.

Peek, J. and Rosengren, E. S. (1997). The International Transmission of Financial Shocks: The Case of Japan. *American Economic Review*, 87(4):495–505.

Pettenuzzo, D., Timmermann, A., and Valkanov, R. (2016). A MIDAS approach to modeling first and second moment dynamics. *Journal of Econometrics*, 193(2):315–334.

Pfarrhofer, M. (2022). Modeling tail risks of inflation using unobserved component quantile regressions. *Journal of Economic Dynamics and Control*, page 104493.

Plagborg-Møller, M., Reichlin, L., Ricco, G., and Hasenzagl, T. (2020). When Is Growth at Risk? *Brookings Papers on Economic Activity*, 2020(1):167–229.

Prasad, A., Elekdag, S., Jeasakul, P., Lafarguette, R., Alter, A., Xiaochen Feng, A., and Wang, C. (2019). Growth at Risk: Concept and Application in IMF Country Surveillance. *IMF Working Papers*, 19(36):1.

Queyranne, M., Lafarguette, R., and Johnson, K. (2022). Inflation-at-Risk in in the Middle East, North Africa, and Central Asia. *IMF Working Paper, WP/22/168*.

Reichlin, L., Ricco, G., and Hasenzagl, T. (2020). Financial Variables as Predictors of Real Growth Vulnerability. *Documents de Travail de l'OFCE*.

Reifschneider, D. and Tulip, P. (2019). Gauging the uncertainty of the economic outlook using historical forecasting errors: The Federal Reserve's approach. *International Journal of Forecasting*, 35(4):1564–1582.

Rey, H. (2015). Dilemma not Trilemma: The Global Financial Cycle and Monetary Policy Independence. *CEPR Discussion Papers*.

Ryngaert, J. M. (2022). Inflation disasters and consumption. *Journal of Monetary Economics*, 129:S67–S81.

Sánchez, A. C. and Röhn, O. (2016). How do policies influence GDP tail risks? *OECD Economics Department Working Papers*, No. 1339.

Stock, J. H. and Watson, M. W. (2002). Macroeconomic forecasting using diffusion indexes. *Journal of Business and Economic Statistics*, 20(2).

Stock, J. H. and Watson, M. W. (2004). Combination forecasts of output growth in a seven-country data set. *Journal of Forecasting*, 23(6):405–430.

Stock, J. H. and Watson, M. W. (2012). Dynamic Factor Models. In *The Oxford Handbook of Economic Forecasting*, pages 35–60.

Yang, Y., Wang, H. J., and He, X. (2015). Posterior Inference in Bayesian Quantile Regression with Asymmetric Laplace Likelihood. *International Statistical Review*, 84(3):327–344.

Yu, K. and Moyeed, R. A. (2001). Bayesian quantile regression. *Statistics & Probability Letters*, 54(4):437–447.

Zou, H. (2006). The adaptive lasso and its oracle properties. *Journal of the American Statistical Association*, 101(476).

Zou, H. and Hastie, T. (2005). Regularization and variable selection via the elastic net. *Journal of the Royal Statistical Society: Series B (Statistical Methodology)*, 67(2):301–320.